Aus der Medizinische Klinik und Poliklinik V
Klinik der Ludwigs-Maximilians-Universität München
Director: Prof. Dr. med. Jürgen Behr

Dissertation

zum Erwerb des Doctor of Philosophy (Ph.D.) an der

Medizinischen Fakultät der

Ludwig-Maximilians-Universität zu München

Cellular and molecular mechanisms of tissue repair by fascia

Vorgelegt von

Haifeng Ye

aus

Jingdezhen, Jiangxi, China

Jahr

2023

Mit Genehmigung der Medizinischen Fakultät der

Ludwig-Maximilians-Universität zu München

First evaluator (1. TAC member): Prof. Dr. med. Jürgen Behr

Second evaluator (2. TAC member): Dr. Yuval Rinkevich

Third evaluator: Prof. Dr. Markus Rehberg

Fourth evaluator: Prof. Dr. Bianca Schaub

Dean: Prof. Dr. med. Thomas Gudermann

Datum der Verteidigung:

11.04.2023

Table of content

Abstract (English):

Aging is an important factor affecting wound healing in the skin. Former research demonstrated that wound healing progresses slowly and is delayed in aging skin compared to adolescent skin. Aged and injured skin also tends to develop into chronic wounds, and that removing senescent cells from the skin can accelerate wound healing(Wilkinson and Hardman, 2020; Yousefzadeh et al., 2018). However, it has also been shown that senescent cells in the skin contribute to wound healing, ultimately leading to the formation of smaller scars. Therefore, it is unclear what the exact mechanism of aging is in affecting wound healing. In this study, we explored the differences and mechanisms between young and aged skin wounds using in vitro skin culture techniques, in vivo skin wound models, skin chimeric grafting experiments, in vitro cell transplantation experiments, real-time imaging techniques, three-dimensional imaging techniques, immunofluorescence staining and histological staining. The cumulative data indicates that the differences in wound healing dynamics between aged and young skin are due to the heterogeneity of fascia fibroblasts. Specifically, the differentiation capacity of fascia fibroblasts is greatly reduced in aging skin, leading to a decrease in fascia contractility and transport into wounds, which ultimately leads to slow skin wound closure and delayed wound healing. The use of a Wnt Signaling agonist (CHIR) can reactivate the differentiation capacity of aged fibroblasts, increasing the contractility capacity of aged fascia, accelerating the closure of aged wounds, and promoting wound healing. These finding explains how wound healing is slowed down during aging, revealing Wnt signaling can activate or reprogram aged fascial fibroblasts to promote wound healing, and provides a new basic research and translational perspectives to accelerate and improve wound healing of aged skin.

List of figures

List of abbreviations

Abbreviation	Definition
UV	Ultraviolet
IL-1	interleukin-1
IL-2	interleukin-2
IL-3	interleukin-3
IL-6	interleukin-6
TNF	tumor necrosis factor
FGF	fibroblast growth factor
EGF	epidermal growth factor
ECM	extracellular matrix
PDGF	Platelet-derived growth factor
DPBS	Dulbecco's phosphate-buffered saline
DMEM/F-12	Dulbecco's Modified Eagle Medium/ F-12
NEAA	Non-Essential Amino Acid
PFA	Paraformaldehyde
PBS	Phosphate-buffered saline
3D	three-dimensional
EQM	echinomycin
DMSO	Dimethyl sulfoxide
PBST	Phosphate-Buffered Saline, 0.05% Tween
DAPI	4',6-diamidino-2-phenylindole
GFP	Green fluorescent protein
a-SMA	Anti-smooth muscle antibody
MOMA-2	Monocyte + Macrophage antibody

Abbreviation	Definition
PDPN	Podoplanin
RUNX2	Runt-related transcription factor 2
NHS-PCB	NHS-Pacific Blue
FRCs	fibroblast-like reticulocytes
Procr	Protein C Receptor
HIF1a	hypoxia inducible factor 1
GSK-3	Glycogen synthase kinase 3
Min	Minute
mL	Milliliter
mm	Millimete

1. Introduction

The skin is the largest organ in the body and has multiple functions; its main function is to act as a protective barrier. It protects the body from harmful chemicals, ultraviolet light and pathogenic microorganisms. Amongst its diverse functions, the skin also synthesizes vitamin D, regulates body temperature and prevents water loss. In the United States, 84.5 million of bedsores, burn victims and chronic skin ulcers are reported each year. And with approximately tens of millions of burn patients and chronic non-healing wounds in China each year, skin wound healing has attracted the attention of researchers worldwide. The cost of skin wound treatment varies depending on the method of prescription, and in the United States, the annual medical cost of chronic wound treatment is approximately $6 to $15 billion. Aging is one of the major causes of aberrant wound healing. Therefore, exploring the differences in wound healing between aging and young skin and improving the speed and quality of wound healing is a major medical problem that needs to be explored and addressed.

1.1 The structure and function of the skin

1.1.1 Basic structure of the skin

The skin consists of three layers: the upper epidermis, the dermis, and the subcutaneous tissue, each with its own unique structure and function. Refer to **Figure A.**

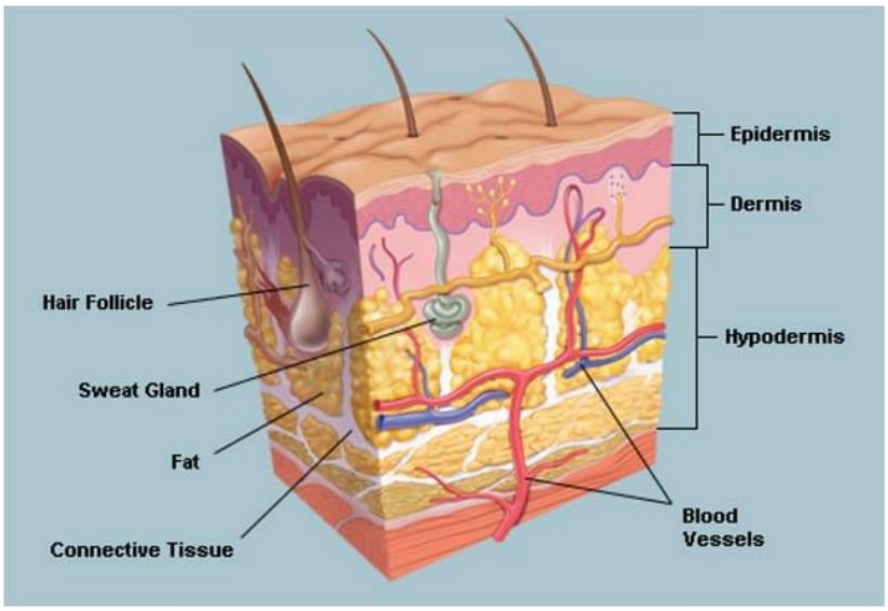

Fig. A The structure of the skin. This image is a reference image (Hoffman and MD, n.d.).

Epidermis: The epidermis is the first layer of the skin. Most epidermal cells are keratin-forming cells, but skin also contains melanocytes, Merkel cells, Langerhans cells, and inflammatory cells (Moreci and Lechler, 2020). Keratin-forming cells are formed in the basal layer, which is the lowest part of the epidermis. New keratin-forming cells delaminate from the basement membrane and slowly migrate through the epidermis to the uppermost part of the epidermis. Once it reaches the skin surface, they gradually fall off and are displaced by new cell from the lower layers, which migrate upward (Mokry and Pisal, 2020; Sotiropoulou and Blanpain, 2012). The outermost layer of the epidermis, also known as the stratum corneum, consists of more than 20 layers of polygonal, non-nucleated keratinocytes that prevent the entry of most bacteria, viruses and other external substances into the body (Baroni et al., 2012; van Smeden et al., 2014). Melanocytes are scattered in the basal layer of the epidermis and produce melanin, the number and distribution of which is a major factor in the formation of skin color. The epidermis also includes Langerhans cells, which are tissue-resident macrophages of the skin and are part of the immune system of the skin. Langerhans cells not only recognize exo- and phagocytosis of source microbial antigens and become full-functioning antigen presenting cell, but also functions in the metaplasia of the skin. The epidermis resists infection by environmental pathogens and regulates skin humidity (Lefèvre-Utile et al., 2021).

Dermis: The dermis is the second layer of the skin and is a thick layer of dense fibers and elastic connective tissue that provides the skin with elasticity and strength. The dermis is composed of two layers; the superficial layer adjoining the epidermis is called the papillary dermis, while the deeper and thicker region is known as the reticular dermis (Wang et al., 2015). The dermis is mainly consisted of three types of cells: macrophages, mast cells and fibroblasts, (Rippa et al., 2019; Woodley, 2017). In addition to its cellular composition, the dermis contains matrix components such as collagen, which gives strength, elastin, which offers elasticity, and extracellular matrix, an extracellular gelatinous substance composed mainly of glycosaminoglycans (most notably hyaluronic acid), proteoglycans, and glycoproteins (Krieg and Aumailley, 2011). The dermis houses sweat glands, nerve endings, blood vessels, sebaceous glands and hair follicles, and their distribution varies from one skin location to another.

Subcutaneous tissue: This is the underlying tissue of the skin and consists largely of loosely packed connective tissue that contains larger blood vessels and nerves than the dermis. (Amano et al., 2020; Ishida et al., 2015). The main cell types that inhabit the subcutaneous tissue are fibroblasts, adipocytes and macrophages. It is the main site of fat storage in the body, helping to insulate against cold and provides a protective padding layer (Li and Ahn, 2011). The subcutaneous tissue contains large numbers of adipocytes within a connective tissue layer termed as fascia (Ahn and Kaptchuk, 2011; Stecco et al., 2011). The structure of mouse skin and human skin are roughly the same. The main differences being that mouse subcutaneous tissue has a very thin muscle layer, whereas human skin does not. Refer to **Figure B.**

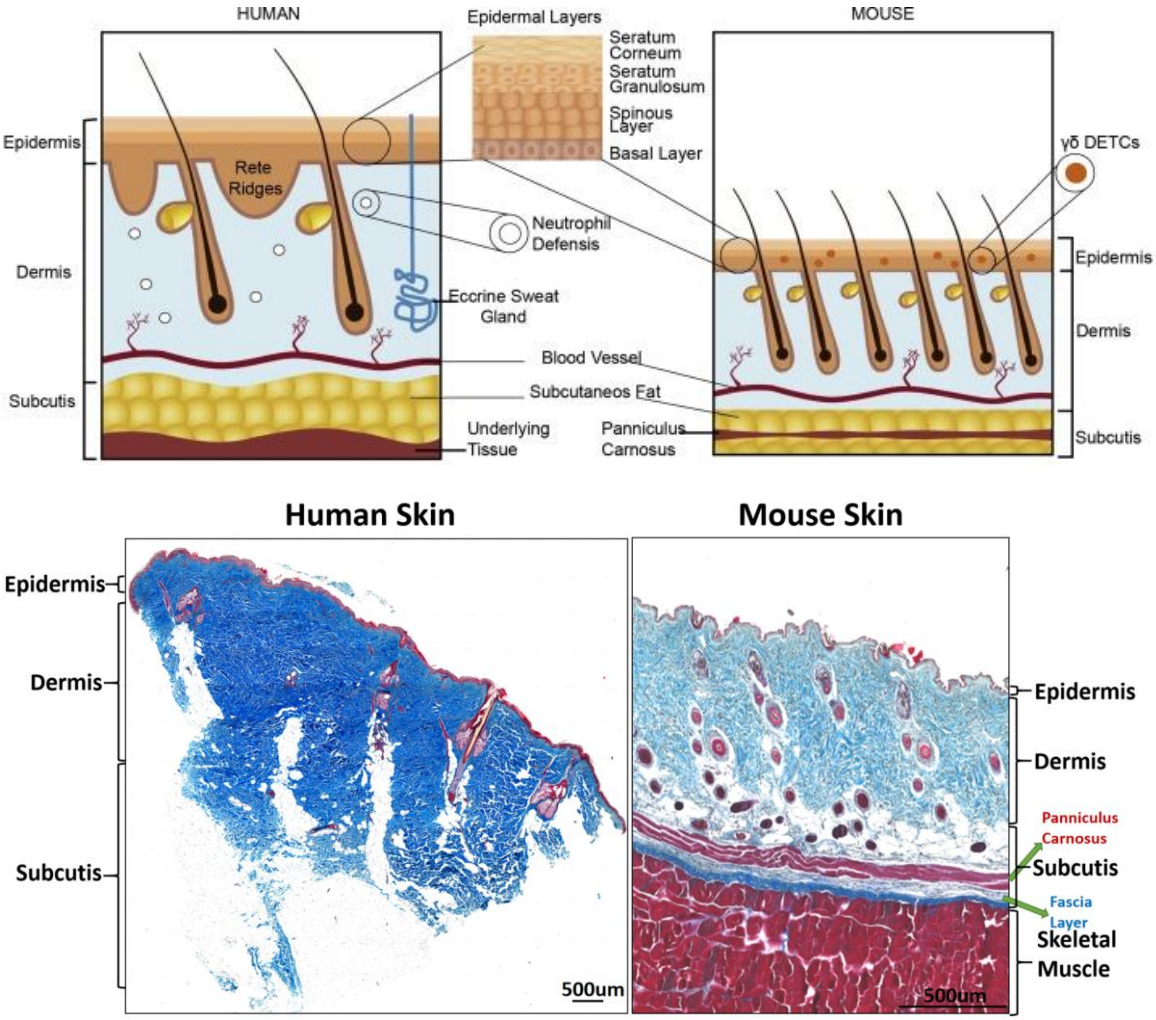

Fig. B Histological differences between mouse and human skin

Above is a cartoon depiction of the difference between mouse and human skin, this image is a reference image (Zomer and Trentin, 2018a). Below is the histological difference between mouse and human skin, scale bar 500 μm.

1.1.2 Skin functions

As the largest organ of the human body, the skin has multiple functions, mainly reflected in the following aspects. **Refer to Figure C.**

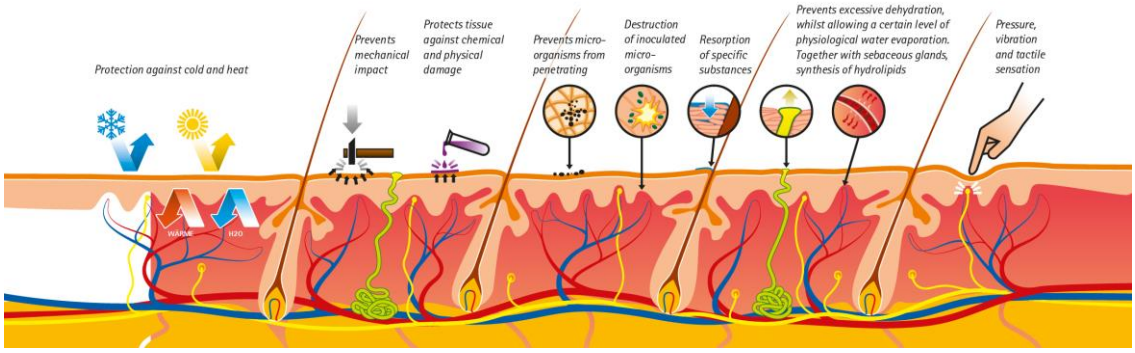

Fig. C The multiple function of skin. This image is a reference image ("What to know about skin," n.d.).

Barrier function: The skin protects the inner organs from mechanically, physically, chemically, and biologically harmful elements derived from the external environment and also prevents the loss of various nutrients, electrolytes, and water from the body (Draelos, 2018; Rawlings and Harding, 2004).

Sensory role: The skin is distributed with sensory and motor nerve endings and special receptors that perceive stimuli and produce various sensations such as touch, cold, temperature, pain, pressure, itch, etc. and elicit the corresponding neural reflexes (Otaka et al., 2019).

Regulation of body temperature: Body temperature is an expression of heat production during the metabolism of substances in the human body and is one of the necessary conditions for various biochemical reactions and physiological activities of cells

(Kodera et al., 2018). The skin is an important component of heat distribution in the body, which can regulate body temperature through skin vasoconstriction, hair erection, and sweat production. It can also distribute heat by radiation, convection, conduction, evaporation and other physical means (Cabanac, 1975).

Absorption: The skin has the ability to absorb external substances through the stratum corneum, hair follicle sebaceous glands and sweat duct openings, called transdermal absorption, or penetration (McCarley and Bunge, 2001), which is indispensable for the maintenance of health and is the theoretical basis of modern dermatological topical medications for the treatment of skin diseases.

Secretion and excretion: The skin has certain secretory and excretory functions, mainly through the secretion of sweat through sweat glands and the excretion of sebum by the sebaceous glands. Sweat functions to cool down body temperature, protecting the skin, excreting drugs, and replacing some of the functions of the kidneys; sebum has the function of forming a lipid film on the skin surface and lubricating the hair and skin (Draelos, 2018).

Immunity: The epidermis and dermis of the skin contain cells that participate in immune regulation, like keratinocytes, Langerhans cells, lymphocytes, and macrophages (Matejuk, 2018). Keratin-forming cells secrete IL-1, IL-2, IL-3, IL-6 and other cytokines, which are involved in the regulation of skin immune function and activate target cells (Williams and Kupper, 1996). Langerhans cells can bind antigens and transmit antigenic information to immunologically active cells to initiate immune responses (Nguyen and Soulika, 2019).

Metabolic effects: The skin, like other tissues and organs of the body, has a common biochemical metabolic process. When the body's metabolism is affected, it also affects the normal metabolism of the skin, which can lead to cosmetic skin disorders. Conversely, when the metabolism of the skin is impaired, it can also affect the metabolism of the entire body. For example, 7-deoxycholesterol in the epidermis synthesizes vitamin D3 after UV exposure, and when this metabolic process is faulty, it affects the body's absorption of calcium, leading to chondromalacia(Pondeljak and Lugović-Mihić, 2020).

1.2 Skin wound healing phases

Skin wound healing progresses by peri-wound resident cells, and it can be classified into three critical phases: the inflammatory phase, the proliferative phase, and the scar formation and remodeling phase. (Wang et al., 2018). Refer to **Figure D**.

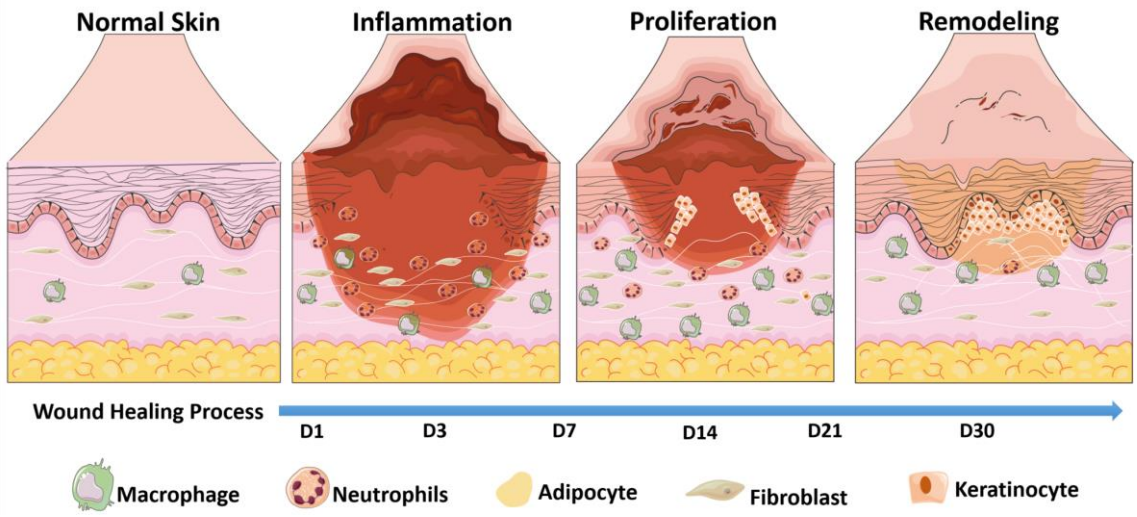

Fig. D The key phases of wound healing

1.2.1 Inflammatory phase

The wound enters the inflammatory phase once it has formed. First, cells in the injured tissue release reactive substances that cause vasoconstriction to prevent further bleeding, while fibrinogen forms an insoluble fibrin network, platelets, granulocytes and lymphocytes form a blood clot to occlude the ruptured vessel and a protection film is formed over the wound to prevent further contamination by pathogens. Immune cells surrounding the injury secrete various inflammatory mediators like TNF, IL and several other cellular factors and growth factors, which together with modulatory signaling promote the progression of the wound healing phase.(Eming et al., 2007).

1.2.2 Proliferative phase

During the proliferative phase, endothelial cells in the vascular wall break the basement membrane and move toward the middle of the wound bed, where these cells divide to form vascular sprouts, which interconnect to form new vessel pathways and then further vascular networks and granulation tissue. The transition of wound healing from the

phase of inflammation to the vascularized granulation phase is achieved by the combined action of various growth factors and cytokines, such as fibroblast growth factor (FGF), which promotes vascular neogenesis and fibroblast proliferation and division (Yamaguchi et al., 2021); epidermal growth factor (EGF), which promotes vasculogenic, fibroblast migration and proliferation, and enhances collagen deposition, thereby promoting wound healing and the growth of new skin tissue (Sorg et al., 2017).

1.2.3 Repair phase

The third stage of wound healing involves the remodeling of the injured tissue and the eventual growth of new skin after a long-term repair. The transition from the formation of granulation tissue to wound re-epithelialization marks the start of dermal tissue remodelling. During this process, the original disordered extracellular matrix (ECM) made up of type III collagen and elastin is displaced by an orderly ECM made of type I collagen and elastin fibers, remodeling the strength and elasticity of the dermis (Rodero and Khosrotehrani, 2010). Platelet-derived growth factor (PDGF) signaling and its receptors are involved in the morphogenesis of hair follicles ("Acute wound healing in the skin: a comprehensive review - PubMed"), and the combination of various factors, the formation of a new epidermis that covers the wound marks the accomplishment of the injury healing process.

1.2.4 New perspective of skin wound healing

The traditional theory of wound healing suggests that wound ECM is mainly derived from fibroblasts migrating to the wound bed, where they proliferate and differentiate into myofibroblasts, which then produce collagen to deposit ECM de novo (Liu et al., 2020; Monika et al., 2021; Yao et al., 2022; Zhao et al., 2017). Recent findings from our laboratory suggest that the fascial layer in the skin is the dominant factor in establishing wound ECM. Prior to wounding the skin, the subcutaneous fascia was injected with NHS-488 dye to specifically label the ECM of the fascial layer. We then made 5-mm-sized whole-skin wounds on the dorsum of mice, and on day 7 samples, we observed that the majority of the wound bed ECM came from the labelled fascia (**refer to Figure 1-D**), suggesting that the fascia is a repository for wound healing. We further found that this influx of fascia ECM into the wound bed is mediated by En1-positive fibroblasts

residing in the fascia (Correa-Gallegos et al., 2019), and that N-Cadherin promotes collective migration of fascia fibroblasts to carry ECM into wounds and promote wound healing (Jiang et al., 2020). We further found that gap junction α1 protein (Connexin43) is essential for large wound repair, and when inhibited, fascial ECM transport into wounds is reduced (Wan et al., 2021), leading to reduced scar formation and laying the foundation for clinical treatment of scarless healing.

1.3 Skin fibroblasts-background and characteristics

1.3.1 Source and classification of skin fibroblasts

Fibroblasts originate from mesenchymal cells in the embryonic mesoderm and neural crest and are the main cellular components of connective tissue (Strutz et al., 1995). Typically, the number of fibroblasts in dense connective tissue is greater than the number of fibroblasts in the same volume of loose connective tissue, which is why fibroblasts are mainly isolated and cultured from dense connective tissue such as the dermis. There are at least two types of fibroblasts in the skin: fibroblasts in the upper layer of connective tissue, which can form skin hair follicles, and fibroblasts in the lower layer of connective tissue, which can form skin collagen fibers (Driskell et al., 2013; Jiang and Rinkevich, 2021a; Stunova and Vistejnova, 2018). In addition, embryonic stem cells differentiate into fibroblasts, through mesenchymal stages.

1.3.2 Biological morphology and characteristics of skin fibroblasts

Fibroblasts are one of the most common cells in loose connective tissue, located near and attached to collagen fibers (Bainbridge, 2013; Bartos, 1970). The morphological structure of this cell can vary according to its functional state. When the functional activity is high, fibroblasts have large, flat star-shaped cell bodies with protrusions. The nucleus is oval in shape, with prominent nucleoli and less chromatin and lighter staining. The cytoplasm is mostly weakly basic and contains abundant structures such as rough endoplasmic reticulum, ribosomes, Golgi complexes, microfilaments and microtubules, indicating that such cells have the ability to synthesize and secrete collagen, elastin and polysaccharides. proteins that form collagen fibers, elastic fibers, reticular fibers, and matrix (Stunova and Vistejnova, 2018). Fibroblasts in healthy conditions are

relatively quiescent or functionally dormant cells (Sorrell and Caplan, 2004). However, in some conditions, like wound repair, inflammation and regeneration of connective tissue, fibroblasts can be converted into functionally active myofibroblasts that actively participate in protein synthesis and secretion, forming fibers and matrix in situ. (Thulabandu et al., 2018).

1.4 Aging of skin fibroblasts and their microenvironment

The skin, as the largest organ of the body, and with ageing, degenerative changes such as structural atrophy and functional decline or loss of function inevitably occurs (Khavkin and Ellis, 2011). Aged skin exhibits dry and rough epidermis, skin laxity, increased and deepened wrinkles, lack of elasticity, and skin pigmentation. The underlying mechanism of skin ageing (Krutmann et al., 2021; Uyar et al., 2020), is associated with its resident fibroblast. Yet mechanistically, skin ageing by fibroblasts is incompletely understood (Campisi, 1998; Zorina et al., 2022).

The fibroblasts are the major structural component of the dermis and can synthesize and secrete extracellular matrix such as collagen fibers, elastic fibers, reticular fibers, and hyaluronic acid (Wong et al., 2016). ECM secretion constitutes the microenvironment in which skin fibroblasts survive (Figure C), as well as help maintain skin strength and elasticity, and repair following damage (Kanitakis, 2002). It is a decisive component in maintaining the youthful state of the skin and is an important part of maintaining the structural stability of the skin. Once the skin collagen system is established, it has a life cycle of 10-15 years. As people age, the number of fibroblasts decreases and the corresponding substances, such as collagen, elastin and hyaluronic acid, will decrease and will not be sufficient to support skin structure (Choi, 2019; Kanitakis, 2002; Khavkin and Ellis, 2011). Consequently, the connective tissue layers become thinner and the skin begins to sag, lose elasticity, and develop wrinkles. Replenishing fibroblasts can address the root cause of skin aging and damage, by allowing skin to regenerate its ECM.

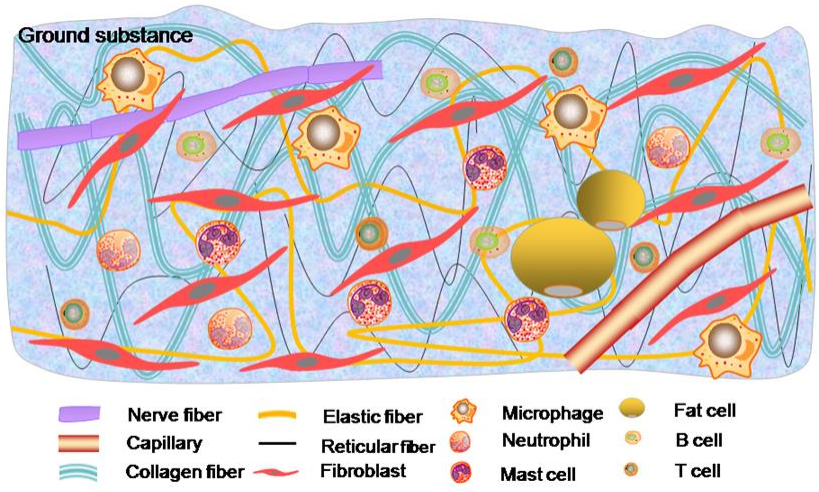

Fig. C The microenvironment of skin fibrobl

2. Material and Methods

2.1 Mice and genotyping

All the mouse strains (C57BL/6J, PDPNCreER x TM4, PDPNCreER x DTA, En1tm2(cre)Wrst/J (En1Cre) and Fox Chase SCID) were obtain from Charles River or Jackson laboratories. Animals are housed in the Helmholtz Central Animal Facility, where cages have air circulation systems and are maintained at constant temperature and humidity, with a 12-hour light cycle, and provided with adequate water and food. All experiments on animals were examined and authorized by the Upper Bavarian State Government and enrolled according to programs 55.2-1-54-2532-16-61 and 55.2-2532-02-19-23 as well as stringent governmental and international guidelines. This study meets all relevant ethics rules for animal research. Young mice 8 to 10 weeks old and older mice 20 to 24 months old were used for animal experiments. Use male and female mice. Cre-positive (Cre+) animals originating from double genetically modified reporter mice were determined by detecting the associated fluorescence in the dorsal dermis. Genomic DNA was extracted from the ears using Quick Extract DNA Extraction Solution according to the instructions.DNA extract (1 µl) was added to each 19 µl PCR. The reaction mixture was set up using GoTaq PCR core kit (Promega) containing 1× GoTaq green master mix, 0.5 µM forward primer 'Procr_Cre_genotype_FW' 5′- GCG GTC TGG CAG TAA AAA CTA TC -3′ (Sigma) and 0.5 µM reverse primer 'Procr_Cre_genotype_RV 5′- GTG AAA CAG CAT TGC TGT CAC TT - 3′ (Sigma). PCRs were performed with initial denaturation for 5 min at 94 °C, amplification for 35 cycles (denaturation for 30 s at 94 °C, hybridization for 30 s at 59 °C, and elongation for 1min at 72 °C) and final elongation for 10 min at 72 °C, and then cooled to 4 °C. PDPNCreER mouse line is homozygous, thus do not need genotyping. In every experiment, negative controls (non-template and extraction) and positive controls were included. The reactions were carried out in an Eppendorf master cycler. Reactions were analyzed by gel electrophoresis.

2.2 Human samples

Skin tissue was obtained in the Klinikum rechts der Isar, and processed in two parts. Skin tissue with underlying fascia tissue was used in in vitro suspension culture. Cul-

ture methods and medium for human skin are the same as those for murine skin. The culture period needs to be extended to about 14-18 days. If skin tissue was obtained without fascial tissue, or if skin wounds or keloids were obtained, these were fixed sectioned and stained.

2.3 Ex-vivo Fascia floating culture

To visualize the contraction rate of the fascia, whole back skin was extracted from the respective mouse line after euthanasia. Back skin of the mouse was first shaved using an animal hair trimmer and then wiped clean using any hair removal cream. The whole back skin was then harvested using scissors and forceps taking care that the fascia remained intact. The sample was then washed twice in ice-cold DPBS, making sure to remove any residual hair fragments from the tissue. The entire dorsal skin was then removed with scissors and forceps, and the fascial layer of the skin was then specifically separated and cut into rice-sized pieces in DPBS. The skin was then placed in a 6-well plate ready for culture, which was supplemented with 3 ml of DMEM/F-12 medium containing 10% FBS, 1x GlutaMAX, 1x MEM non-essential amino acids and 1x Penicillin/Streptomycin. the medium was changed every other day DMSO was used as a control group and other treatment groups were added with yes concentrations of chemicals. After the start of the experiment, samples were maintained in a humidified incubator at 37°C with 5% CO2 for 7 days and then fixed overnight with 2% PFA refrigerated, followed by histological treatment.

2.4 3D Matrigel Culture of Fascia

The Matrigel was taken out of the -20° freezer in advance and slowly dissolved on ice. Then, the full-thickness skin of the mouse was isolated and placed in cold PBS. Several fascial tissues of similar size were processed with scissors and forceps. Then add 150μl of the prepared Matrigel to the middle of the 35 mm Petri dish, and then quickly embed the prepared fascia into the middle of the Matrigel. Then, the culture dish was gently transferred to the incubator for 1 hour, and after the matrigel solidified, 3ml of complete medium was added to continue the culture. The samples were photographed once a day, the medium was replaced in every alternate day and samples were collected for fixation and staining after 6 days of culture.

2.5 Fascial Ablation Experiment

2-month-old C57BL/6J mice were selected, and the fascia layer was marked with NHS-488 in advance. Two full-thickness excisional wounds were then made on the back using a 5 mm punch. The control group received no additional treatment, and the experimental group used ophthalmic scissors to remove the fascia tissue on the wound bed and wound edge after the wound was done. Samples were collected on the seventh day after wounding for fixed sectioning and staining.

2.6 Fascial cell clearance experiment

The dorsal skin of the mouse was taken according to the conventional method, and the fascia tissue of similar size was separated with scissors and forceps. The isolated fascial tissue was then freeze-thawed several times at -80° to kill all cells in the fascial tissue. The fascial tissue that has been cleared of cells can be further subjected to 3D Matrigel culture, in vitro suspension culture experiments and cell transplantation experiments.

2.7 Re-transplantation of cells into decellularized fascia

Decellularized fascial tissue was obtained by repeated freezing and thawing at -80°, and then these tissues were placed in trans-wells for culture. The positive control group was normal fascial tissue, the control group was decellularized fascial tissue, and the treatment group was transplanted with different cells into decellularized fascial tissue. Prepare the cell suspension to be transplanted in advance, and then inject 50 microliters (about $5*10^4$ cells) of the cell suspension into the center of the fascia. Add an appropriate amount of medium to the bottom of the trans-well, and then put the entire culture dish into the incubator to continue culturing. After culturing for two hours, 100μl was added to the trans-well to continue culturing. Photographs were taken two days after culture to analyse the contraction of the fascia.

2.8 Type I Collagen Contraction Assay

The type I collagen from rat tail was dissolved on ice, and then diluted in half with medium. The control group was the no-cell group, the experimental group was added with $1x10^5$ cells and mixed in the gel, and the negative control group was added with cells. in Matrigel. The culture plate was then placed in an incubator for half an hour. After the

type I collagen and Matrigel were solidified, the culture medium was added to continue the culture. Photographs were taken after one day of culture to observe the contractile ability of different cells.

2.9 Live and 3D imaging of fascia

In order to monitor the shrinkage trend of the fascia, we cultured the fascia of En1XTM4 mice using a Matrigel 3D culture model and used the Thunder microscope in vivo culture system to take pictures in real time, taking pictures every ten minutes, and taking pictures continuously for 12-16 hours. To examine cell morphology after fascial culture, we collected Matrigel-cultured samples for fixation and then imaged using two-photon microscopy. To monitor cell migration in fascial tissue, we cultured the En1XTM4 mouse fascia using a Matrigel 3D culture model and took real-time photographs using a T two-photon microscope in vivo culture system. Imaris was used for analysis and video production after all the above experimental imaging was completed.

2.10 Recombinant Chimeric Transplantation Experiment

We collected full-thickness skin from 20-month-old TM4 mice and 2-month-old VT2GK3 mice, and then isolated the fascia layer and epidermis-dermis layer, respectively, and then the fascia layer of these two groups of young and aged mice and the epidermis-dermis exchange reorganization. Simply put, it is the combination of the epidermis-dermis layer of VT2GK3 mice and the fascia layer of TM4 mice, and the combination of the epidermis-dermis layer of TM4 mice and the fascia layer of VT2GK3 mice. After the combination was completed, new explants were formed, and then we used a 2 mm punch to make a small wound in the middle of the combined explants, and then transplanted the wounded explants into immunodeficient mice. Fourteen days after transplantation, samples were collected, fixed, sectioned and stained.

2.11 Lineage tracing experiment in skin wounds

8-week-old PDPNCreER x TM4 mice were selected and injected with 1mg tamoxifen per mouse per day 3 days in advance before wounding. Pacific Blue dye at 2mg/mL (prepared with 0.1M sodium bicarbonate in normal saline) was injected four days prior and two days prior to wounding to label the fascial layer. The experiment was divided into two groups, the treatment group was injected subcutaneously with 50mg/mL of EQM and the control group was injected subcutaneously with 50mg/mL of DMSO.

Samples were collected on day 3 and day 7 after wounding and subsequently fixed, frozen sections, immunofluorescence stained and photographed.

2.12 Excisional wounds on the dorsal skin of mice

We selected 2-month-old and 20-month-old C57BL/6J mice, labeled the skin and fascia layer with NHS-488 in advance, and then used a 5 mm punch to make two full-thickness skin wounds on the back. Samples were collected on days five, seven, and fourteen, and then fixed, sectioned, and stained. Then in our drug treatment experiment, we selected 20-month-old C57BL/6J mice and divided them into a control group and an experimental group. The fascia was marked in advance by the same method. After the wound was made, the treatment group was treated with 10uM CHIR treatment, the control group was treated with 10uM DMSO, injected every other day, the samples were collected on the third, fifth, seventh, and fourteenth days, and then the samples were fixed, sectioned and stained.

2.13 Masson's Trichrome Staining

Wound and fascia samples were fixed with 2% paraformaldehyde at 4°C for 12 hours. After fixation the samples were rinsed three times with PBS, embedded in OCT and frozen in dry ice. Frozen sections of 6 mm were then made. Masson trichrome staining was performed according to the kit instructions. Sections were placed in acetone at -20°C for 10 minutes and then air dried for 5 minutes. Sections were rinsed in deionized water for 2 min and then heated in Bouin's solution at 56°C for 15 min. Wash slowly in running tap water until the yellow color is removed from the slices, then place in Weigert's iron hematoxylin solution for 3 min, followed by washing in running tap water for 5 min, three times. Place in Bie-brich Scarlet-Acid fuchsin solution for 5 min, then rinse with deionized water. Place in phosphotungstic acid/phosphomolybdic acid solution for 5 min, then incubate in aniline blue solution for 10 min, then place in 1% acetic acid for 2 min, and finally rinse with deionized water for 5 min 3 times. The sections were then dehydrated in 80% ethanol->90% ethanol->100% ethanol for 5 min each and then cleared with Roti-Histol and mounted with Roti-Histokitt.

2.14 Immunofluorescence staining

For immunolabeling, sections are rinsed three times with PBST solution containing 0.05% Tween and closed with 5% donkey serum for 1 hour at room temperature. The primary antibody was then incubated overnight at four degrees. The sections were then rinsed three times with PBST and the secondary antibody was incubated for 60

minutes at room temperature. Finally, the antibody is rinsed three times with PBST and mounted with fluorescent mounting medium containing DAPI. Primary antibodies used: GFP, a-SMA, MOMA-2, PDPN, Phospho- Stat3, and RUNX2. For Phospho-Stat3, and RUNX2 antibodies, antigen repair is required prior to staining.

2.15 Microscopy

Ex vivo fascia tissues were imaged every 24hr from the start of the experiment until the end to record the contraction pattern of the tissue under control and treatment conditions. Whole-mount bright-field images were taken with a Leica M50 stereo-microscope (Leica) with a Leica DFC310 FX camera (Leica) and saved with Leica Application Suite (v4.8). Histological sections were imaged using a using a ZEISS AxioImager.Z2m (Carl Zeiss) and thunder.

2.16 Image analysis and Statistics

Images were processed and analysed with ImageJ (version 1. 52e). Statistical analyses were performed using GraphPad Prism software (v.9.2). Statistical significance was assessed by Student's t-test to compare two groups or one-way ANOVA with Tukey's multiple comparisons. Significant differences were considered with p-values below 0.05.

3. Results

3.1 Fibroblast-mediated contraction of fascia leads to wound closure

3.1.1 The contraction of the fascia leads to the closure of a full-thickness skin wound

To clearly track the dynamic changes of the fascia after injury, we used 10mg/ml NHS-PCB to pre-label the fascia layer, and then made two 5mm full-thickness excisional wounds on the back of the mice, and then at different times Points (D1, D3, D5, D7) are collected, and the specific method is shown in Figure 1-A. First, in order to verify the role of the fascia layer in wound healing, we used the excisional mouse wound model wherein two 5 mm full-thickness excisional wounds are made on the back of 2-month-old En1Cre-mTmG mice, while the control group was left untreated. In the treatment group, the residual fascia around the wound was carefully removed with ophthalmic scissors after the wound was punched, and the skin was photographed on the 1st, 3rd, and 5th day after the wound was punched. 1-B), it can be seen from the statistical chart that after the fascia is removed, the rate of wound closure is greatly delayed (Fig. 1-C). Histologically, in the uninjured group, the fascial layer was specifically labelled by NHS-PCB, and was very stable. After injury, marked fascia transferred into the wound, but in the treatment group, marked fascia entering the wound was greatly reduced if the peri-wound and wound bed regions (Fig. 1-D). After the fascia was removed, the width of the open wound increased, with reduced scar (Fig. 1-E).

A

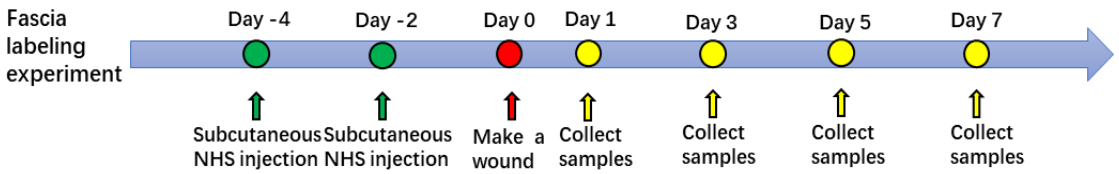

B

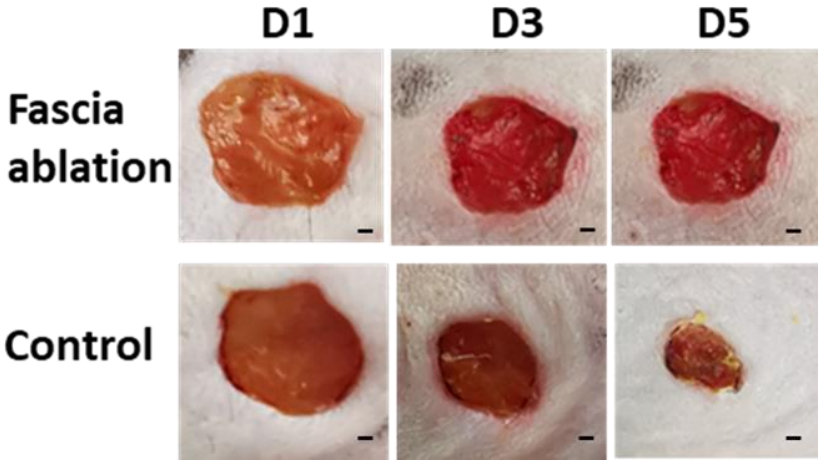
D1
D3
D5
Fascia ablation
Control

C

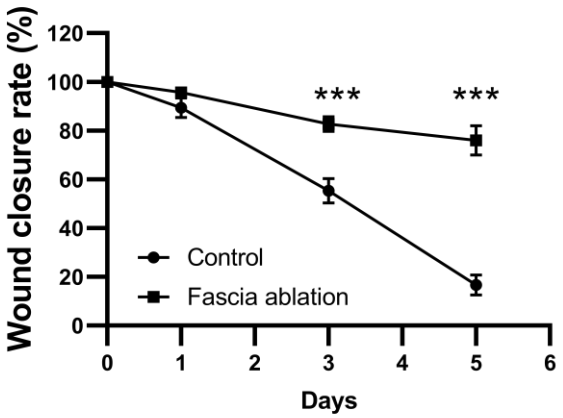
Wound closure rate (%)
120
100
80
60
40
20
0
***
***
Control
Fascia ablation
0
1
2
3
4
5
6
Days

D

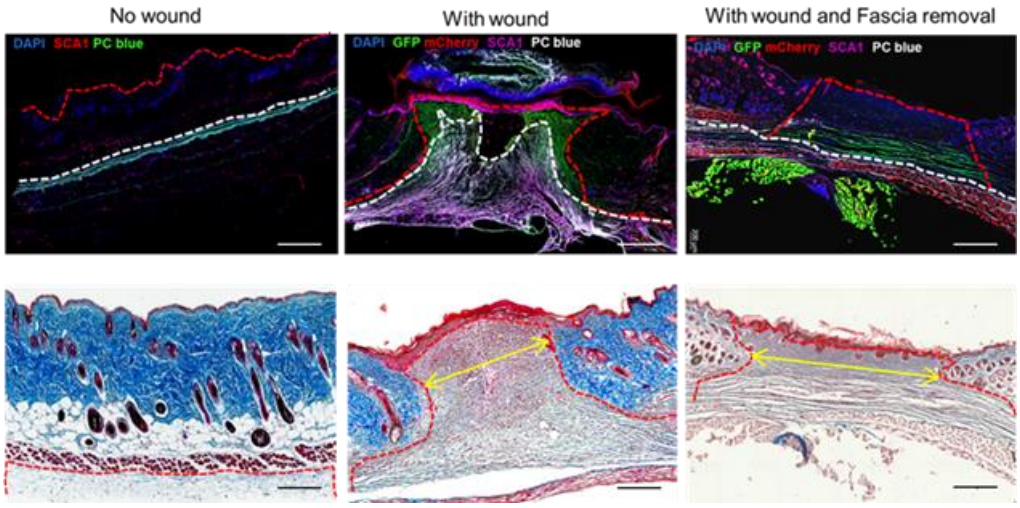
No wound
With wound
With wound and Fascia removal
DAPI SCA1 PC blue
DAPI GFP mCherry SCA1 PC blue
GFP mCherry SCA1 PC blue

E

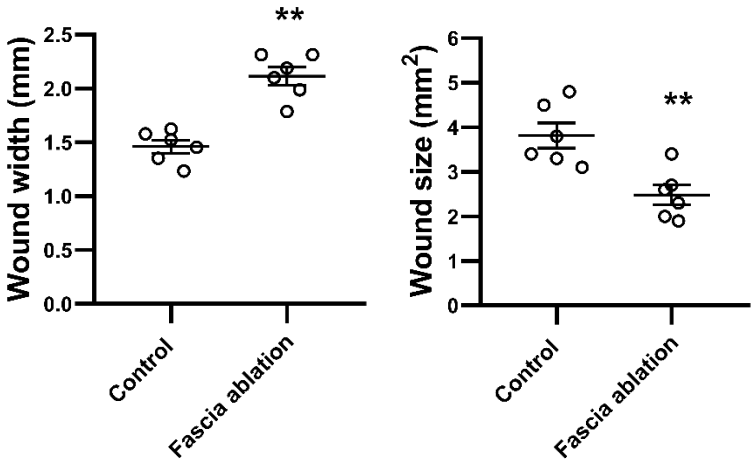

Fig.1 The contraction of the fascia leads to the closure of a full thickness skin wound.

(A) Fascia labelling experiment. **(B)** The graph of wound size change in control and the fascia removal treatment groups. **(C)** Quantitative analysis of wound width and wound area in control and treatment groups. **(D)** Using the fascia marker model, the control group made a normal skin full-thickness wound, and the treatment group continued to remove the fascia tissue from the wound edge and wound bed after making the skin full-thickness wound, scale bars: 500μm. **(E)** Quantitative analysis of wound width and wound area in control and treatment groups. Mean ± SEM, n = 6. All p-values (p) indicated were obtained from two-tailed T-tests, **p < 0.01. Scale bars = 500 μm

3.1.2 The contraction of fascia is centripetal

In normal skin, fascia is immobile. When there is a wound, the fascia contracts concen-
A
trically toward the center of the wound, which results in rapid wound closure. As seen in Figure 2-A-B, the NHS488-labeled fascia moves from the wound edge toward the wound center, and the residual fascia in the wound bed moves upward, creating a centripetal movement toward the wound center. A similar phenomenon was observed in in vitro fascial culture experiments, where the fascia tissue continuously contracted toward the center and formed scar-like tissue during the culture process (Figure 2-C).

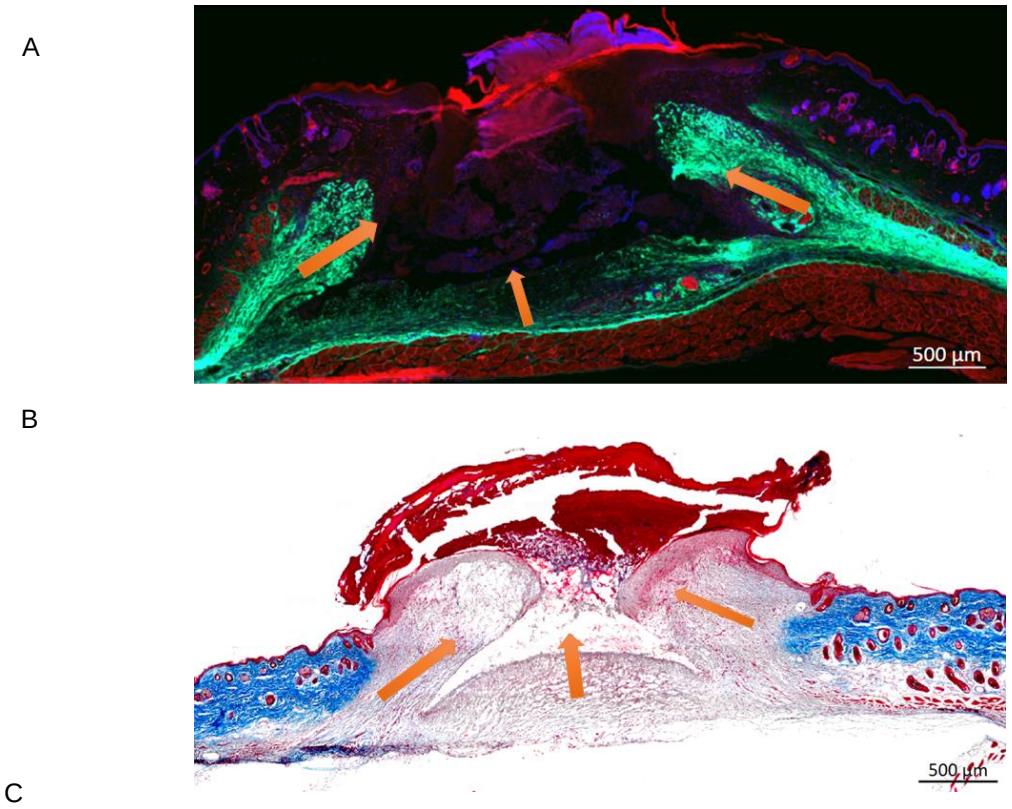

Fig.2 The contraction of fascia is centripetal

(**A**) Fluorescence images of wounds on day 5 of fascia labelling experiment, nuclei (blue), labelled fascia (green), and mouse background colour (red). (**B**) Masson's trichrome stain of wound on day 5 in the fascia labelling experiment. (**C**) Bright field images and cartoon of fascia on day 0 and day 6 in in vitro floating culture. Scale bars: 500 μm.

3.1.3 The contraction of fascia is dependent on fibroblasts

As shown in Figure 3-A-B, in our skin in vitro floating culture system, after six days of culture, we observed that the first group (full-thickness skin with fascia) shrank, and the second group (full-thickness skin without fascia) lacked any shrinkage. The third group (PC muscle) does not shrink, and the fourth group (fascia tissue alone) shrank rapidly.

A

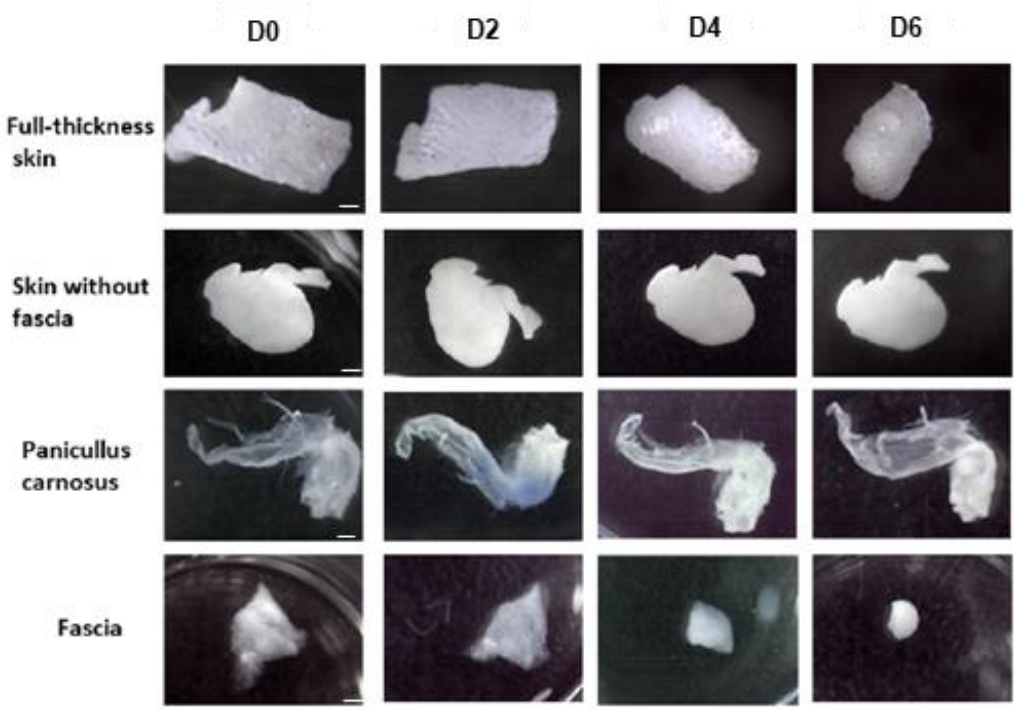

B

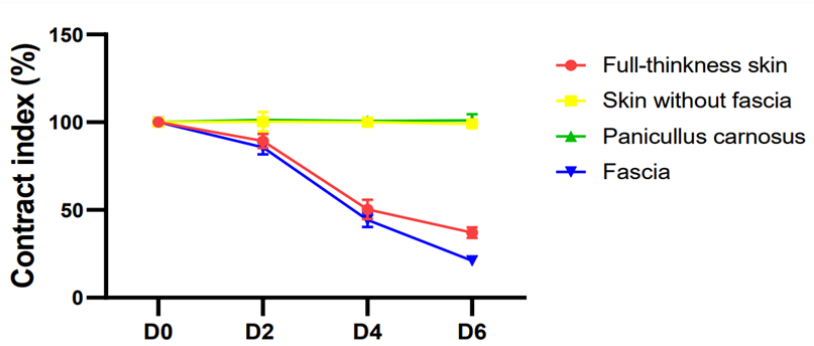

Fig. 3 In vitro suspension culture of different parts of skin tissue

(**A**) Variation trend of in vitro suspension culture of different parts of the skin, (**B**) Quantitative analysis of the shrinkage rate of different skin tissues during in vitro suspension

culture. Mean ± SEM, n = 4. All p-values (p) indicated were obtained from two-tailed T-tests. Scale bars: 500 μm.

We developed another 3D Matrigel culture system to understand fascia cell dynamics. The exact procedure is shown in Figure 4-A. As can be seen in Figure 4-B, the fascia slowly contracted as it was cultured, and then after 36 hours fibroblasts began to migrate out of the fascia. We then used repeated freeze-thawing at -80° to deplete cells from the fascia, followed by 3D incubation. We found that the fascia neither contracted nor migrated out without cells (Figure 4-C). Figure 4-D shows the results of the fascia floating culture model. We found that the fascia did not contract after cell removal compared to control groups. After decellularization of the fascia, we transplanted fibroblasts, neutrophils and macrophages into cell-depleted fascia tissue, respectively, and found that the contractility of the fascia could be restored again after transplantation of fibroblasts, whereas the fascia could not contract after transplantation of neutrophils or macrophages. Figure 4-E shows another in vitro model where we see that only the addition of fibroblasts can cause contraction of type I collagen, while the addition of neutrophils and/or macrophages cannot cause contraction of type I collagen.

A

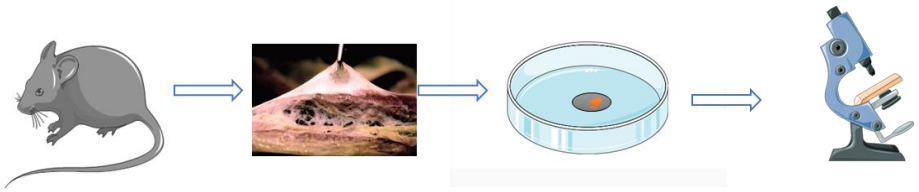

B

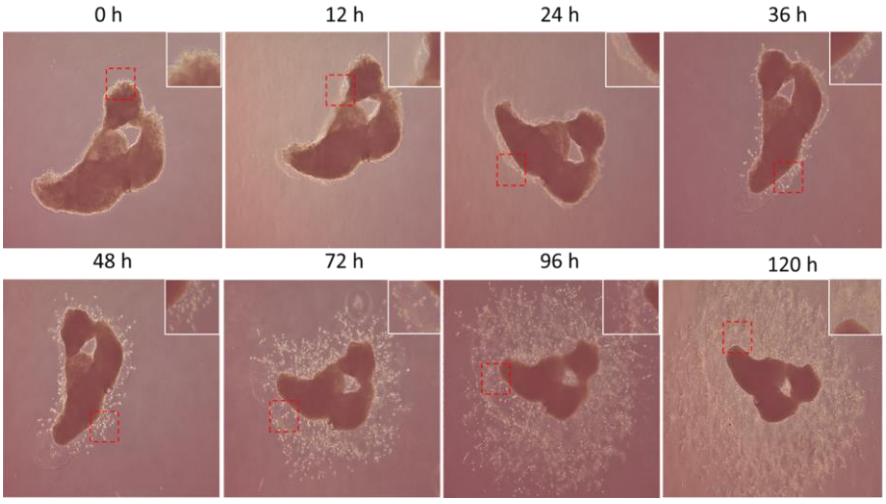

C

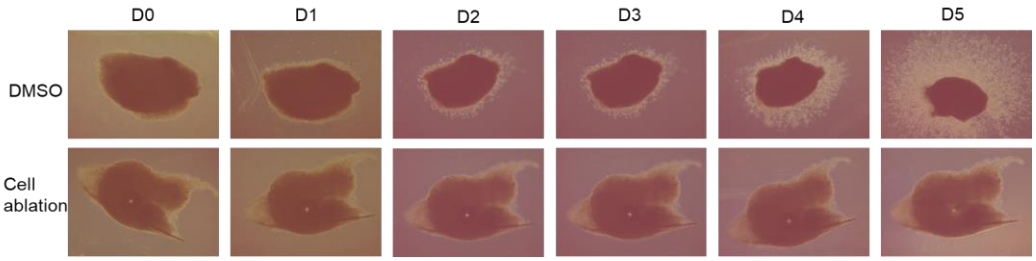
D0
D1
D2
D3
D4
D5
DMSO
Cell ablation

D

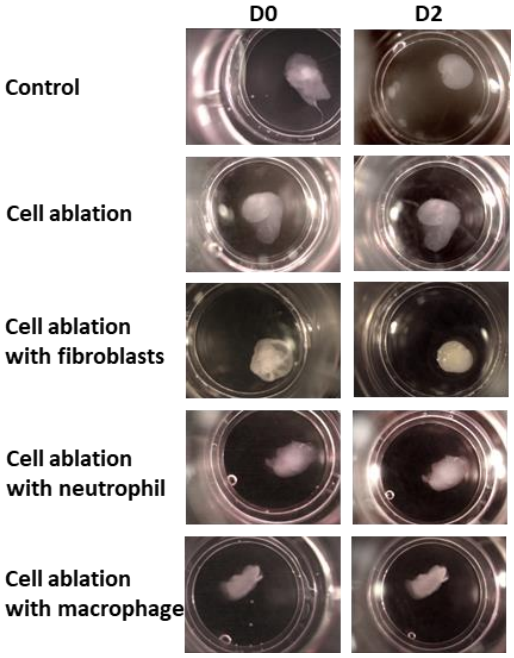
D0
D2
Control
Cell ablation
Cell ablation with fibroblasts
Cell ablation with neutrophil
Cell ablation with macrophage

E

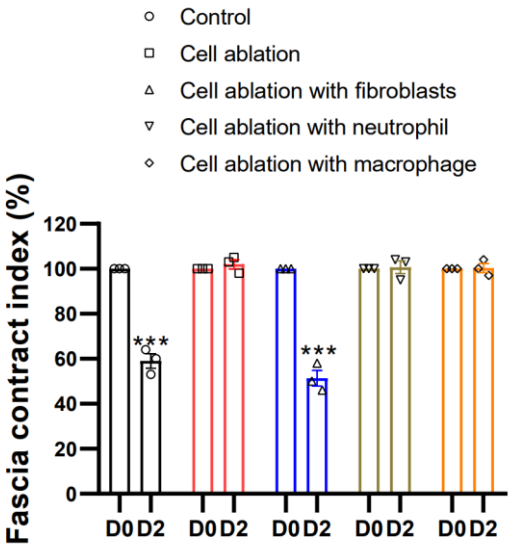
Control
Cell ablation
Cell ablation with fibroblasts
Cell ablation with neutrophil
Cell ablation with macrophage
Fascia contract index (%)
120
100
80
60
40
20
0
***
***
D0 D2
D0 D2
D0 D2
D0 D2
D0 D2

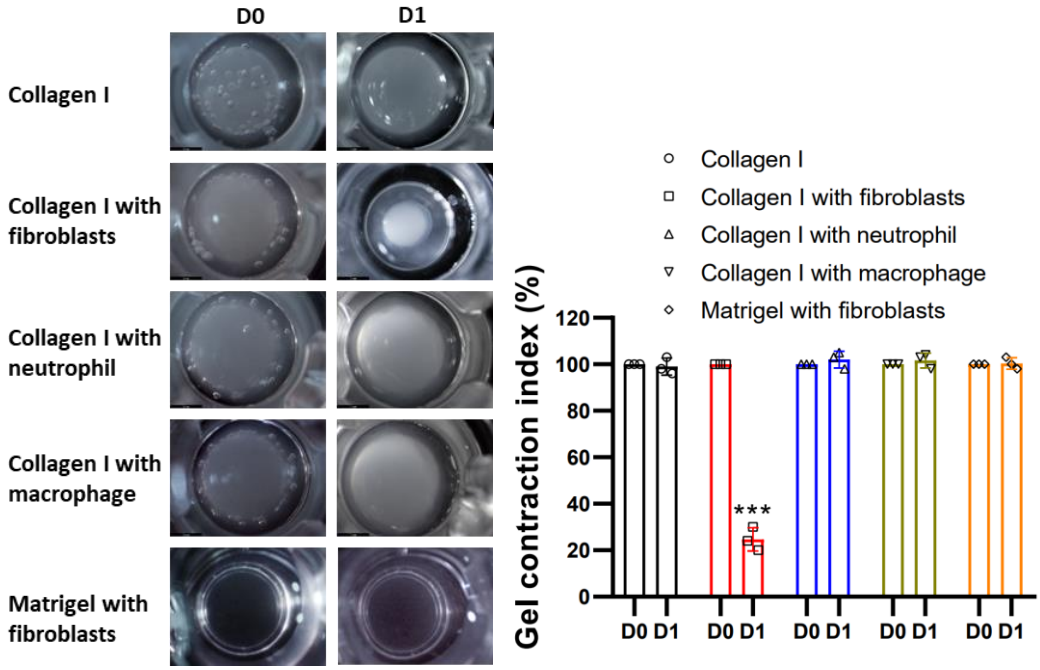

Fig. 4 The contraction of fascia is solely dependent on fibroblasts

(**A**) Schematic diagram of the fascia 3D matrigel culture. (**B**) Dynamic image of 3D Matrigel culture of fascia from 0 hr to 120 hr. (**C**) Dynamic image of fascia cultured in Matrigel after decellularization. (**D**) On the left, cells were transplanted into the fascia for suspension culture after decellularization of the fascia, and on the right was the quantitative analysis of the contraction rate of the cultured fascia. (**E**) On the left is the experiment of transplanting cells into type I collagen and Matrigel, and on the right is the quantitative analysis of the shrinkage rate of the corresponding glue after one day of culture. Mean ± SEM, n = 3. All p-values (p) indicated were obtained from two-tailed T-tests.

3.2 Fascial fibroblasts undergo differentiation to contract fascia connective tissue

3.2.1 After skin injury, mouse fascia fibroblasts undergo different stages of differentiation and cause fascia contraction

From our previous single-cell sequencing results (Figure 5-A), we found that fascia fibroblasts in the skin undergo a graduated differentiation process after injury, from a naïve fibroblast state to proinflammatory fibroblasts, then into promyofibroblasts and finally to myofibroblasts. Different stages of fascia fibroblast differentiation express dif-

ferent markers. For example, pro-inflammatory fibroblasts, express PDPN, proto-myofibroblasts express Pstat3, and myofibroblasts express Runx2. The complete differentiation trajectory of fascia fibroblasts after injury is shown in Figure 5-B. We then examined the expression of the above-mentioned genes related to the differentiation stages of fascia fibroblasts at different time points using immunofluorescence staining in both in vitro and in vivo models, respectively. As shown in Figure 5-C, in the in vitro model, in normal fascia at day 0, only PDPN was expressed in lymphatic vessels and a-SMA was expressed in vascular smooth muscle. PDPN, pSTAT3, a-SMA and Runx2 were not expressed in fascia fibroblasts. Fascia then began to express PDPN on the first day after culture, peaking on the third day, and then expression began to decline, with nearly all fibroblasts no longer expressing PDPN after the sixth day. pSTAT3 then began to be expressed around the second day after culture, peaking on the fourth and fifth days, and a-SMA and Runx2 began to be expressed on the third day, peaking on the sixth day. Then in the in vivo experiments, the expression of PDPN, pSTAT3, a-SMA and Runx2 was consistent with in vitro and also underwent fibroblast differentiation (Figure 5-D).

A

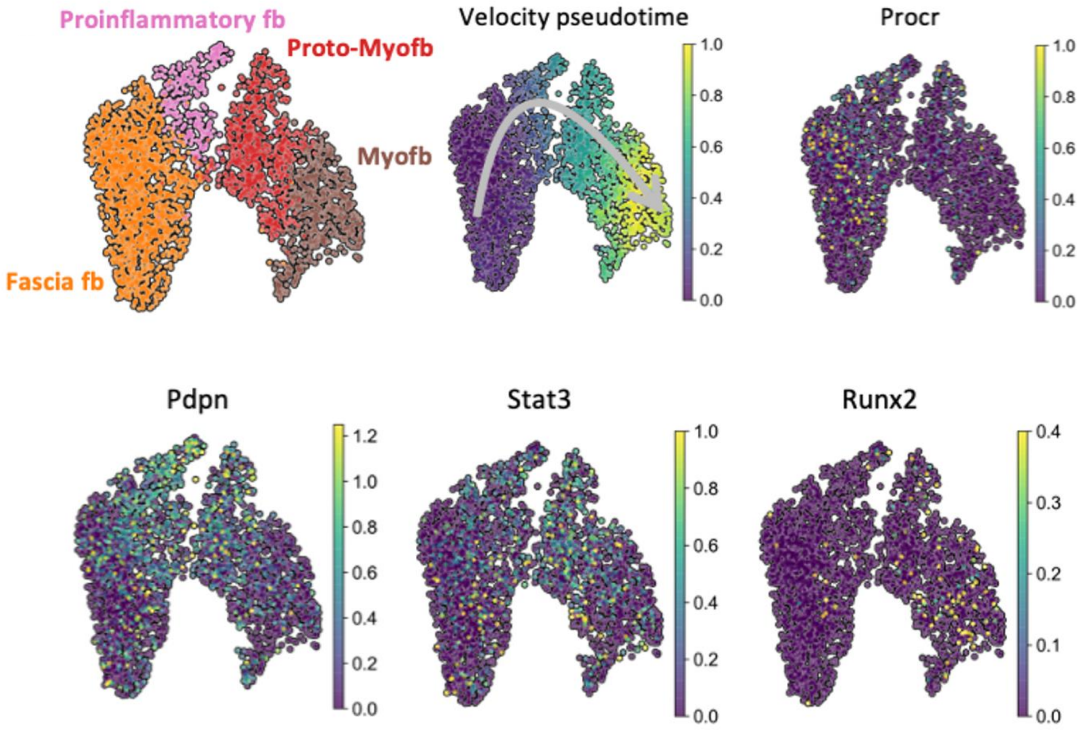

B

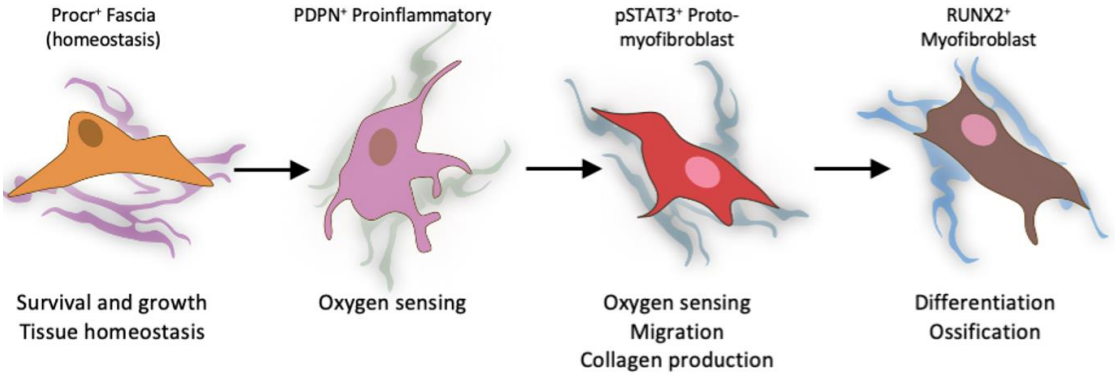
Procr+ Fascia (homeostasis)
PDPN+ Proinflammatory
pSTAT3+ Proto-myofibroblast
RUNX2+ Myofibroblast
Survival and growth
Tissue homeostasis
Oxygen sensing
Oxygen sensing
Migration
Collagen production
Differentiation
Ossification

C

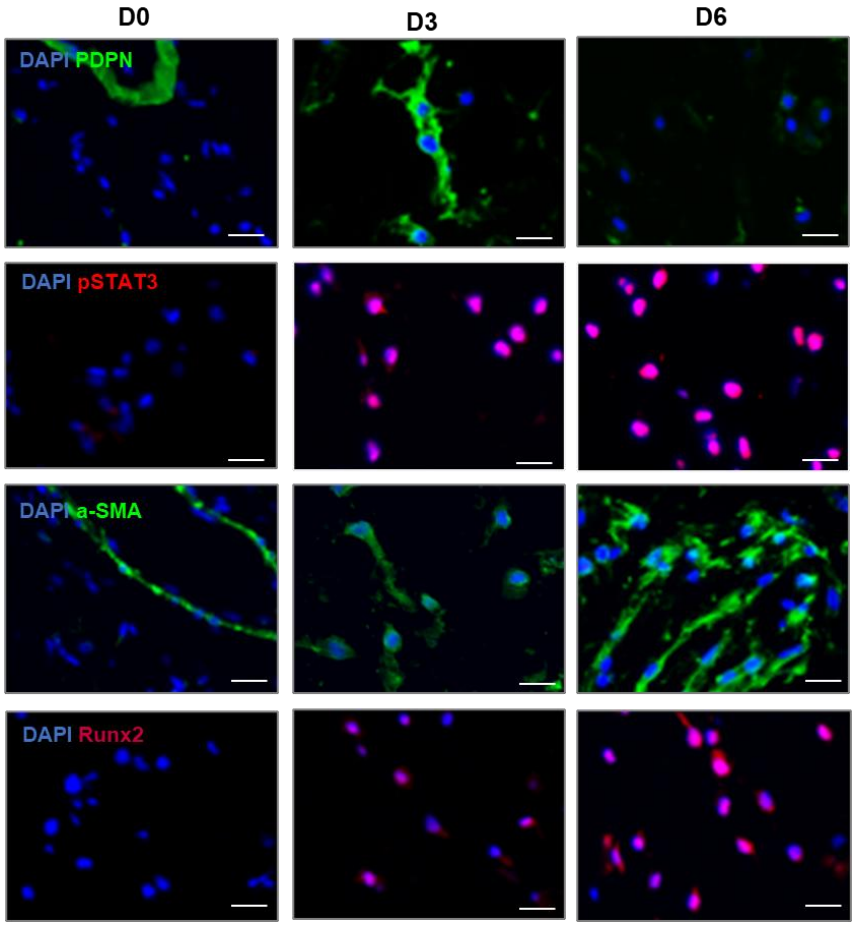
D0
D3
D6
DAPI PDPN
DAPI pSTAT3
DAPI a-SMA
DAPI Runx2

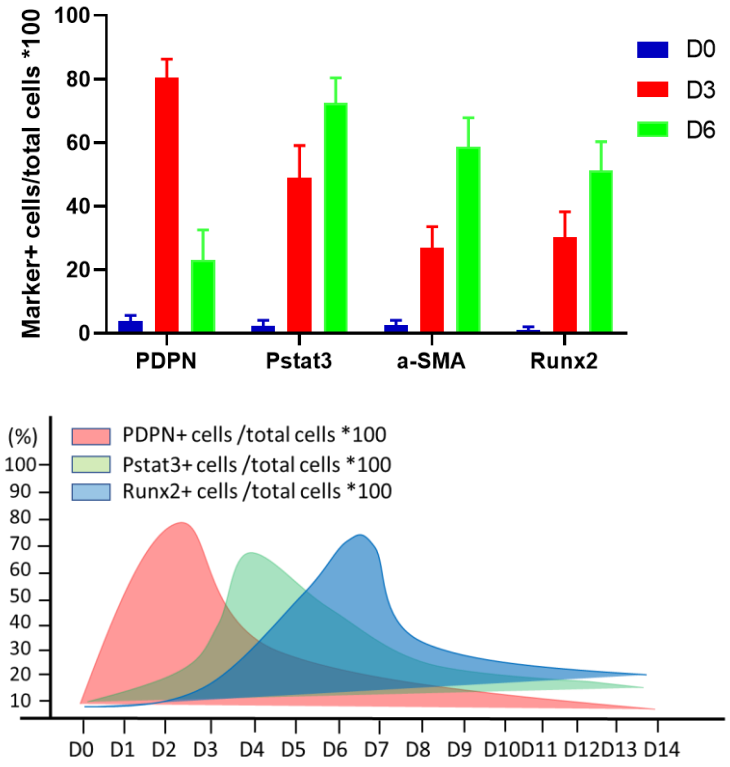
Marker+ cells/total cells *100
100
80
60
40
20
0
D0
D3
D6
PDPN
Pstat3
a-SMA
Runx2
(%)
PDPN+ cells /total cells *100
Pstat3+ cells /total cells *100
Runx2+ cells /total cells *100
100
90
80
70
60
50
40
30
20
10
D0 D1 D2 D3 D4 D5 D6 D7 D8 D9 D10 D11 D12 D13 D14

D

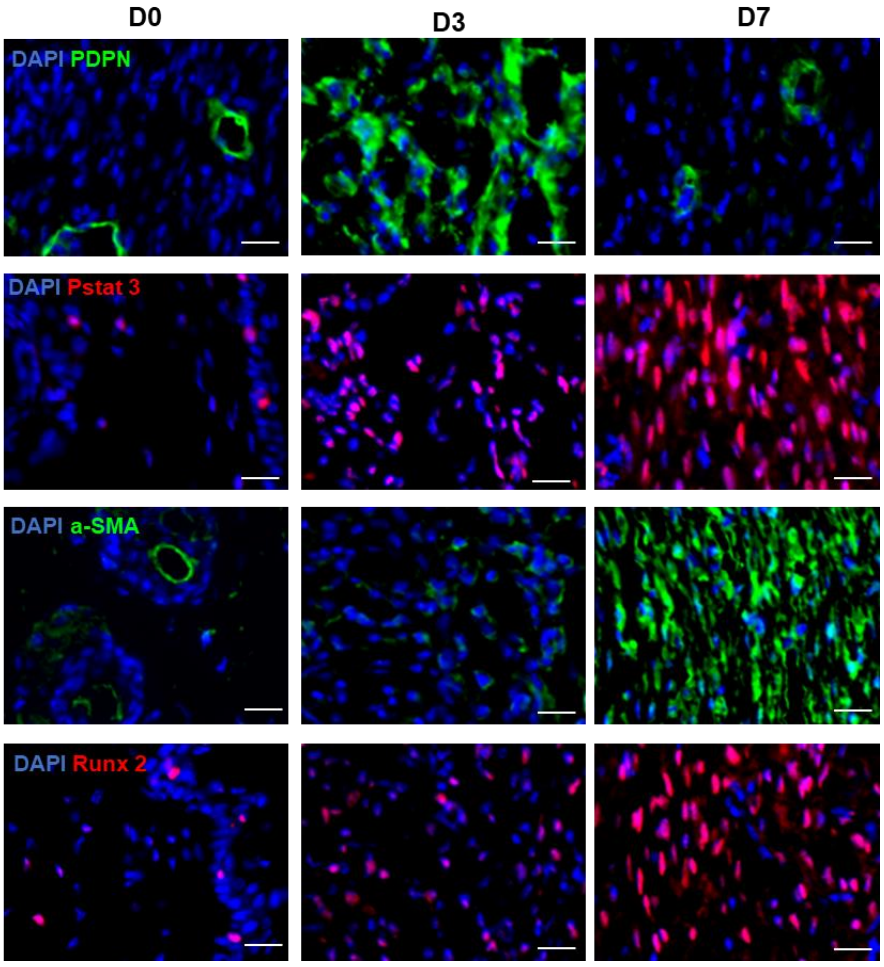
D0
D3
D7
DAPI PDPN
DAPI Pstat 3
DAPI a-SMA
DAPI Runx 2

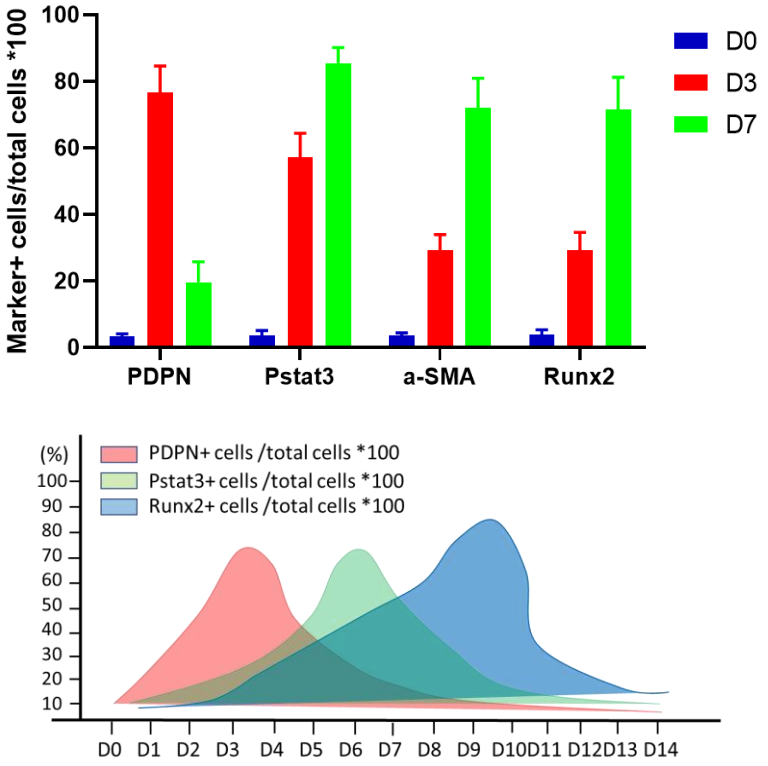

Fig.5 Differentiation trajectory of fascia fibroblasts after injury

(**A**) UMAP representations of fibroblast cells color-coded for individual clusters (left), velocity pseudotime score, and expression of defined markers (right). (**B**) Schematics of the fibroblastic states along the fascia-to-myofibroblast differentiation trajectory and their function revealed from scRNAseq analysis (reference Donovan). (**C**) Immunofluorescence staining of in vitro fascia cultured tissue, there are three groups of D0, D3 and D6, each group was stained with PDPN, pSTAT3, a-SMA and Runx2 respectively. Then, quantitative analysis of the expression of different genes in the three groups of fascia tissue was carried out. Finally, the time-expression correlation diagram of PDPN, pSTAT3 and Runx2 in fascia cultured in vitro. (**D**) Immunofluorescence staining of wounds in vivo, there are three groups of D0, D3 and D7, each group was stained with PDPN, pSTAT3, a-SMA and Runx2 respectively. Then, quantitative analysis of the expression of different genes in the three groups of wounds was carried out. Finally, the time-expression correlation diagram of PDPN, pSTAT3 and Runx2 in wounds in vivo. All p-values (p) indicated were obtained from two-tailed T-tests. Scale bars = 20 μm

3.2.2 Human fascia fibroblast differentiation phenocopies is similar to that of mouse fascia

A general view of human ventral skin tissue is shown in Figure 6-A. The fascia is seen as white transparent layer of connective tissue at the base of the fat layer. Human fascia cultures (Figure 6-B-C) showed that the dermal tissue barely contracted in culture. whereas the fascia tissue contracted similarly to mouse fascia tissue. Immunofluorescence staining shows that fibroblast differentiation also occurs in human fascia tissue during culture (shown in Figure 6-D), mimicking mouse fascia fibroblast differentiation, but with a longer differentiation tempo.

A

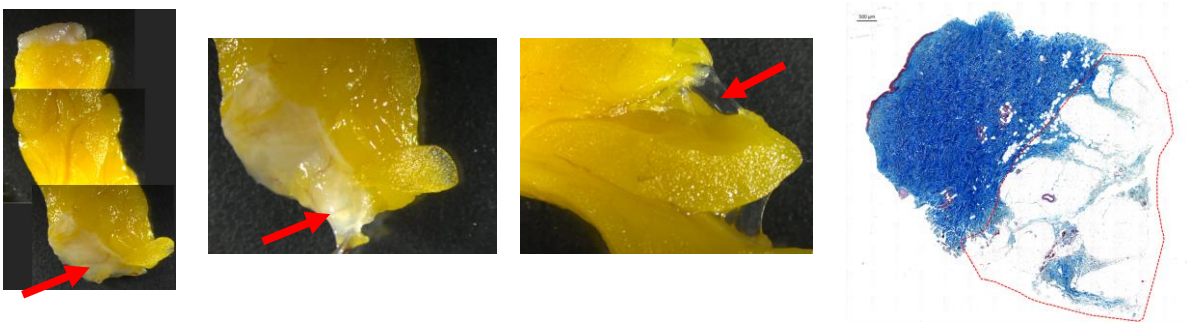

B

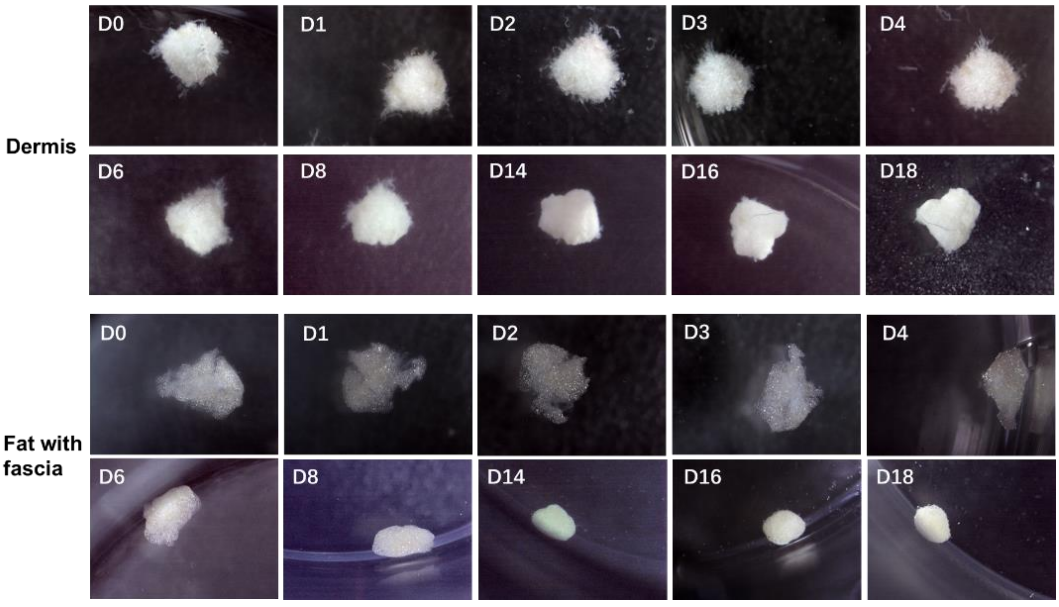

C

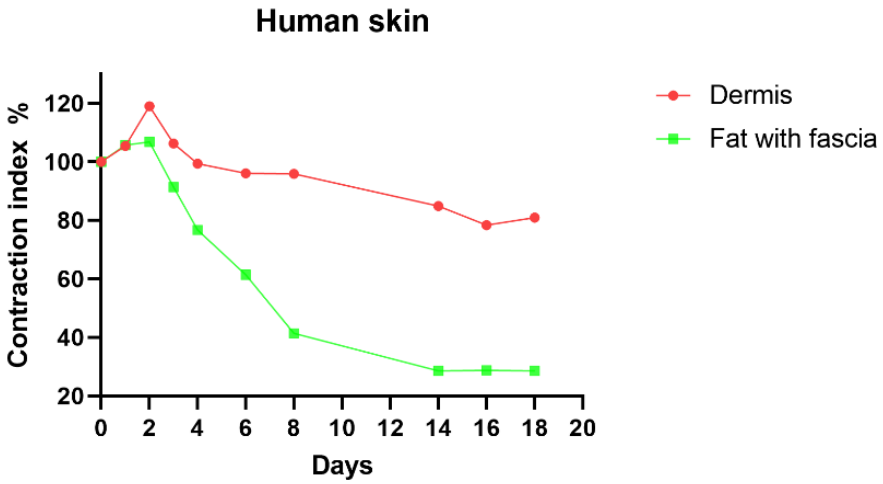
Human skin
Contraction index %
120
100
80
60
40
20
0
2
4
6
8
10
12
14
16
18
20
Days
Dermis
Fat with fascia

D

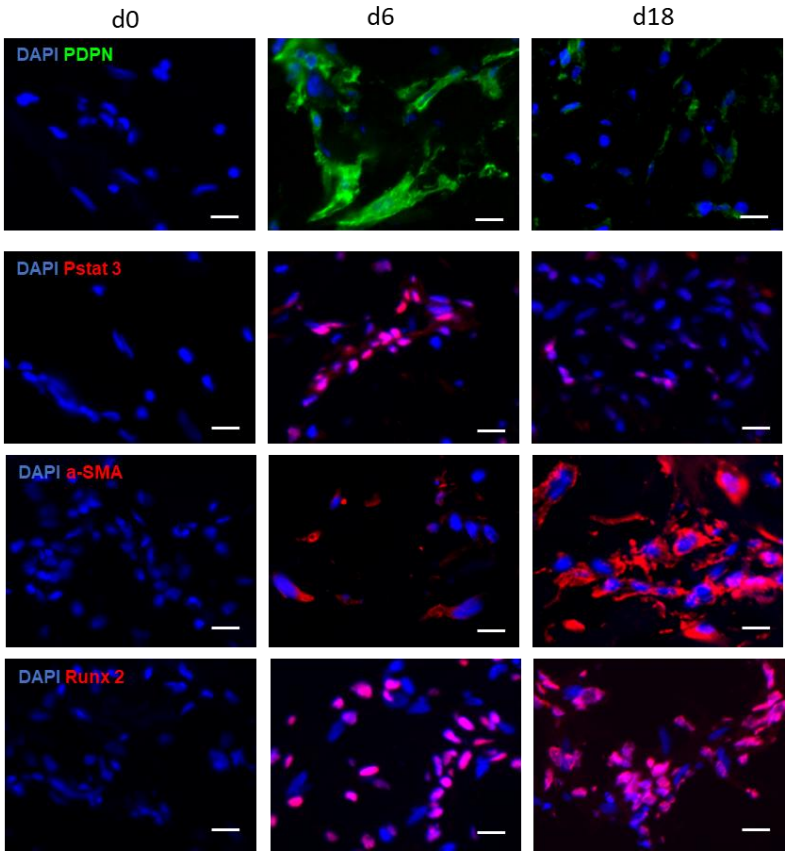
d0
d6
d18
DAPI PDPN
DAPI Pstat 3
DAPI a-SMA
DAPI Runx 2

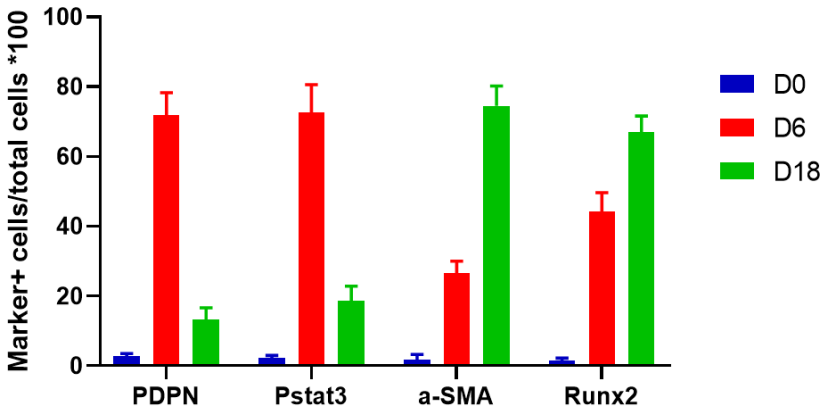

Fig.6 Human skin-derived fascia fibroblasts undergo differentiation after injury

(A) Gross view and Masson collagen staining of human abdominal full-thickness skin. (**B**) Timeline diagram of in vitro suspension culture of human dermal tissue and fascia tissue. (**C**) Quantitative analysis of the shrinkage rate of human dermal and fascia tissue cultured in vitro. (**D**) Immunofluorescence staining of in vitro human fascia cultured tissue, there are three groups of D0, D6 and D18, each group was stained with PDPN, pSTAT3, a-SMA and Runx2 respectively. Then, quantitative analysis of the expression of different genes in the three groups of fascia tissue was carried out. All p-values (p) indicated were obtained from two-tailed T-tests. Scale bars = 20 μm

3.3 Blocking fascia fibroblast differentiation leads to heterogeneity of wound healing

3.3.1 Blockade of fibroblast differentiation delays wound healing

To verify the functional effects of signalling pathways on fascia differentiation, we used Hif-1a inhibitors and Pstat3 antagonists to block the differentiation process of fibroblasts in the fascia. In the control group, we could see that the fascia gradually contracted in culture. Whereas when we used the inhibitor, the fascia no longer contracted but kept swelling (Figure 7-A-B). In in vivo experiments, we found that the use of EQM greatly slowed down the rate of wound closure (Figure 7-C). Masson staining of the wounds on day 7, showed that in the EQM group wound re-epithelialization was greatly slowed down and the wound remained open (Figure 7- D). Immunofluorescence staining of the experimental samples in vivo revealed that the normal control group underwent fibroblast transformation after injury, while EQM inhibitors greatly hindered the fibroblast transformation process (Figure 7-E-F).

A

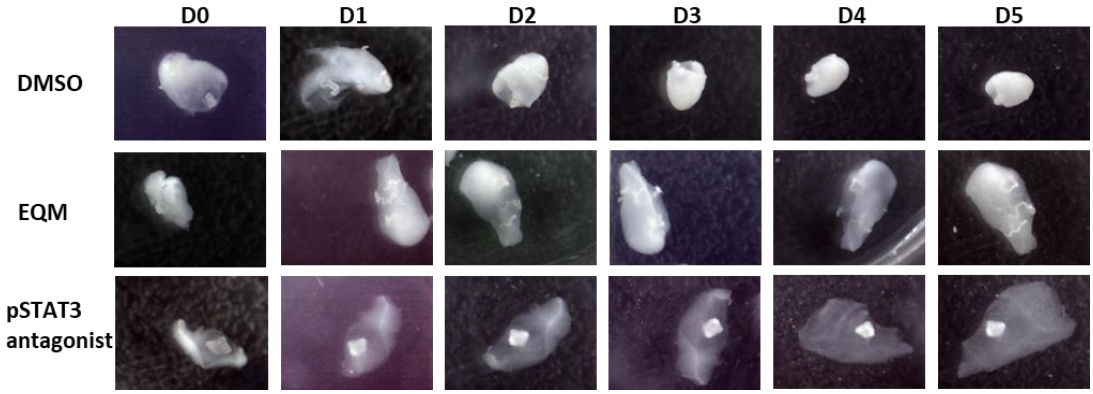
D0
D1
D2
D3
D4
D5
DMSO
EQM
pSTAT3
antagonist

B

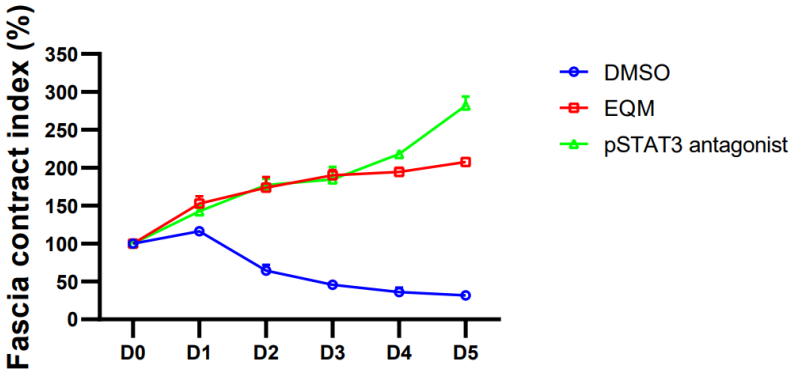
Fascia contract index (%)
350
300
250
200
150
100
50
0
D0
D1
D2
D3
D4
D5
DMSO
EQM
pSTAT3 antagonist

C

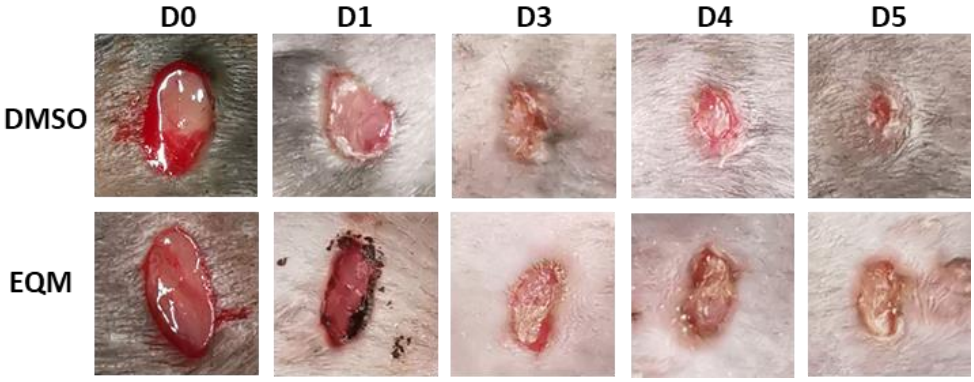
D0
D1
D3
D4
D5
DMSO
EQM

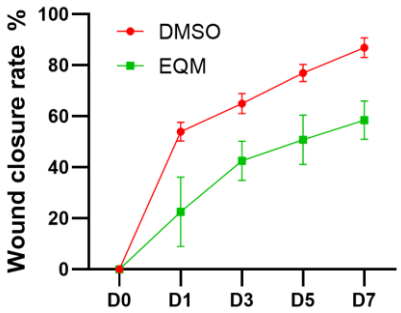
Wound closure rate %
100
80
60
40
20
0
D0
D1
D3
D5
D7
DMSO
EQM

D

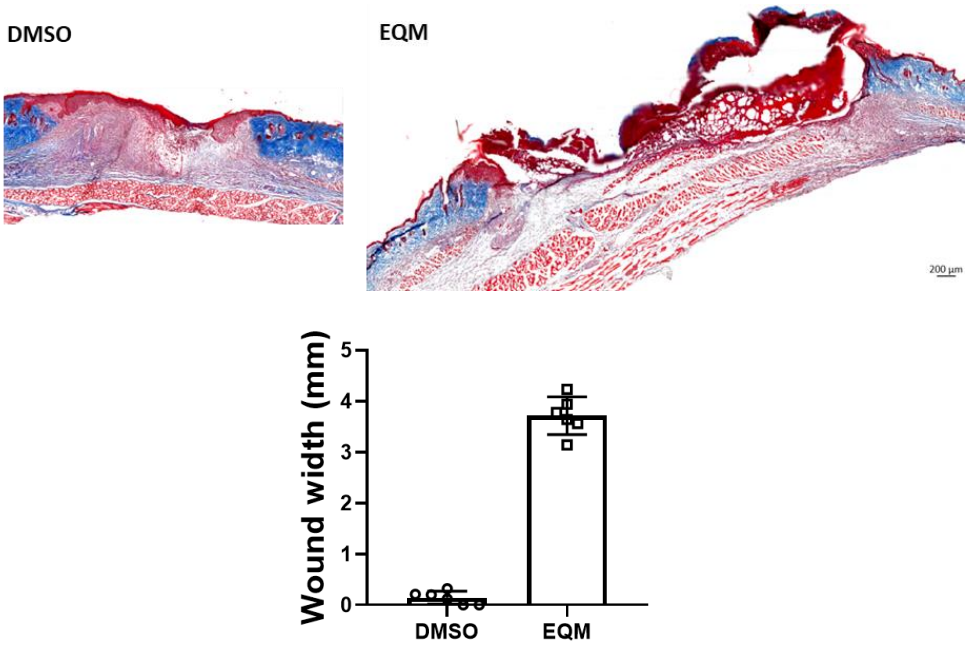
DMSO
EQM
200 μm
Wound width (mm)
5
4
3
2
1
0
DMSO
EQM

E

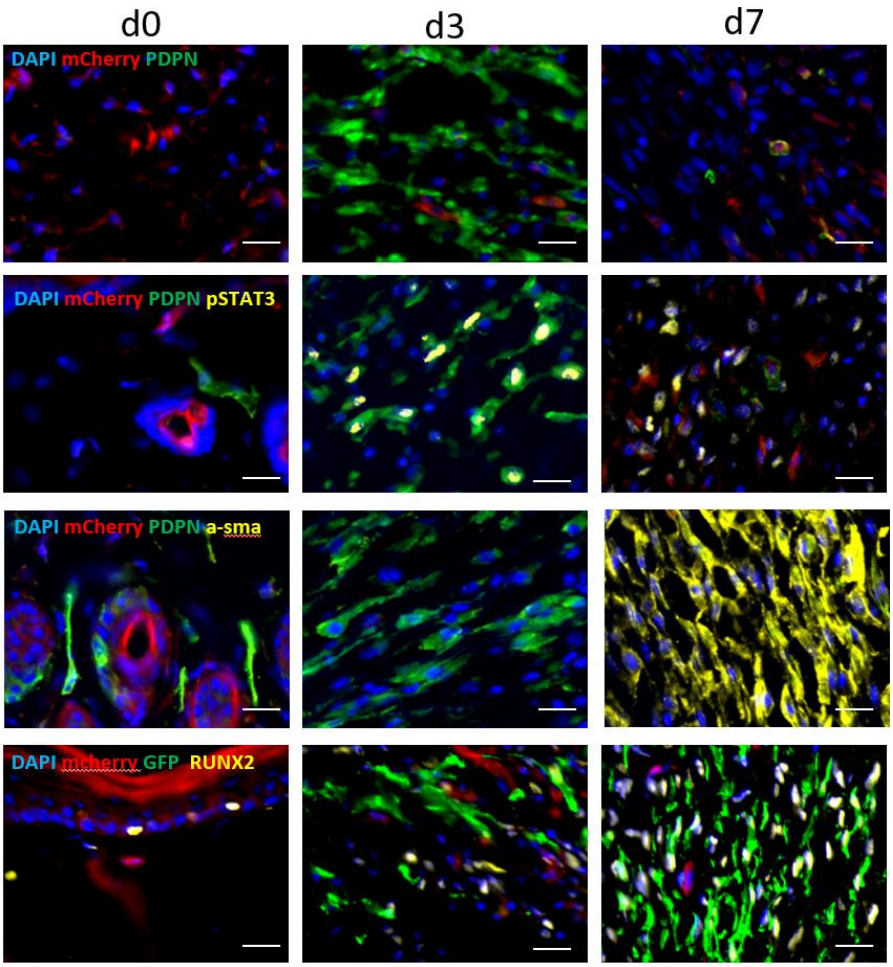
d0
d3
d7
DAPI mCherry PDPN
DAPI mCherry PDPN pSTAT3
DAPI mCherry PDPN a-sma
DAPI mcherry GFP RUNX2

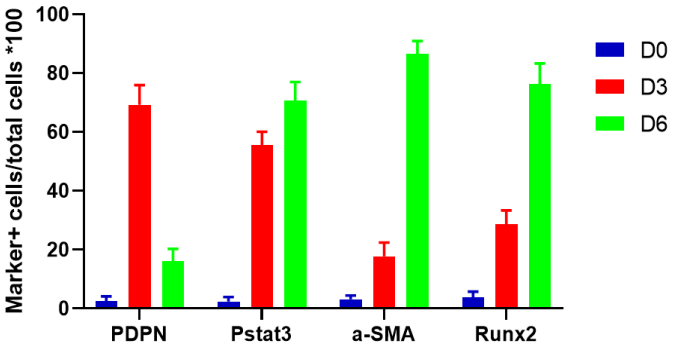
Marker+ cells/total cells *100
100
80
60
40
20
0
PDPN
Pstat3
a-SMA
Runx2
D0
D3
D6

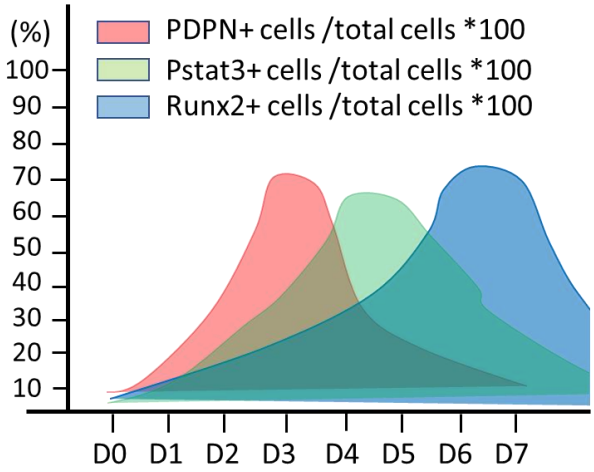
(%)
PDPN+ cells /total cells *100
Pstat3+ cells /total cells *100
Runx2+ cells /total cells *100
100
90
80
70
60
50
40
30
20
10
D0 D1 D2 D3 D4 D5 D6 D7

F

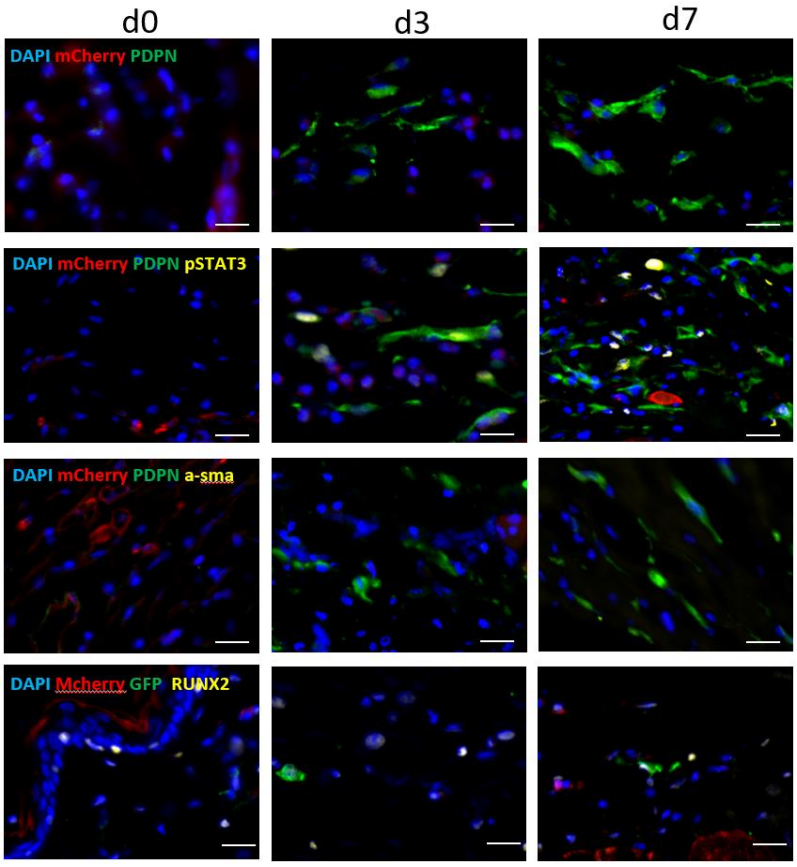
d0
d3
d7
DAPI mCherry PDPN
DAPI mCherry PDPN pSTAT3
DAPI mCherry PDPN a-sma
DAPI Mcherry GFP RUNX2

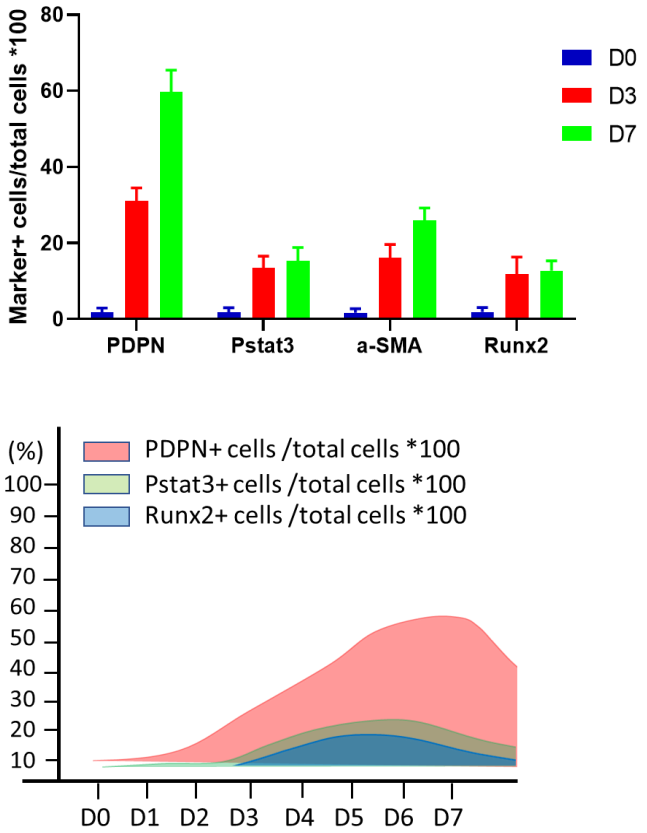

Fig.7 Blockade of fibroblast differentiation delays wound healing

(A)Young mouse fascia floating culture, the control group is DMSO, the treatment groups are EQM inhibitor and pSTAT3 antagonist (B)Quantitative analysis of the contractile index of three groups of fascia (DMSO, EQM, and pSTAT3) (C)Changes in wound size and quantitative analysis of wound closure rate in excisional wound experiments with Hif-a inhibitor EQM (D)Masson trichrome staining of wounds on the seventh day after Hif-a inhibitor EQM treatment, quantitative analysis of wound width. (E)The first figure is immunofluorescence staining of the wounds of the DMSO group in vivo, there are three groups D0, D3, and D7, each group was stained with GFP, PDPN, pSTAT3, a-SMA, and Runx2 respectively. The second figure is the quantitative analysis of the expression of different genes in the three groups of wounds. The third figure is the time-expression correlation diagram of PDPN, pSTAT3, and Runx2 in wounds in vivo. (F)The first figure is immunofluorescence staining of the wounds of the EQM treatment group in vivo, there are three groups D0, D3, and D7, each group was stained with GFP, PDPN, pSTAT3, a-SMA, and Runx2 respectively. The second figure is the quantitative analysis of the expression of different genes in the three groups of wounds. The third figure is the time-expression correlation diagram of PDPN, pSTAT3, and Runx2 in wounds in vivo. All p-values (p) indicated were obtained from two-tailed T-tests. Scale bars (D) = 200 μm, Scale bars (E, F) = 20 μm.

3.3.2 Genetic depletion of PDPN+ fascia fibroblasts greatly slows wound healing

We depleted PDPN+ fibroblasts using the genetic DTA system crossed to PDPNCre-ER. in the in vitro model (shown in Figure 8-A), the fascia of the first two control groups could still contract. In the experimental group, the contraction process of the fascia was inhibited when the PDPN+ cells were conditionally knocked down. In the in vivo experiment (shown in Figure 8-B), the wounds of the first two control groups healed normally, and the wounds were largely healed on day 7. In the PDPN knockout group wounds barely closed. Masson staining (Figure 8-C), day 7 wound re-epithelialization was completed in the control group, the wound area was smaller than that of the experimental group, and more mature collagen fibers appeared on the wound surface. In the experimental group, wound re-epithelialization was severely inhibited, the wound area was larger than that of the control group, and mature collagen fibers had not yet appeared on the wound surface. The wounds were then immunofluorescently stained on the third and seventh days (as shown in Figure 8-D). On the third day post injury, there were a large number of PDPN-positive cells as well as macrophages infiltrating the wounds in control groups. Whereas in the experimental group there was a large decrease in PDPN-positive cells and a decrease in macrophages. On day 7 of wound, there were almost no PDPN-positive cells and a large number of macrophages in the control group. The experimental group began to show a large number of PDPN-positive cells, along with some macrophages.

A

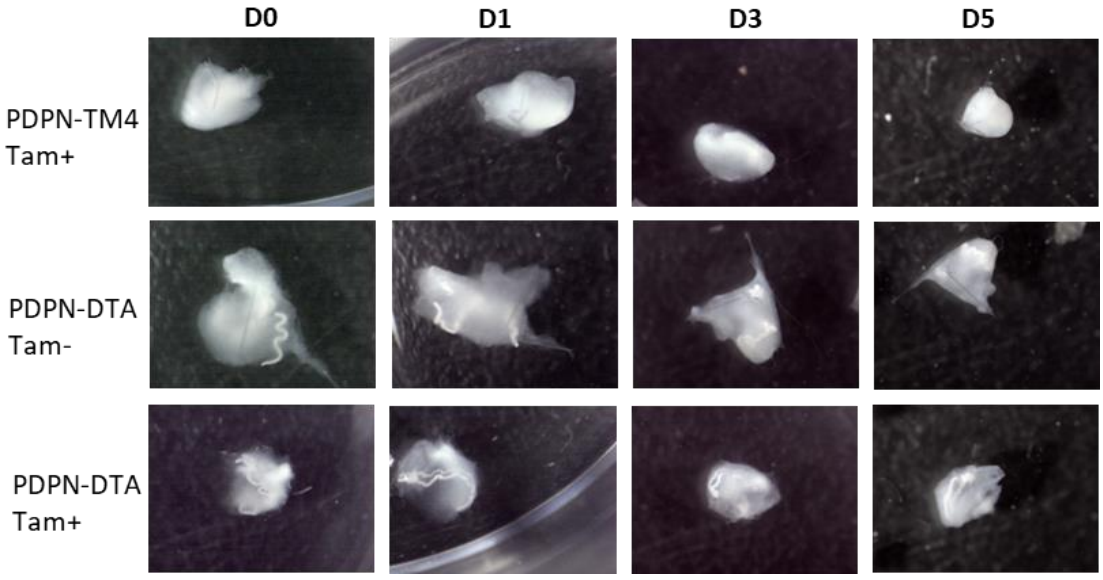

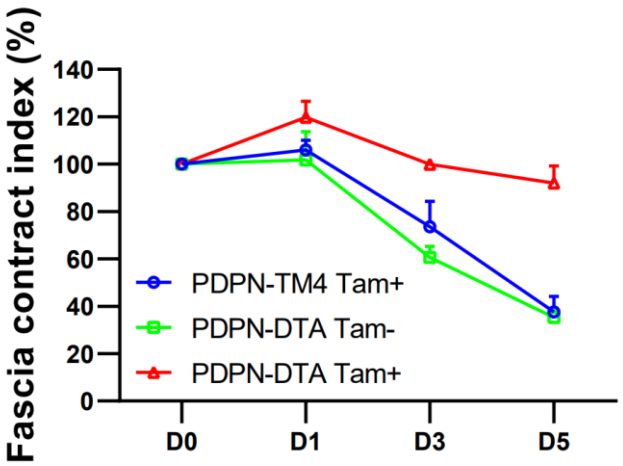
Fascia contract index (%)
140
120
100
80
60
40
20
0
D0
D1
D3
D5
PDPN-TM4 Tam+
PDPN-DTA Tam-
PDPN-DTA Tam+

B

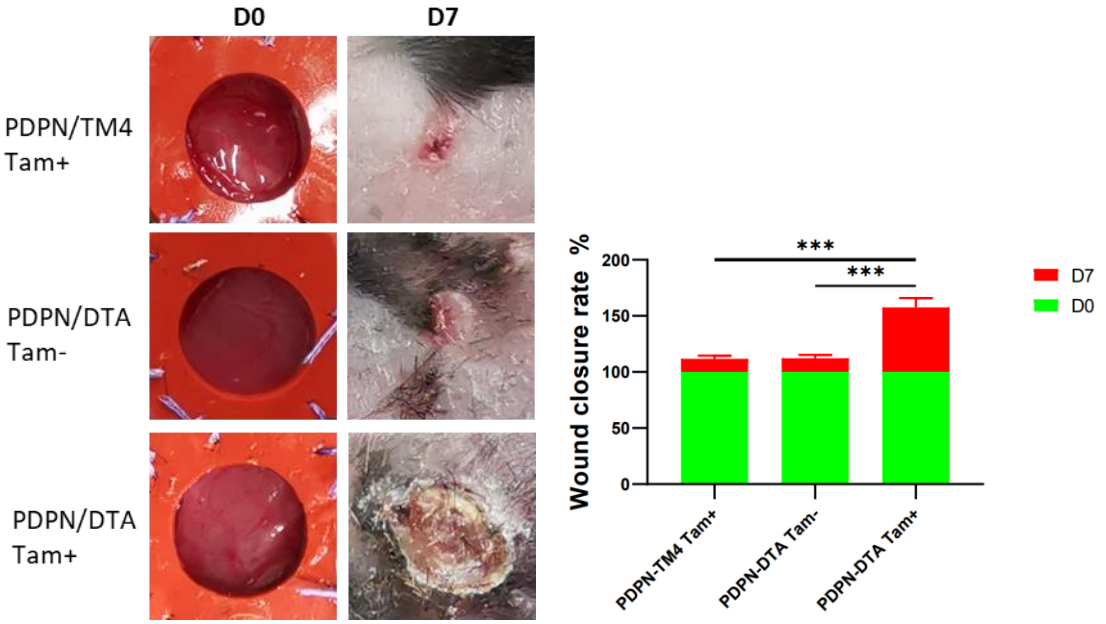
D0
D7
PDPN/TM4 Tam+
PDPN/DTA Tam-
PDPN/DTA Tam+
Wound closure rate %
200
150
100
50
0
***
***
D7
D0
PDPN-TM4 Tam+
PDPN-DTA Tam-
PDPN-DTA Tam+

C

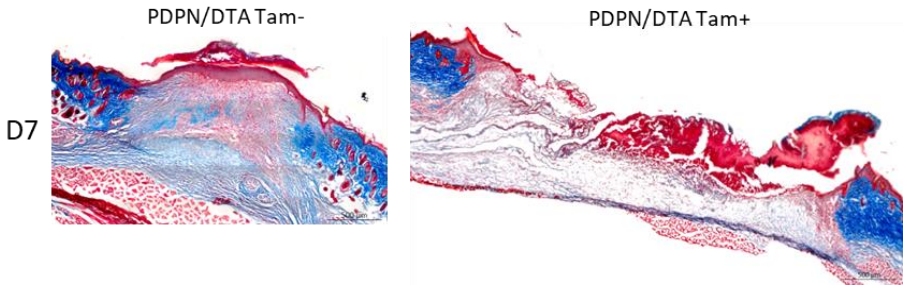
PDPN/DTA Tam-
PDPN/DTA Tam+
D7

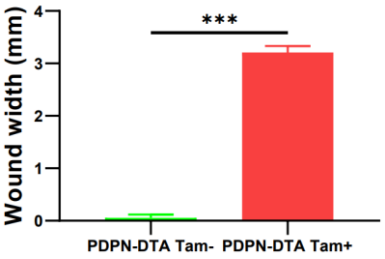

D

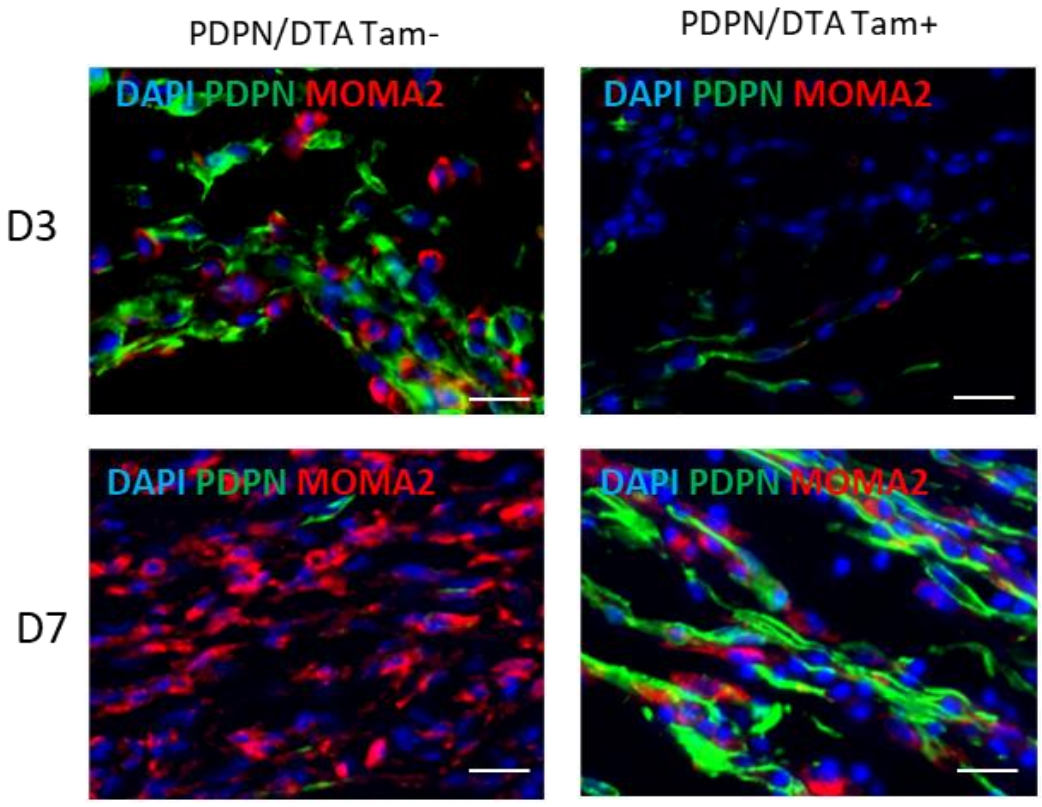

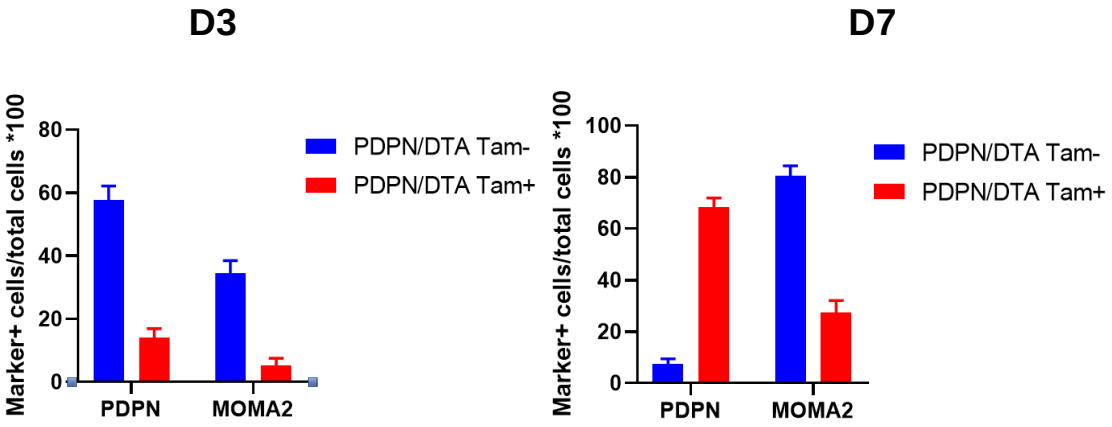

Fig.8 Conditional depletion of PDPN+ cells slows wound healing

(A) The left side of the picture is the suspension culture experiment of fascia after conditional knockout of PDPN, the upper two groups are the control group, and the lower group is the treatment group. The right side of the picture is the quantitative analysis of fascia contraction in each group. **(B)** In vivo full-thickness skin wound experiment after conditional knockout of PDPN, the upper two groups are the control group, and the lower group is the conditional knockout PDPN group. The right side of the figure is a quantitative analysis of the wound closure rate for the three groups. **(C)** The left side of the picture is the Masson collagen staining of the wounds of the control group and the experimental group on the seventh day, and the right side of the picture is the quantitative analysis of the wound width. **(D)** Above the picture is the immunofluorescence staining of wounds on the third and seventh days in the control and experimental groups, DAPI (blue), PDPN (green), MOMA2 (red). Below the picture is a quantitative analysis of the percentage of PDPN+ and MOMA2+ cells. All p-values (p) indicated were obtained from two-tailed T-tests. Scale bars (C) = 500 μm, Scale bars (D) = 20 μm.

3.3.3 Abnormal differentiation of human fascia fibroblasts in human keloids

To study the relevance of our mouse fascia findings on human disease, we analyzed human keloid samples. As shown in Figure 9-A, human keloids contain fascia embedded in fat tissue. Histological staining showed that the collagen fibers of normal skin are arranged in. areticular pattern, whereas the collagen fibers of the keloid are arranged in a very disorganized, swirling pattern. In immunofluorescence staining (as shown in Figure 9-B-C), keloid samples were found to express more a-SMA than normal skin, Pstat3 was barely expressed in normal skin and keloid, and Runx2 was highly expressed in keloid but not in normal skin, indicating that fascia fibroblasts in keloid samples have transitioned entirely to a myofibroblastic fate (Figure 9-D).

A

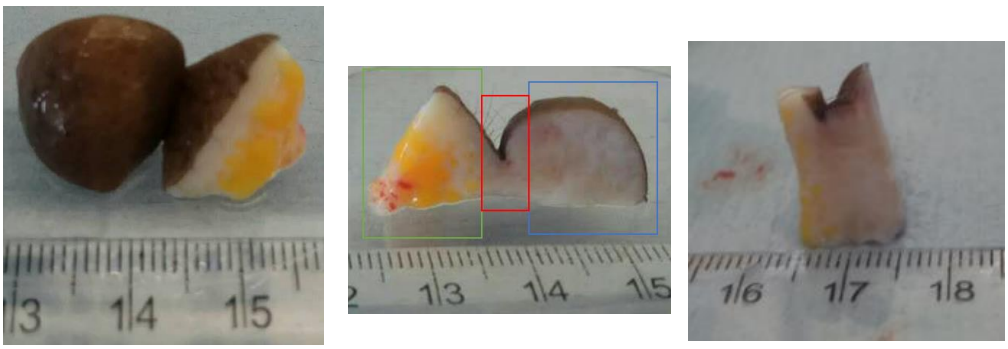

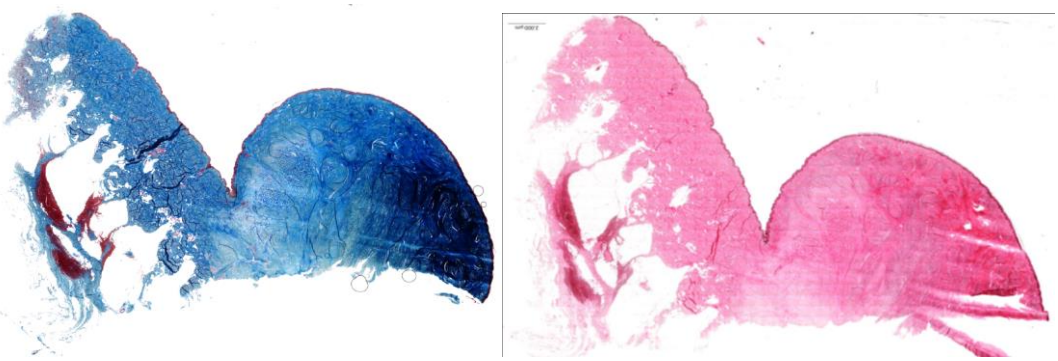

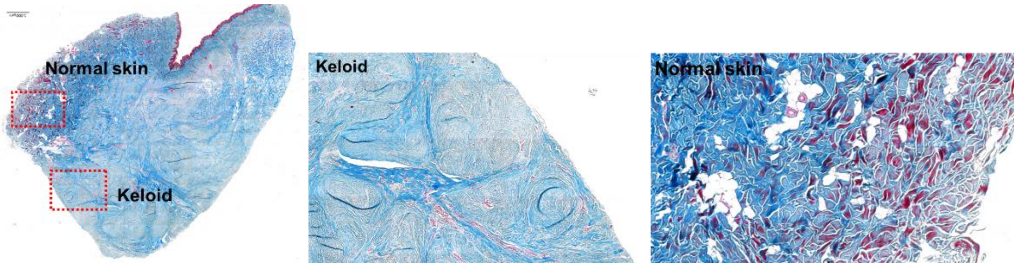
Normal skin
Keloid
Keloid
Normal skin

B

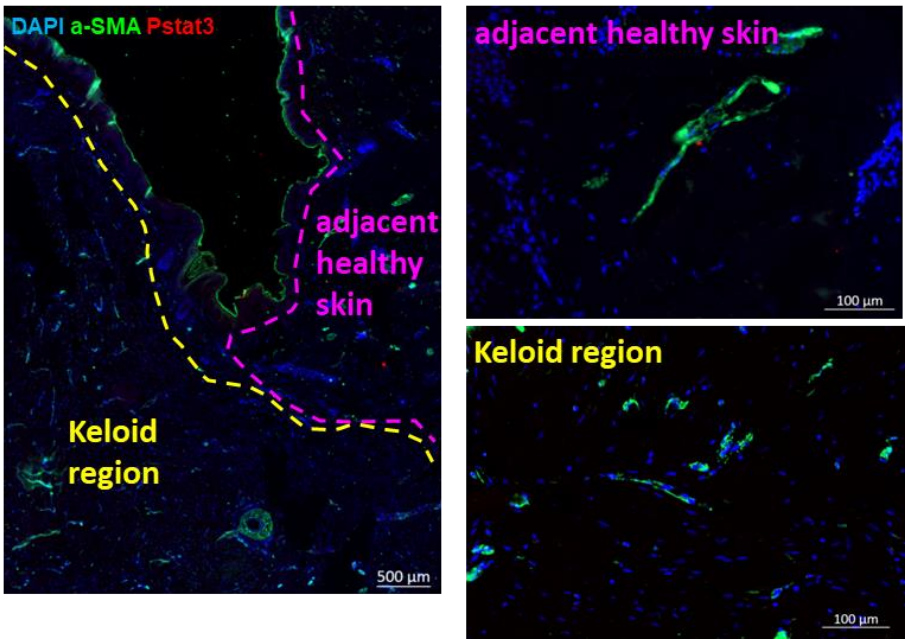
DAPI a-SMA Pstat3
adjacent healthy skin
Keloid region
500 µm
adjacent healthy skin
100 µm
Keloid region
100 µm

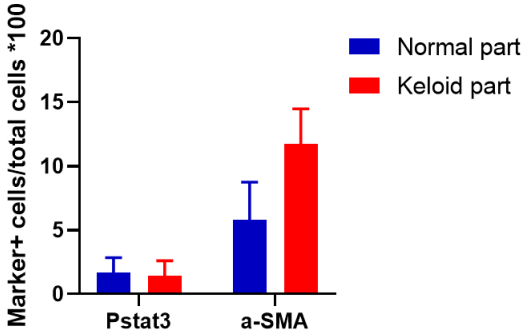
Marker+ cells/total cells *100
20
15
10
5
0
Pstat3
a-SMA
Normal part
Keloid part

C

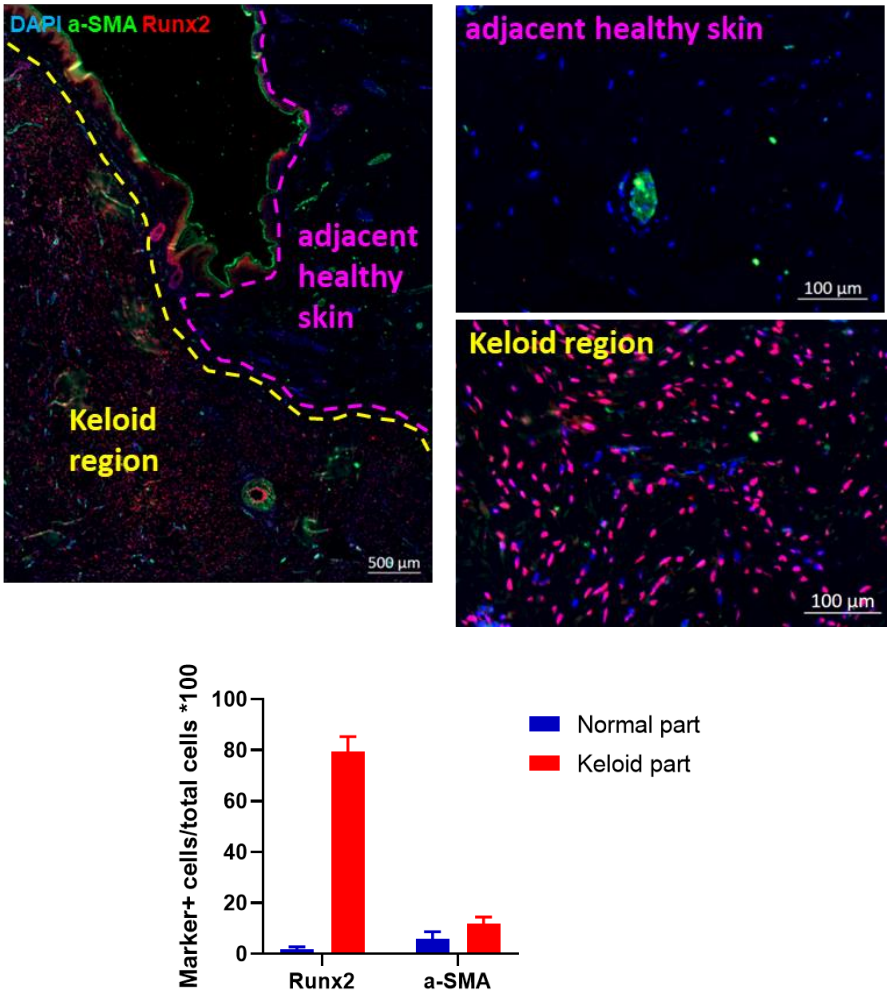

D

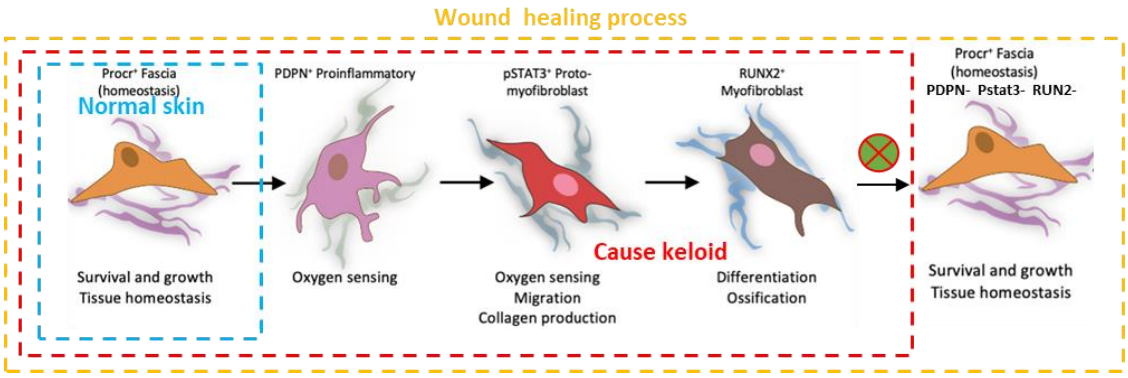

Fig. 9 Abnormal fascia fibroblast differentiation in human keloid samples

(**A**) The upper part of the picture is the physical image of human skin keloid, and the lower part is histological image (masson trichrome staining and HE staining). (**B**) Immunofluorescence staining of keloid (blue: DAPI, green: a-SMA, red: Pstat3) and quantitative analysis of related genes (**C**) Immunofluorescence staining of keloids (blue:

DAPI, green: a-SMA, red: Runx2) and quantitative analysis of related genes (D) Schematic illustration of the differentiation of fascial fibroblasts during wound healing. All p-values (p) indicated were obtained from two-tailed T-tests.

3.4 Fascia fibroblast differentitation is delayed in aged skin

3.4.1 Aged wounds heal slower than younger wounds

Aged skin exhibits drastic histologic changed as compared to young skin, as shown in Figure 10-A. On the left is the Masson staining of the dorsal skin of 2-month-old mice, and on the right is the histological staining of the dorsal skin of 20-month-old mice. In aged skin, the thickness of the dermis and fascia layer became significantly thinner, except for the epidermal thickness, which did not change significantly, and a large amount of adipose tissue also appeared in the aging fascia. Density of fibroblasts in the fascia also decreases significantly with age (Figure 10-B). As seen in the mouse dorsal excision wound model in Figure 10-C-D, the wound closes and heals rapidly after a back injury in 2-month-old mice, especially between the first and second day. When mice reach middle age (9 months), the rate of wound closure is similar to young mice. However, when mice reach 20 months of age, wound closure was significantly slower. Masson staining of the wounds on days 3 and 7 (Figure 10-E) shows that the older wounds were wider and closed more slowly than the younger wounds on day 3. By day 7, the young wound had almost completed epithelialization, while the old wound still had not closed.

A

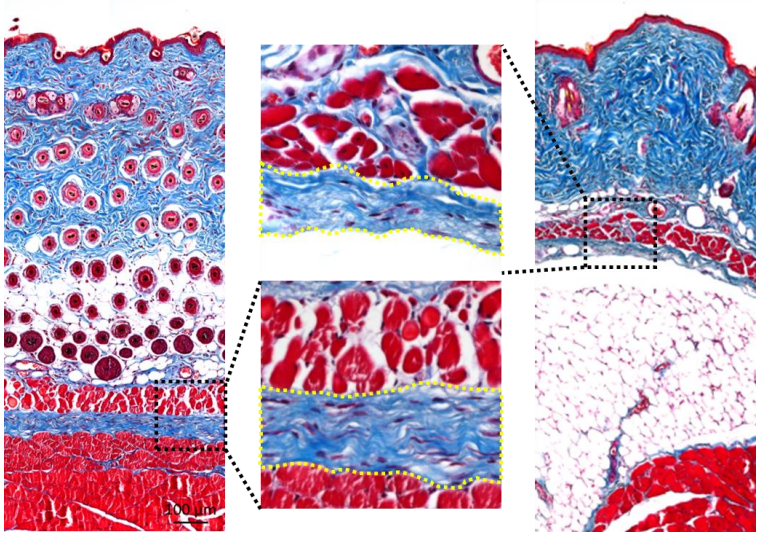

B

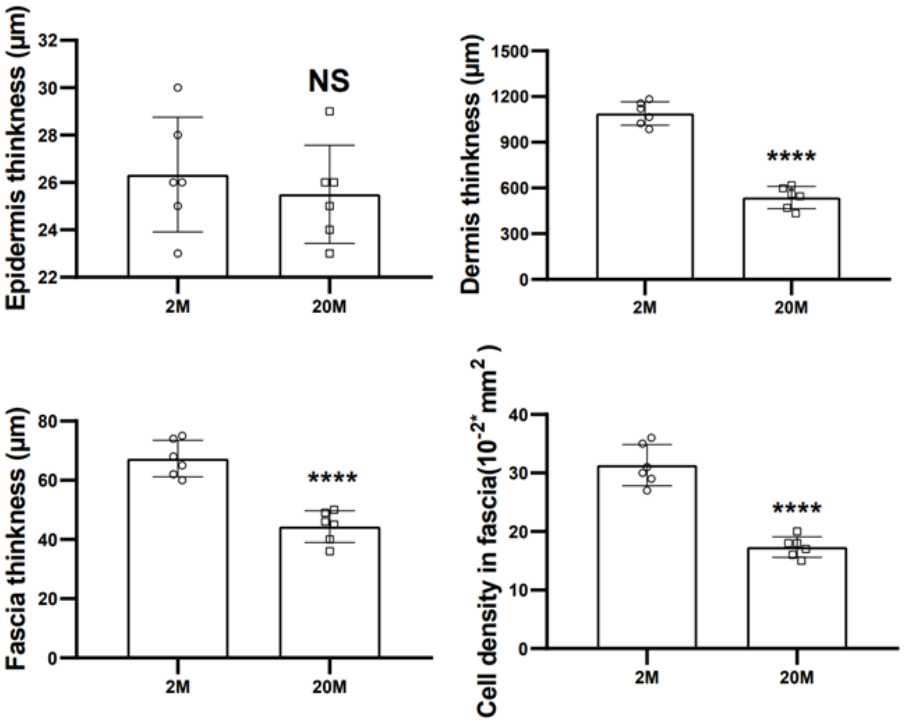
Epidermis thinkness (μm)
NS
2M
20M
Dermis thinkness (μm)
****
Fascia thinkness (μm)
****
Cell density in fascia(10-2* mm2)
****

C

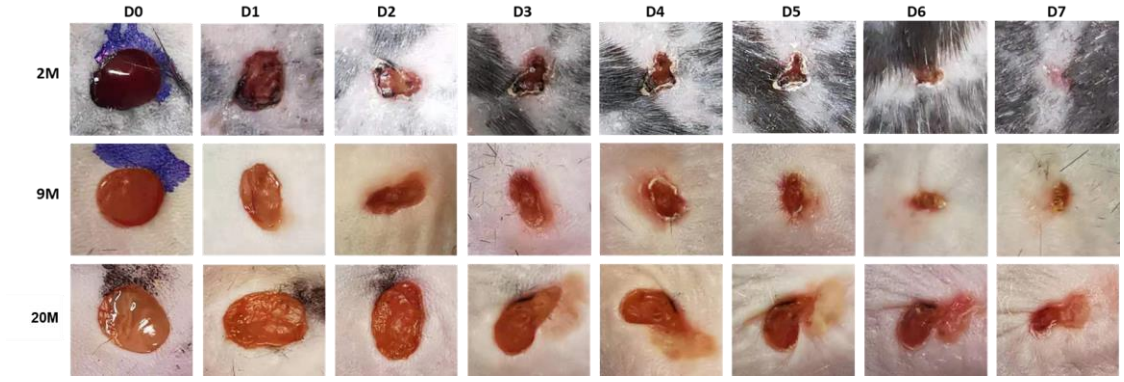
D0
D1
D2
D3
D4
D5
D6
D7
2M
9M
20M

D

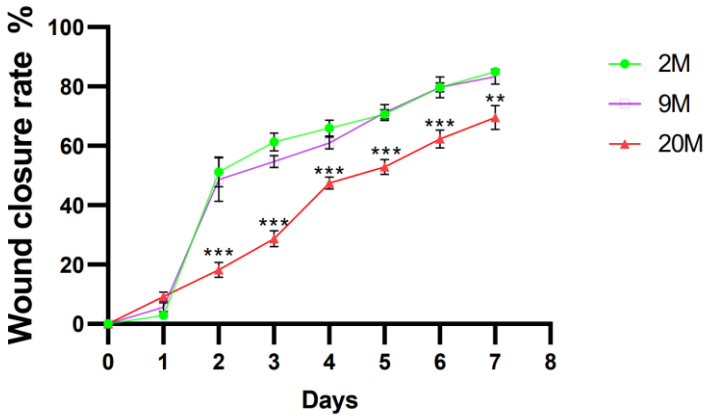
Wound closure rate %
Days
2M
9M
20M
***
**

E

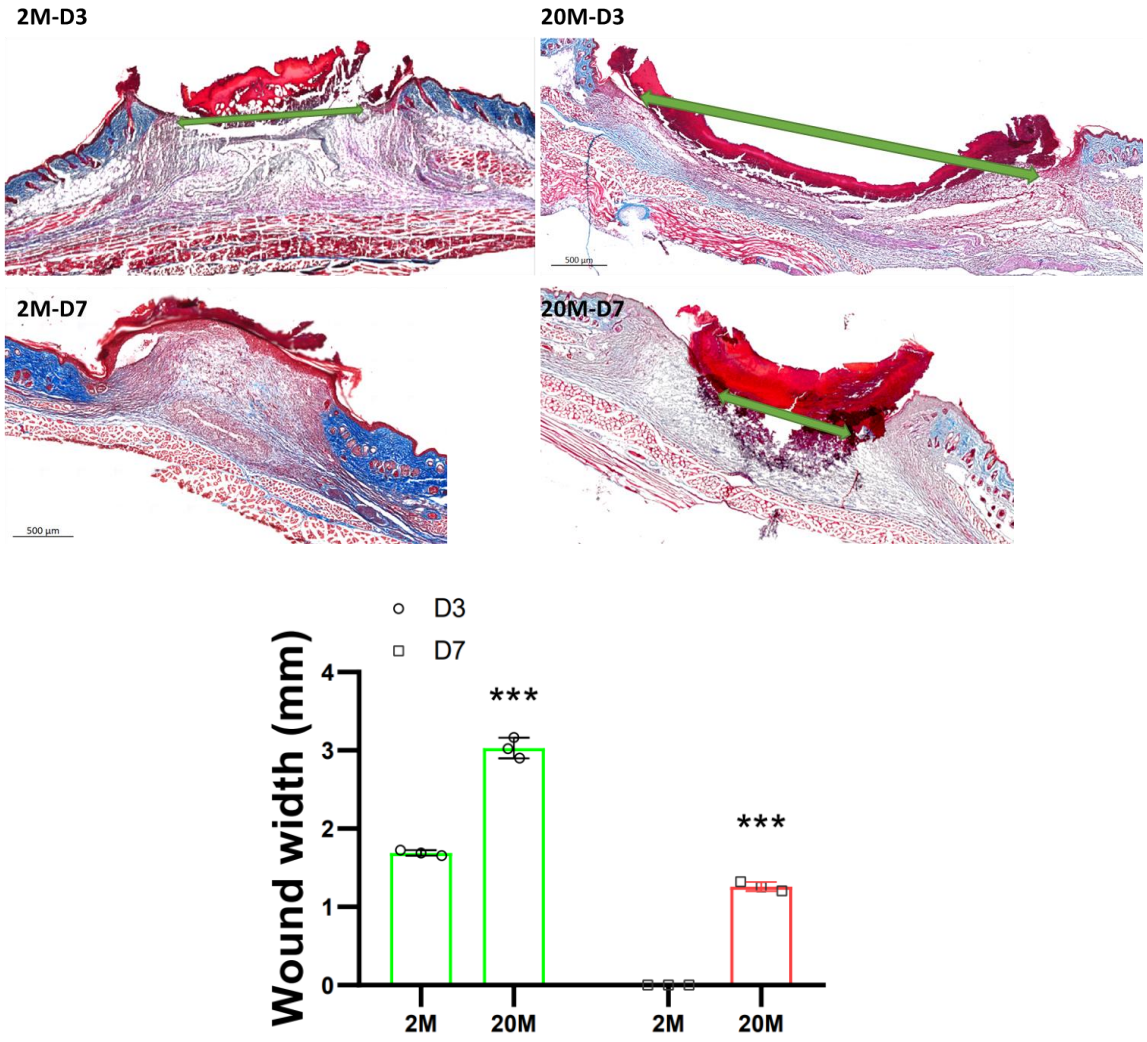

Fig.10 Aged wounds heal slower than younger wounds

(**A**) Masson trichrome staining of young mouse skin on the left, Masson trichrome staining of aged mouse skin on the right, and the corresponding high magnification image in the middle. (**B**) Quantitative analysis of epidermis, dermis, fascial layer thickness and fascial layer cell density in young and aged skin. (**C**) Wound change graph of excisional wounds of young mice, middle-aged mice and aged mice (**D**) Quantitative graph of wound closure rates of excisional wounds of young mice, middle-aged mice and aged mice (**E**) Quantitative statistics of wound Masson trichrome staining images and wound width on day 3 and day 7 of young and aged mice. All p-values (p) indicated were obtained from two-tailed T-tests. Scale bars (A) = 100 μm, Scale bars (E) = 500 μm.

3.4.2 Slowed wound healing in aged skin is attributed to the fascia

In our in vivo wound experiments with fascia ECM labelling, it can be seen that in day 7 wounds, the young wounds were all filled with pre-labelled fascia, while in wounds from aged mice, the labelled fascia barely entered, with a significant difference in the entry rate of fascia from the young wounds (Figure 11-A). In vitro tissue culture of young and aged fascia shows that fascia undergoes a process of expansion followed by contraction during culture, and young fascia shrinks faster than old fascia during culture (Figure 11-B). Figure 11-C shows the real-time images of the fascia after two days of 3D Matrigel culture. Young fascia contracted very quickly, while the aged fascia contracted very slowly. In our skin intercalation chimeric graft experiment, the experimental flow chart is shown in Figure 11-D. On the 14th day after fascia grafting, as shown in Figure 11-E, the amount of young fascia entering the wound on the left side was much larger than that seen with engraftments of aged fascia. Immunofluorescence results (Figure 11-F), shows young fascia entering the wound significantly more than aged fascia. These experiments indicate that wound healing phenotypes of aged skin are attributed to the fascia itself.

A

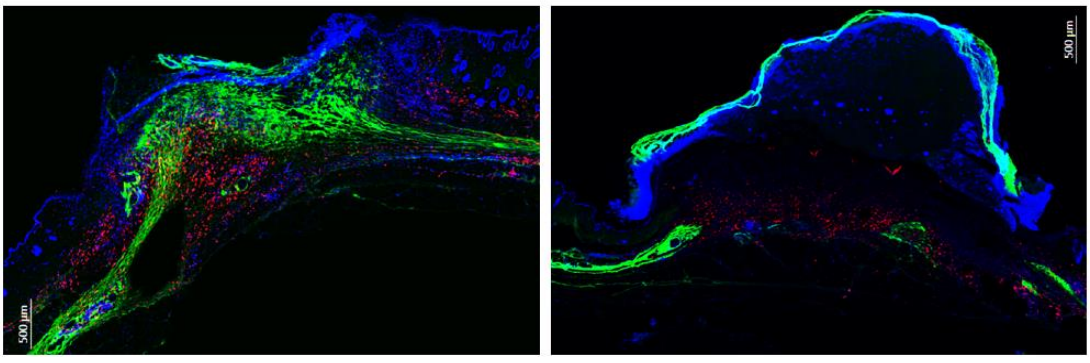

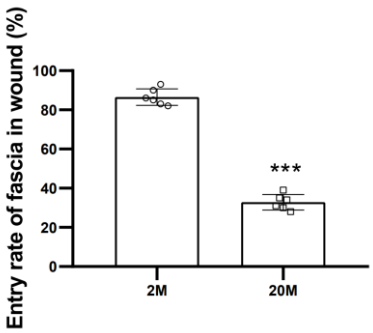

B

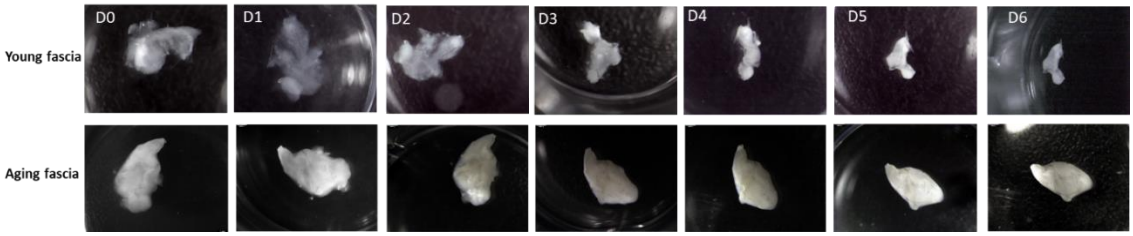
Young fascia
Aging fascia
D0
D1
D2
D3
D4
D5
D6

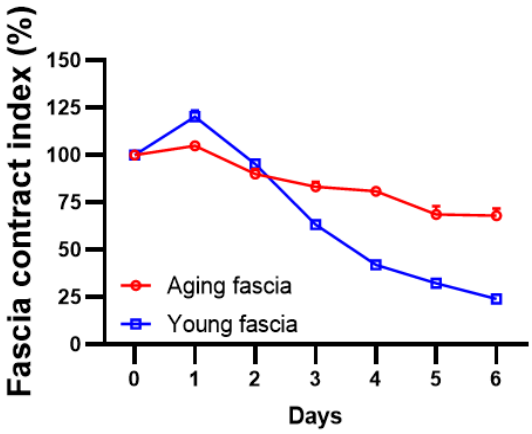
Fascia contract index (%)
150
125
100
75
50
25
0
0
1
2
3
4
5
6
Days
Aging fascia
Young fascia

C

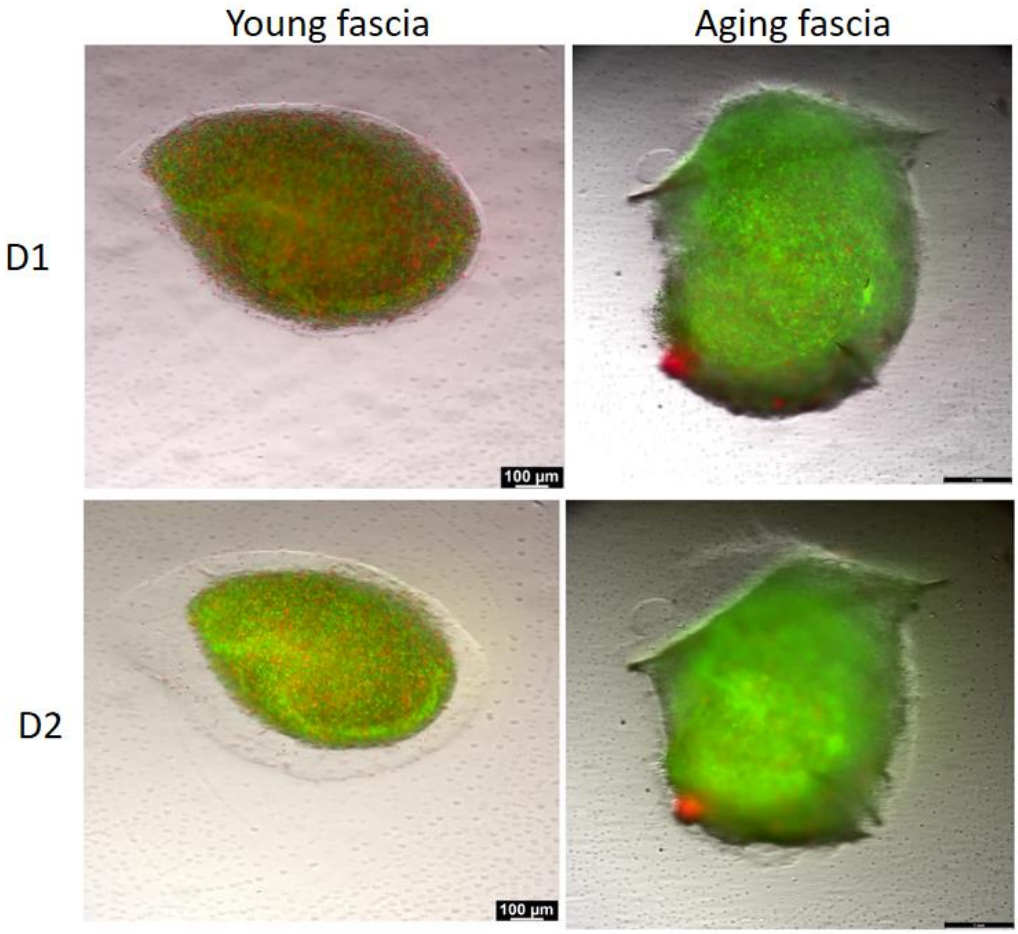
Young fascia
Aging fascia
D1
D2
100 μm
100 μm

D

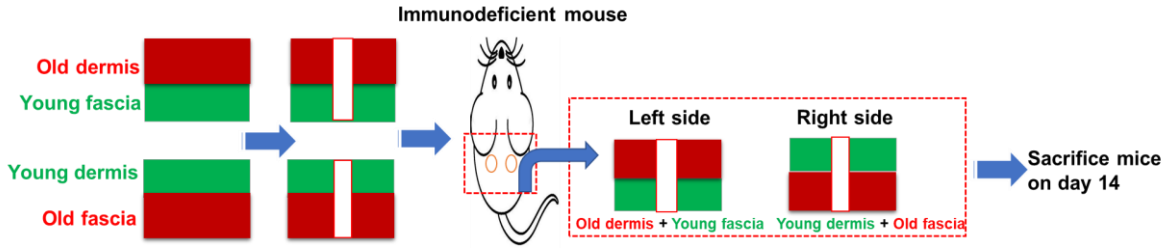
Immunodeficient mouse
Old dermis
Young fascia
Young dermis
Old fascia
Left side
Right side
Old dermis + Young fascia
Young dermis + Old fascia
Sacrifice mice on day 14

E

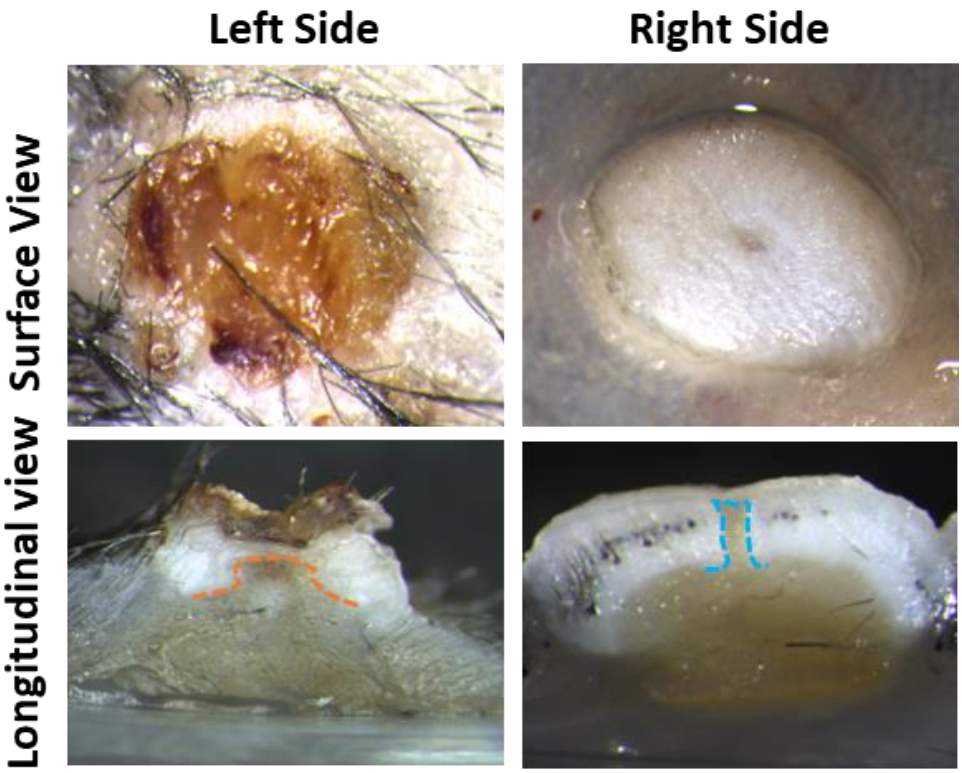
Left Side
Right Side
Surface View
Longitudinal view

F

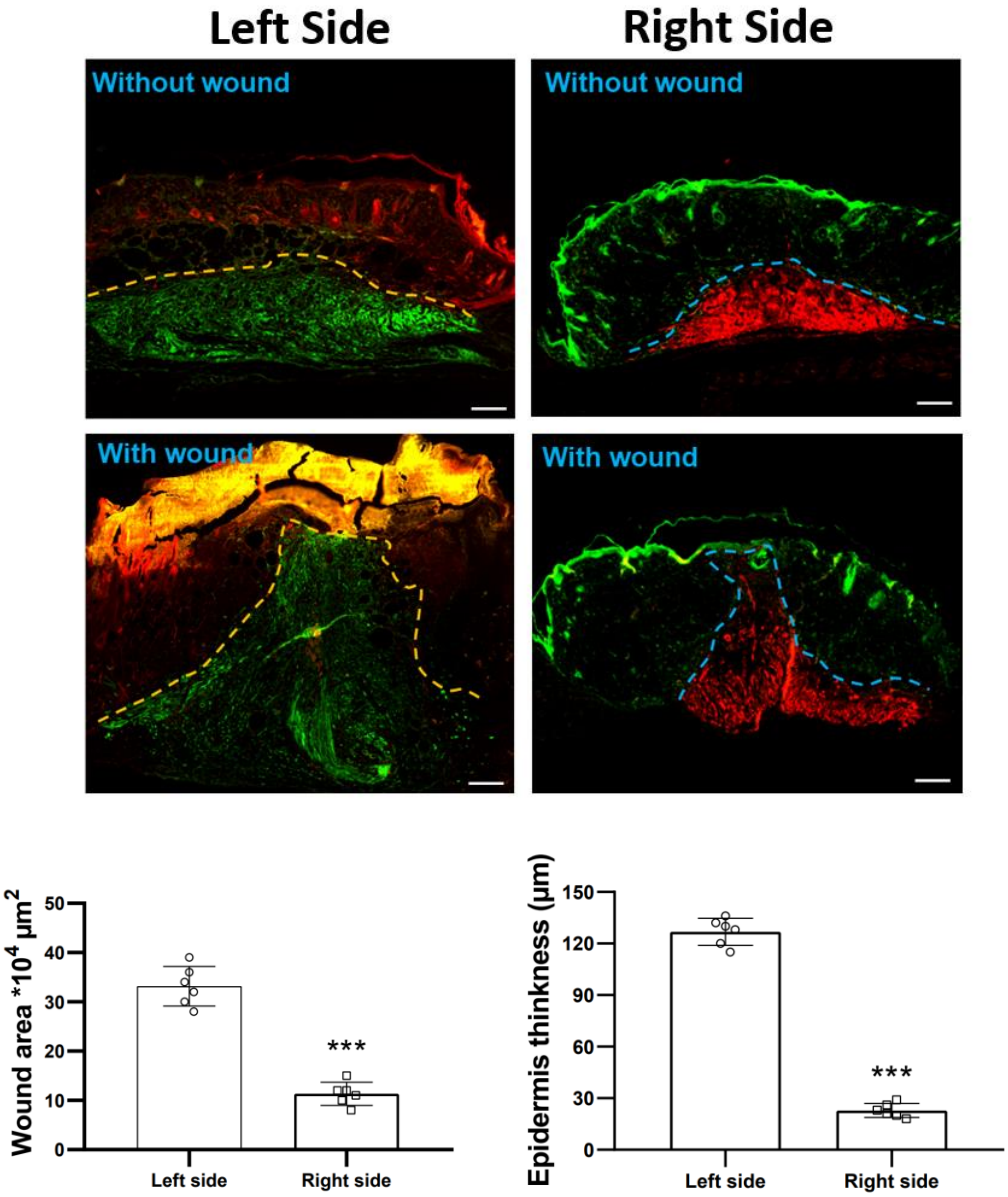

Fig.11 Slowed wound healing in aged skin is atributed to the fascia

(**A**) In vivo fascia ECM labelling. The left side of the figure is the situation of the marked fascia entering the wound on the seventh day of youth, and the right side of the figure is the situation of the marked fascia entering the wound on the seventh day of aging, and the bottom of the figure is the corresponding Quantitative analysis. (**B**) Size change and quantitative analysis of in vitro suspension cultures of young and aged fascia. (**C**) 3D Matrigel cultures of young and aged fascia, recording the process of fascial contraction using real-time microscopy. (**D**) Skin reorganization embedded Schematic diagram of the synthesis experiment. (**E**) Surface view and longitudinal section of the graft wound on the 14th day of the skin reorganization chimera experiment.

(**F**) Immunofluorescence images of the graft wound on the 14th day of the skin reorganization chimera experiment and related quantitative analysis. All p-values (p) indicated were obtained from two-tailed T-tests. Scale bars (A) = 500 μm, Scale bars (C) = 100 μm, Scale bars (F) = 200 μm.

3.4.3 Contractility dysfunction in aged fascia is atributed to fascia fibroblasts

Figure 12-A shows a schematic diagram of 3D fascia cultured in vitro. After a few days of culture, we found that there were significantly more fibroblasts in the young fascia than in the aged fascia (Figure 12-B-C). On the fifth day of culture, we fixed the tissue and then photographed it with a two-photon microscope. As shown in Figure 12-D, the fibroblasts migrating out of the young fascia were sparse and lacked the intercellular membrane connections seen in young fascia tissue. In Figure 12-E, we can see the dynamic process of fibroblast migration in the fascia. We can see that young fibroblasts are very active and migrate rapidly, while fibroblasts from aged fascia lack migratory capacity with minimal fibroblasts migrating outwards. As shown in Figure 12-F-G, type 1 collagen contraction experiments we can see that the effect of type 1 collagen contraction is different after adding fibroblasts from different young/aged skin sources. The ability of older fascia fibroblasts to contract type 1 collagen is greatly reduced compared to younger fascial fibroblasts. We also found that dermal-derived fibroblasts have a lower ability to contract type 1 collagen than fascia-derived fibroblasts. Both human skin-derived fibroblasts and human keloid-derived fibroblasts were able to contract type 1 collagen much more than dermal fibroblasts.

A

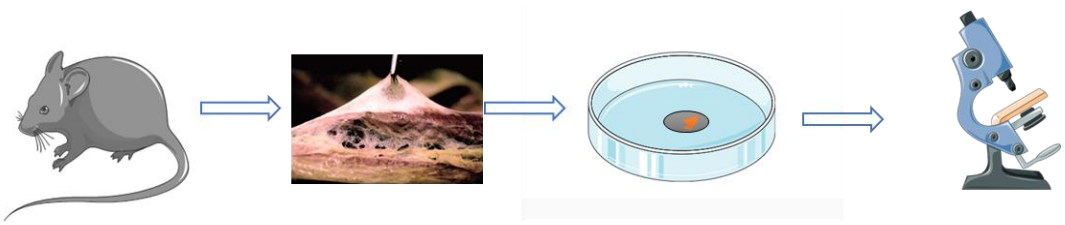

B

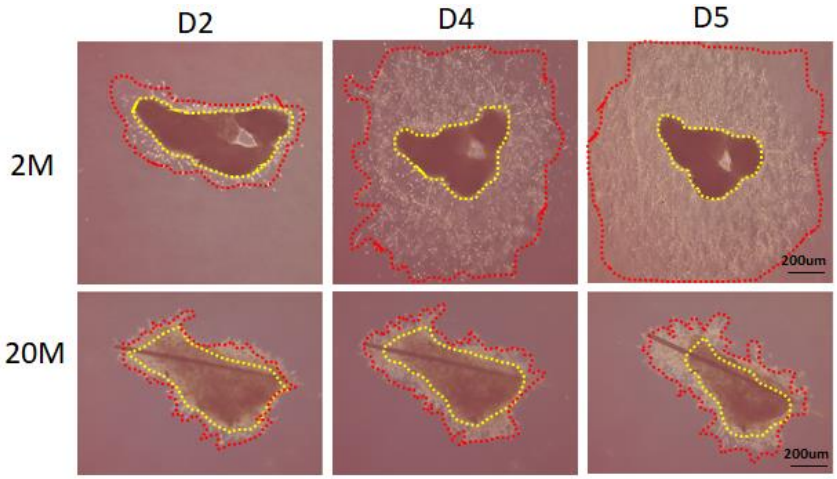
D2
D4
D5
2M
20M
200um
200um

C

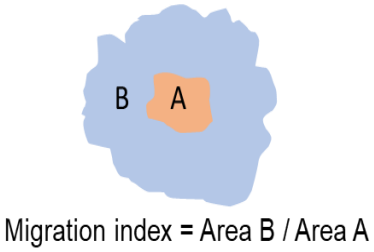
B
A
Migration index = Area B / Area A

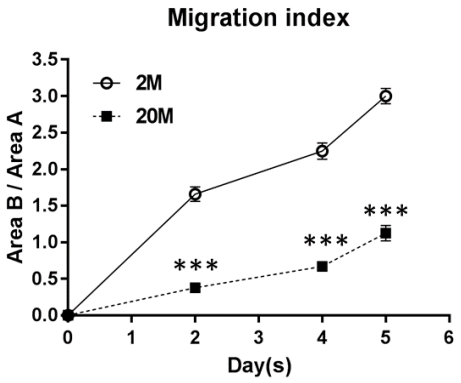
Migration index
2M
20M
Area B / Area A
Day(s)
***
***
***

D

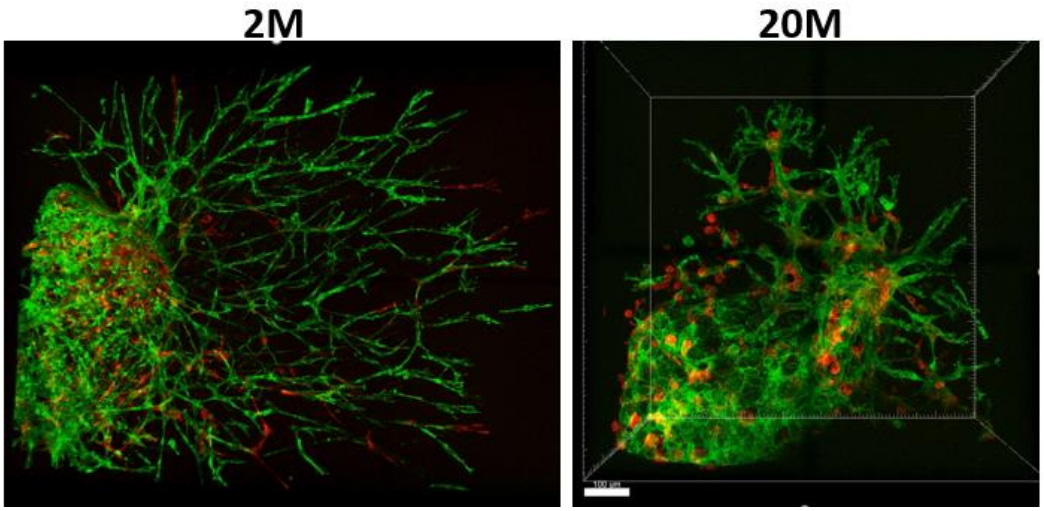
2M
20M

E

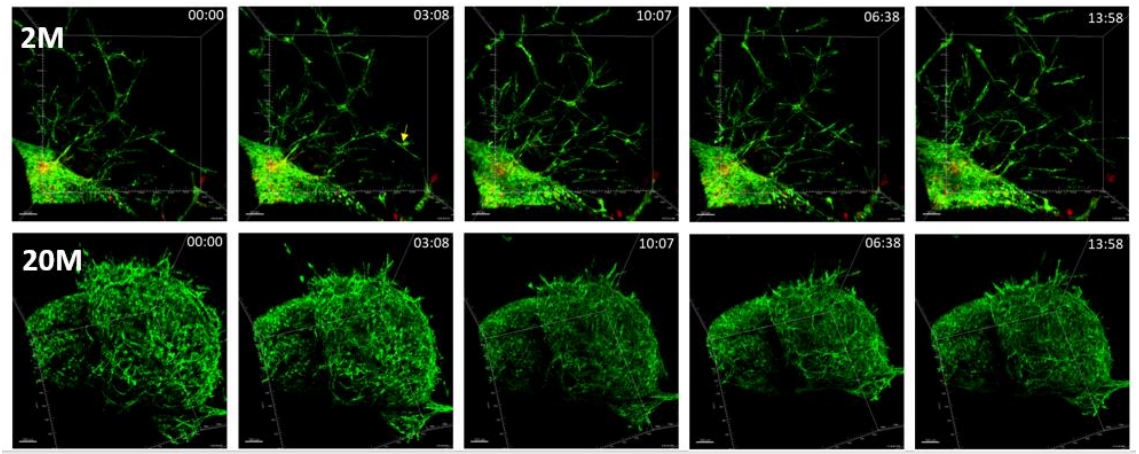

F

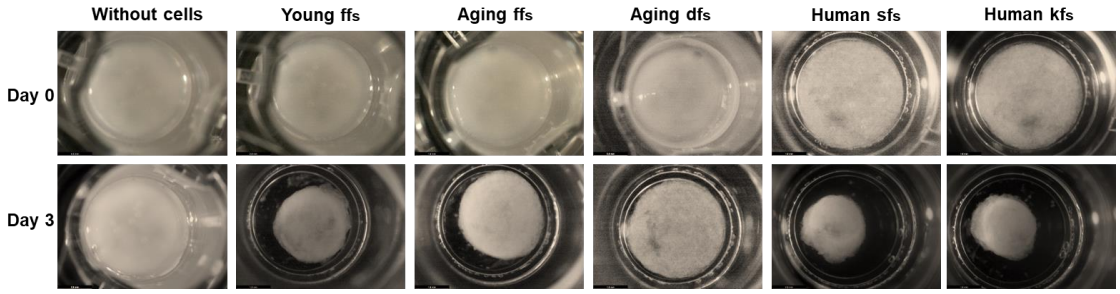

G

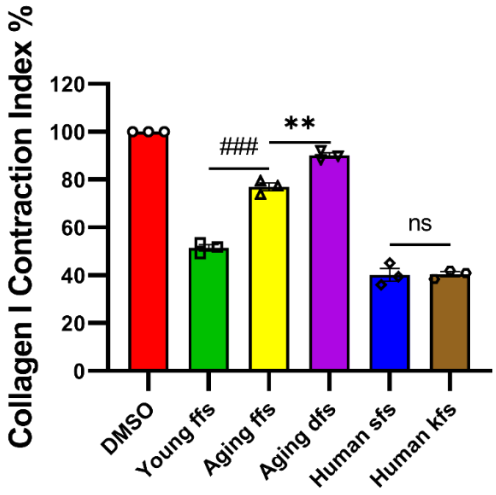

Fig.12 Contractility disfunctions of aged fascia is atributed to its fibroblasts

(**A**) Schematic diagram of 3D Matrigel culture of fascia. (**B**) Changes of young and aged fascia cultured in Matrigel. (**C**) Quantitative analysis of 3D Matrigel culture of fascia. (**D**) Young and aged fascia Morphology of membrane 3D Matrigel on the fifth day

after culture. (**E**) Real-time dynamic image of 3D Matrigel culture of young fascia and aged fascia. (**F**) Contraction experiments of transplanting different cells into type I collagen. (**G**) Quantitative analysis of the contraction assay of type I collagen. All p-values (p) indicated were obtained from two-tailed T-tests. Scale bars (B) = 200 μm, Scale bars (D) = 100 μm.

3.5 Wnt signaling can rejuvenate aged fibroblasts and accelerate wound healing

3.5.1 Impaired fibroblast differentiation in aging wounds leads to slowed wound healing

In in vitro fascia floating culture experiments (shown in Figure 13-A), the contractility of the aged fascia was greatly reduced compared to young fascia. Immunofluorescence staining of in vitro samples (Figure 13-B), showed that fibroblast differentiation is delayed in aged fascia than in young fascia, with young fascia completing the differentiation trajectory into contractile myofibroblasts at approximately day 6, whereas aged fascia completes differentiation within 10 days (Figure 13-C). In in vivo experiments (Figure 13-D), wound closure was slower in aged wounds than in young mice, and there was no significant difference in the rate of wound closure between young and middle-aged mice. Immunofluorescence staining results showed that fibroblast differentiation was completed in approximately 14 days in aged wounds and 7 days for younger wounds (Figure 13-E). Moreover, fascia fibroblast differentiation in vivo occurred mainly on days 3 to 10 in young mice, whereas in old mice, fascia fibroblast differentiation in vivo occurred mainly between day 10 to day 14. (Figure 13-F)

A

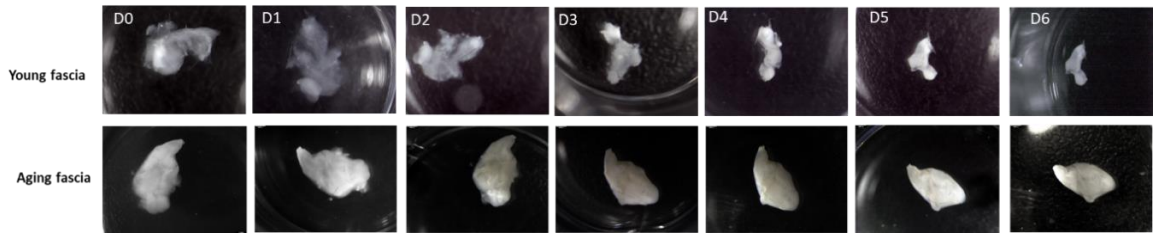
D0
D1
D2
D3
D4
D5
D6
Young fascia
Aging fascia

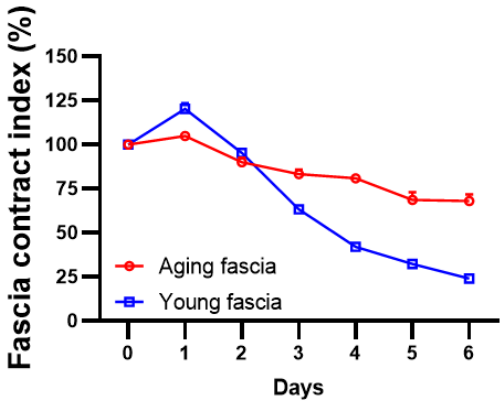
Fascia contract index (%)
150
125
100
75
50
25
0
0
1
2
3
4
5
6
Days
Aging fascia
Young fascia

B

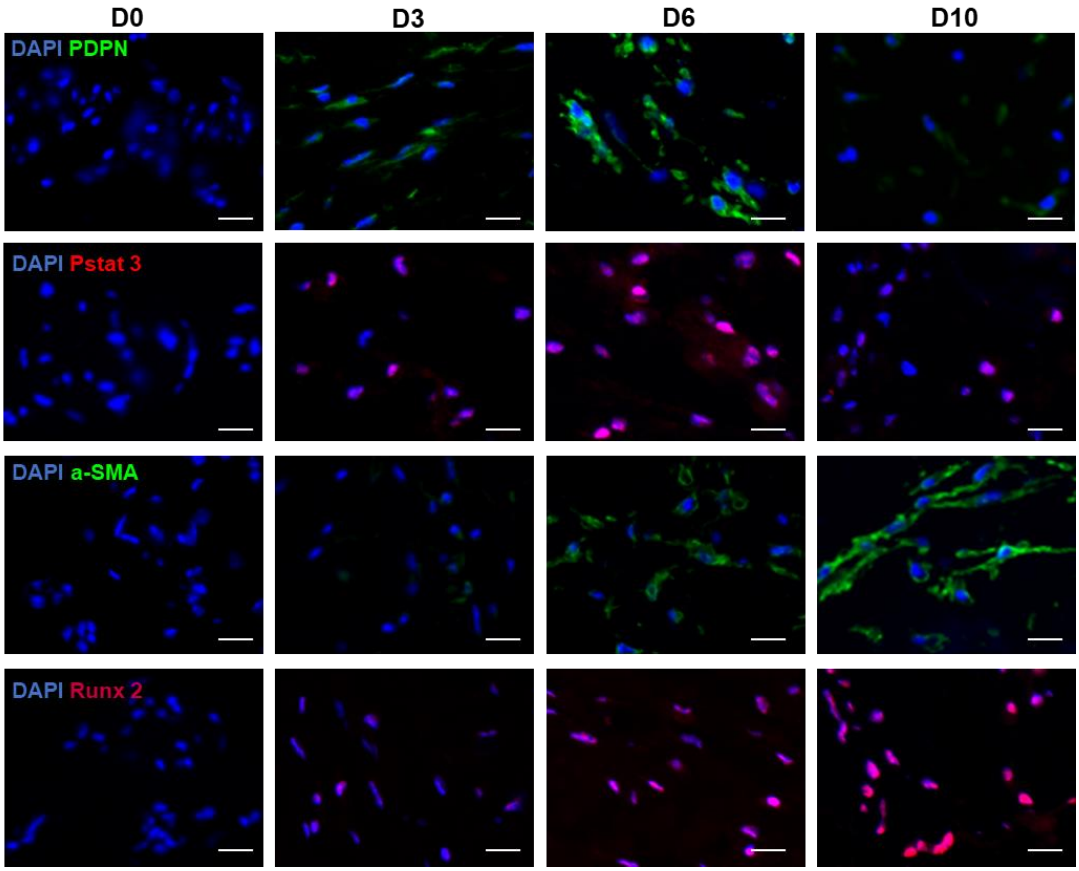
D0
D3
D6
D10
DAPI PDPN
DAPI Pstat 3
DAPI a-SMA
DAPI Runx 2

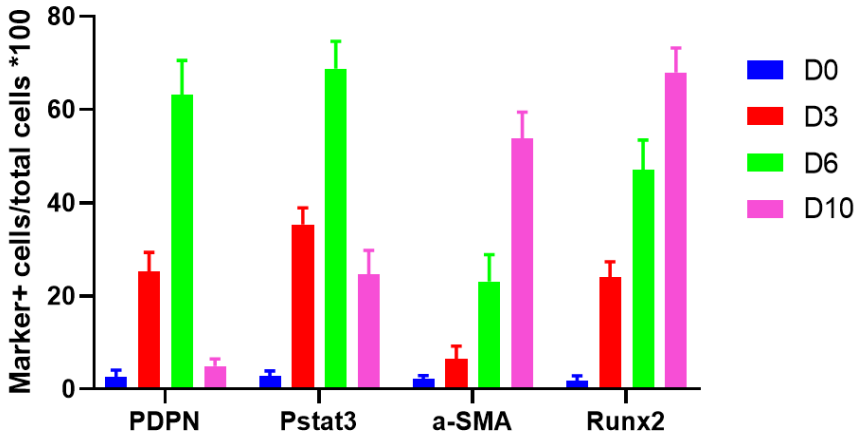
Marker+ cells/total cells *100
80
60
40
20
0
PDPN
Pstat3
a-SMA
Runx2
D0
D3
D6
D10

C

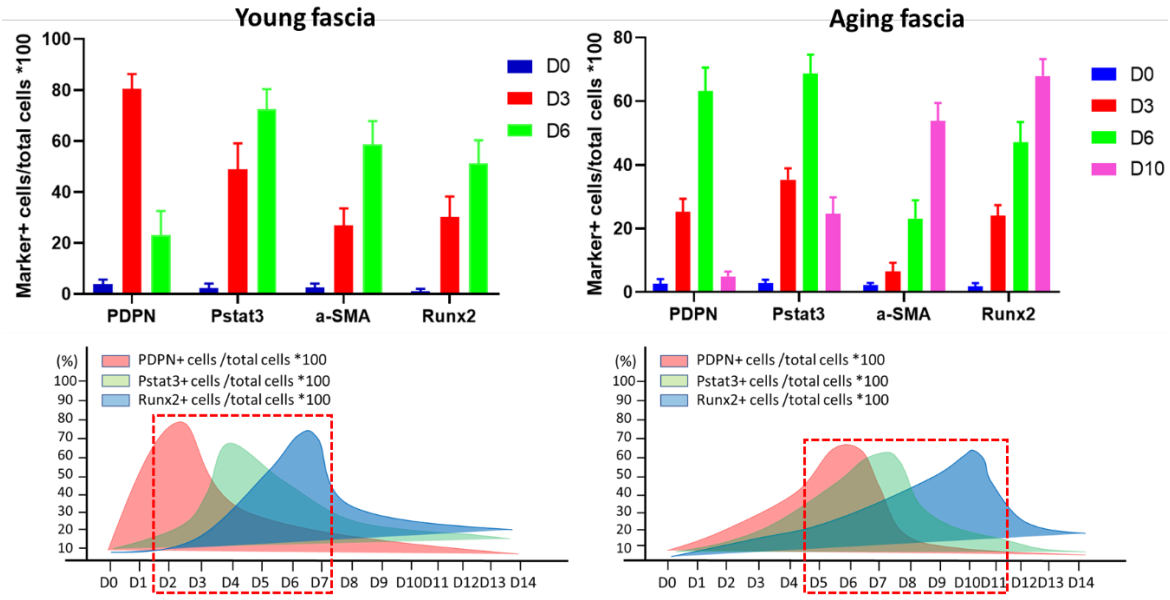
Young fascia
Aging fascia
Marker+ cells/total cells *100
PDPN
Pstat3
a-SMA
Runx2
D0
D3
D6
D10
(%)
PDPN+ cells /total cells *100
Pstat3+ cells /total cells *100
Runx2+ cells /total cells *100
D0 D1 D2 D3 D4 D5 D6 D7 D8 D9 D10 D11 D12 D13 D14

D

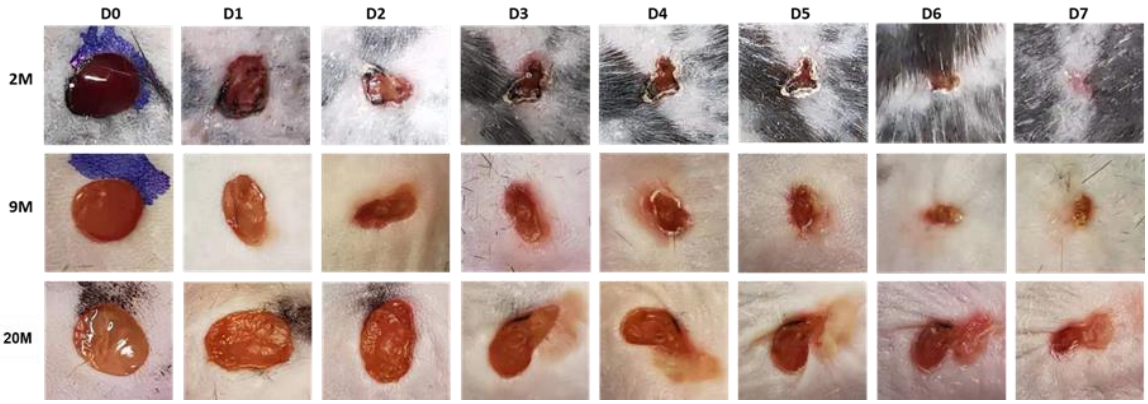
D0
D1
D2
D3
D4
D5
D6
D7
2M
9M
20M

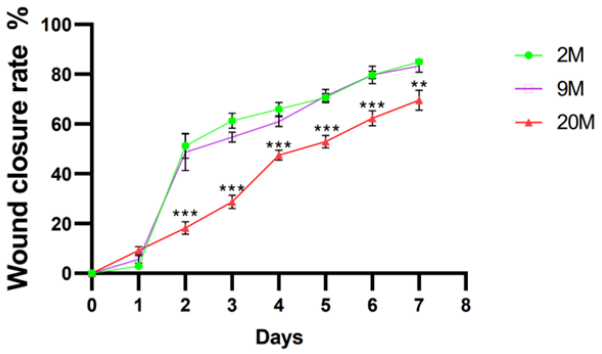
Wound closure rate %
100
80
60
40
20
0
0 1 2 3 4 5 6 7 8
Days
2M
9M
20M
***
***
***
***
***
**

E

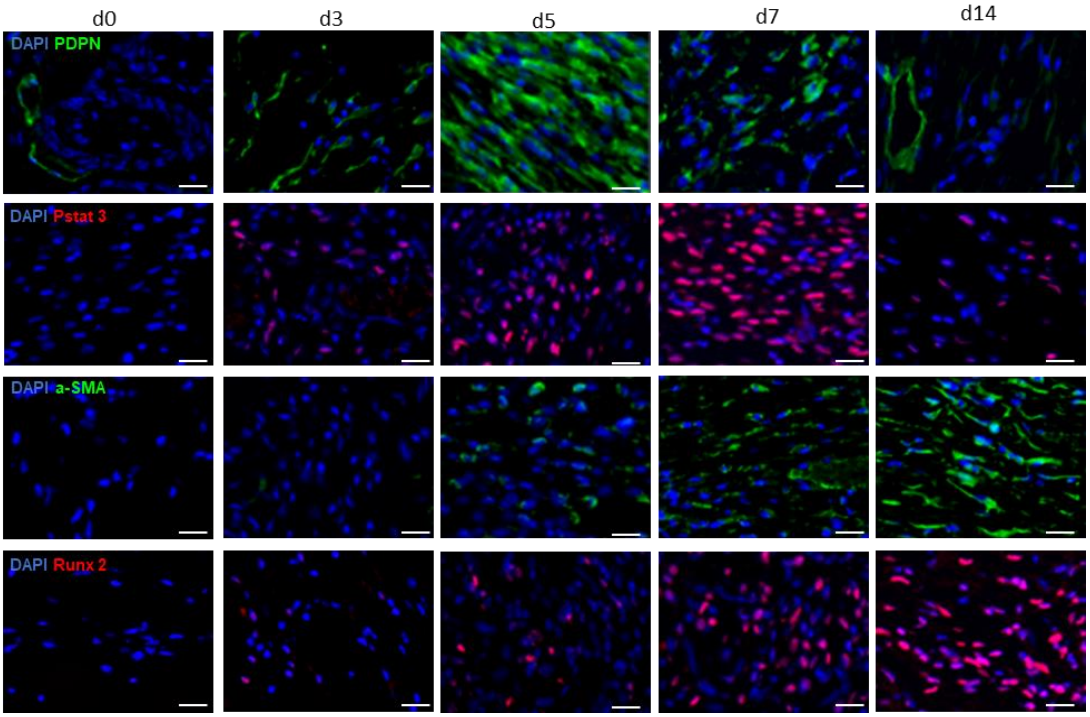
d0
d3
d5
d7
d14
DAPI PDPN
DAPI Pstat 3
DAPI a-SMA
DAPI Runx 2

F

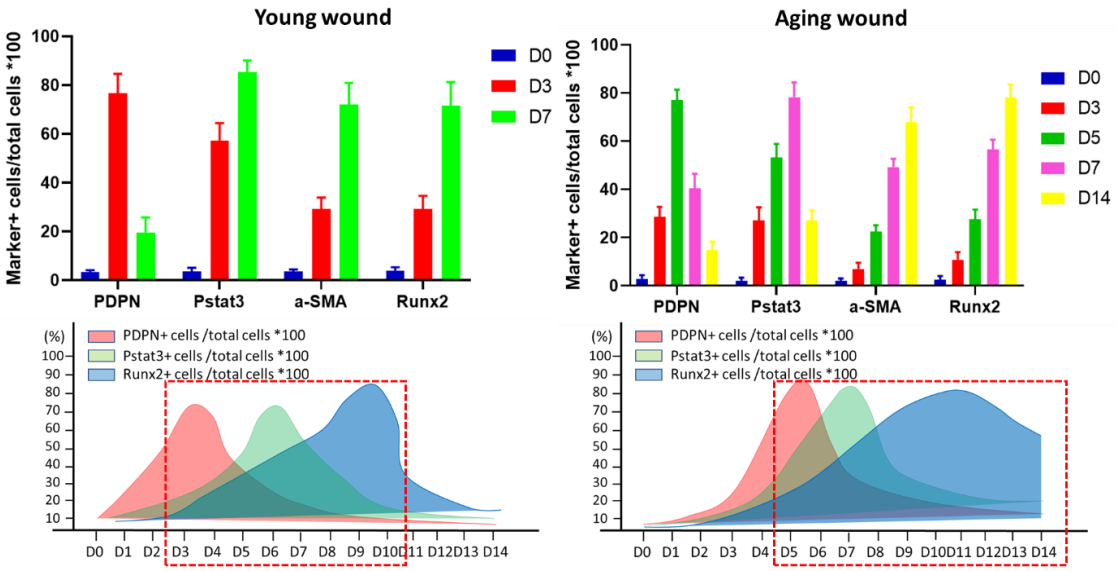
Young wound
Aging wound
Marker+ cells/total cells *100
D0
D3
D5
D7
D14
PDPN
Pstat3
a-SMA
Runx2
(%)
PDPN+ cells /total cells *100
Pstat3+ cells /total cells *100
Runx2+ cells /total cells *100
D0 D1 D2 D3 D4 D5 D6 D7 D8 D9 D10 D11 D12 D13 D14

Fig.13 Impaired fibroblast differentiation in aged wounds leads to delayed wound healing

(**A**)Suspension cultures of young fascia and aging and quantitative analysis of their contractility index (**B**) Immunofluorescence staining of cultured aging fascia, there are four groups of D0, D3, D6 and D10, each group was stained with PDPN, pSTAT3, a-SMA and Runx2 respectively. Then, a quantitative analysis of the expression of different genes in the four groups of fascia tissue was carried out. (**C**) During fascia suspension culture, PDPN, pSTAT3, a-SMA and Runx2 in Expression differences in young fascia and aging fascia. (**D**) Healing differences and quantitative analysis of excisional wounds in young and aging mice (**E**) Immunofluorescence staining of the aging wound, there are five groups of D0, D3, D5, D7 and D10, each group was stained with PDPN, pSTAT3, a-SMA and Runx2 respectively. Then, a quantitative analysis of the expression of different genes in the four groups of fascia tissue was carried out. (**F**) In vivo wound Differential expressions of PDPN, pSTAT3, a-SMA and Runx2 in young and aged wound fascia during healing. All p-values (p) indicated were obtained from two-tailed T-tests. Scale bars = 20 μm.

3.5.2 Wnt signaling enhances the rate of differentiation of aged fibroblasts and accelerates wound healing

In the in vitro fascia floating experiments (Fig. 14-A), we found that Wnt signalling agonists (CHIR) can accelerate the contractility of aged fascia, mimicking a young fascia phenotype. Immunofluorescence staining (Fig. 14-B), showed that CHIR can activate and accelerate the differentiation of aged fibroblasts (Fig. 14-C). CHIR further accelerates the closing speed of aged skin wounds, by promoting the transport and movements of fascia toward the wound (Fig. 14-D-E). Immunofluorescence staining (Fig. 14-F) showed that CHIR also activated and accelerated the differentiation capacity of aged fibroblasts in vivo (Fig. 14-G).

A

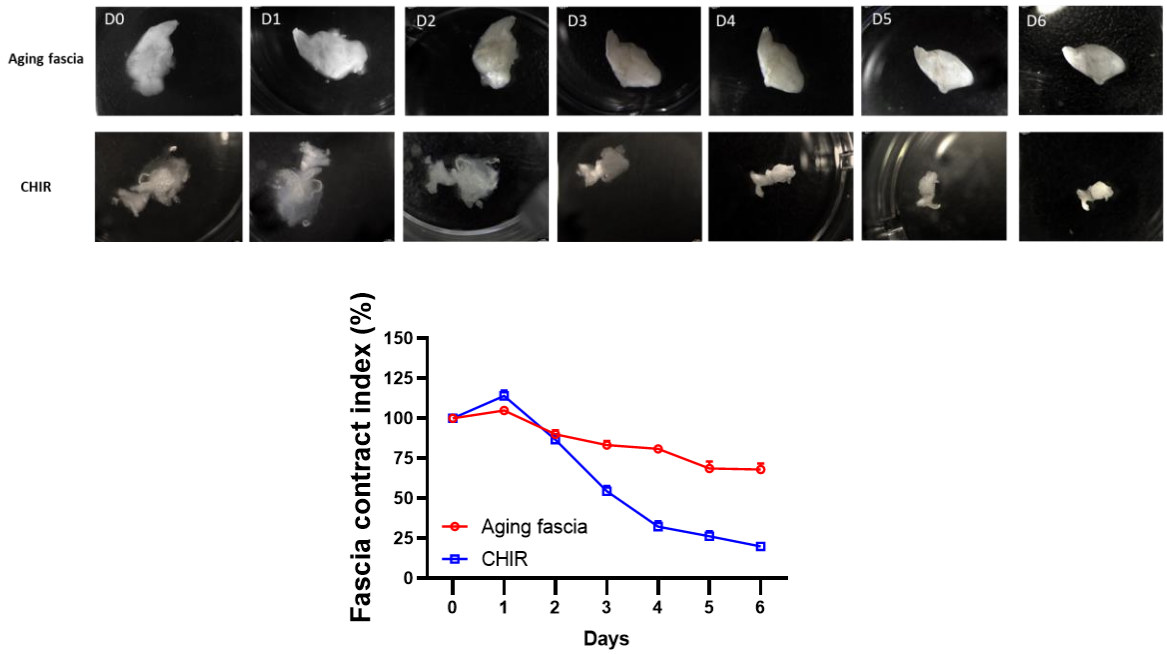
Aging fascia
CHIR
D0
D1
D2
D3
D4
D5
D6
Fascia contract index (%)
150
125
100
75
50
25
0
0
1
2
3
4
5
6
Days
Aging fascia
CHIR

B

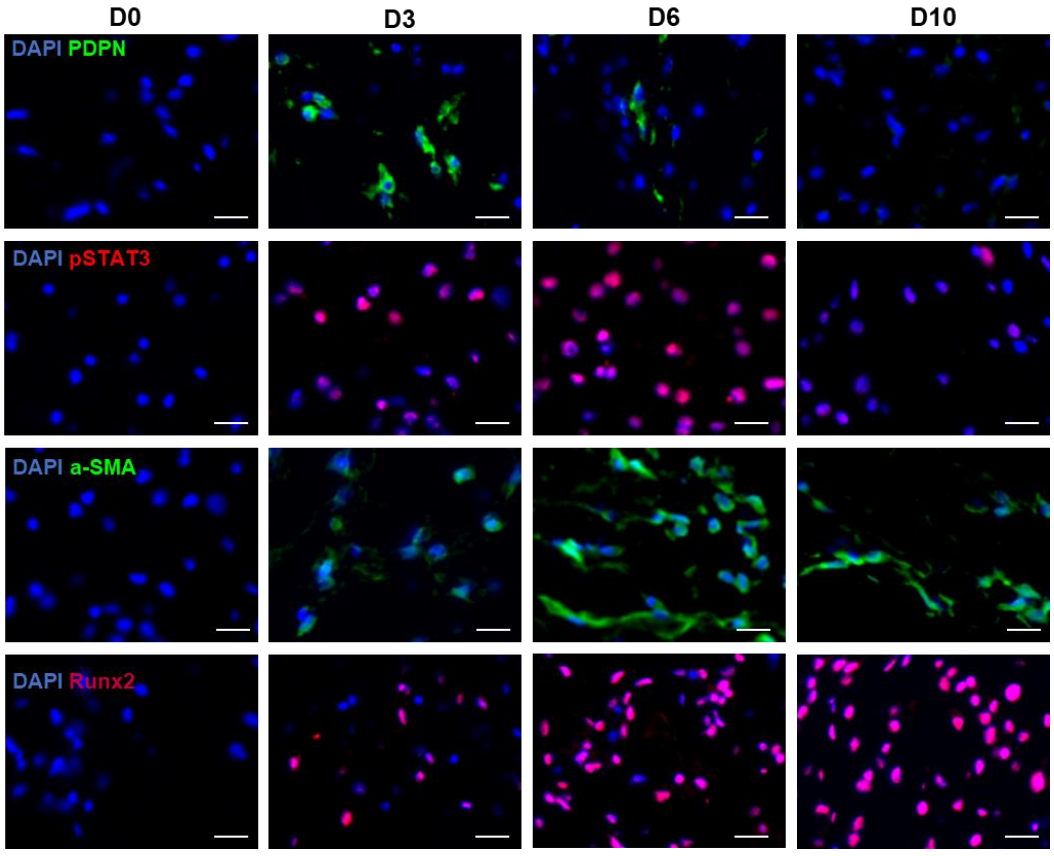
D0
D3
D6
D10
DAPI PDPN
DAPI pSTAT3
DAPI a-SMA
DAPI Runx2

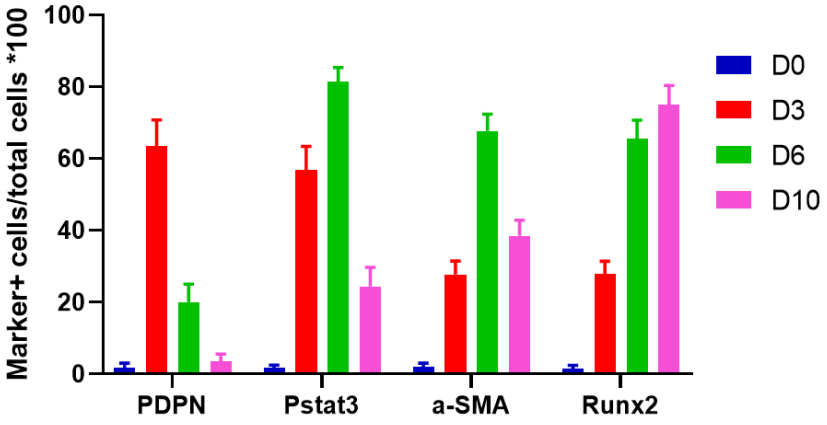
Marker+ cells/total cells *100
100
80
60
40
20
0
PDPN
Pstat3
a-SMA
Runx2
D0
D3
D6
D10

C

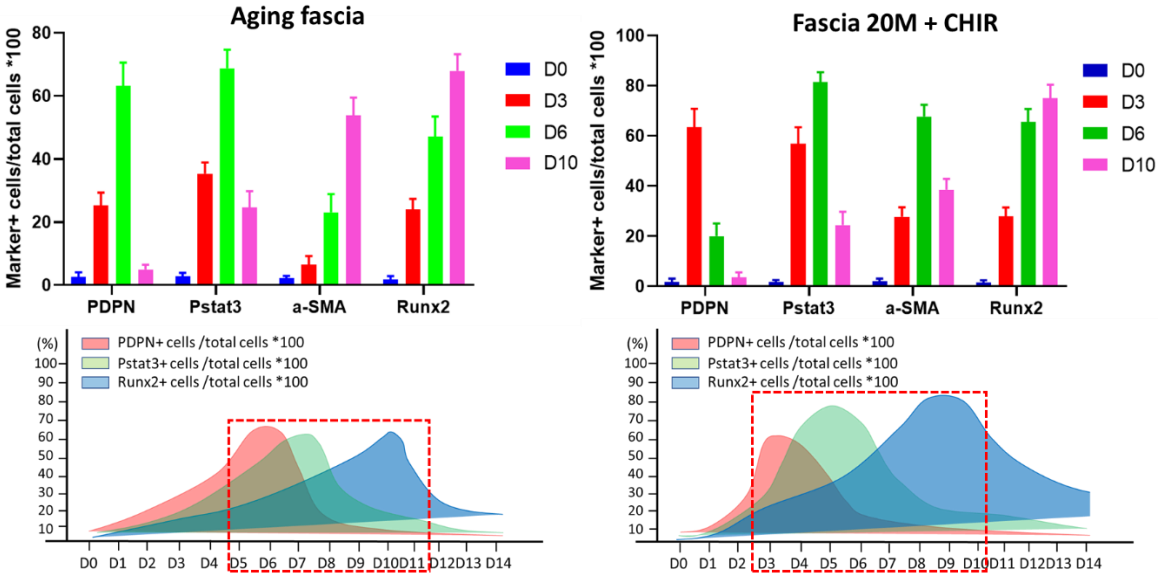
Aging fascia
Fascia 20M + CHIR
Marker+ cells/total cells *100
PDPN
Pstat3
a-SMA
Runx2
D0
D3
D6
D10
(%)
PDPN+ cells /total cells *100
Pstat3+ cells /total cells *100
Runx2+ cells /total cells *100
D0 D1 D2 D3 D4 D5 D6 D7 D8 D9 D10 D11 D12 D13 D14

D

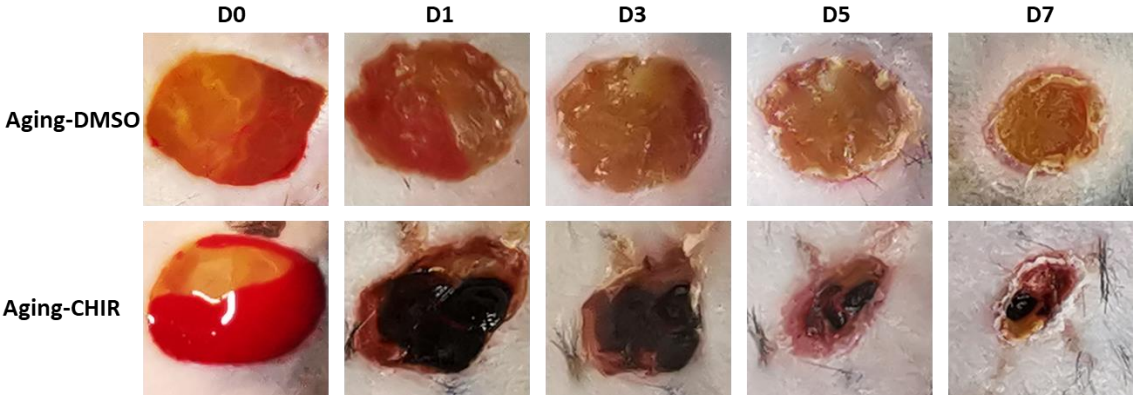
D0
D1
D3
D5
D7
Aging-DMSO
Aging-CHIR

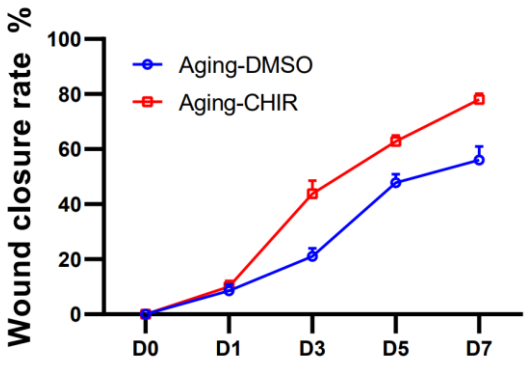
Wound closure rate %
100
80
60
40
20
0
Aging-DMSO
Aging-CHIR
D0
D1
D3
D5
D7

E

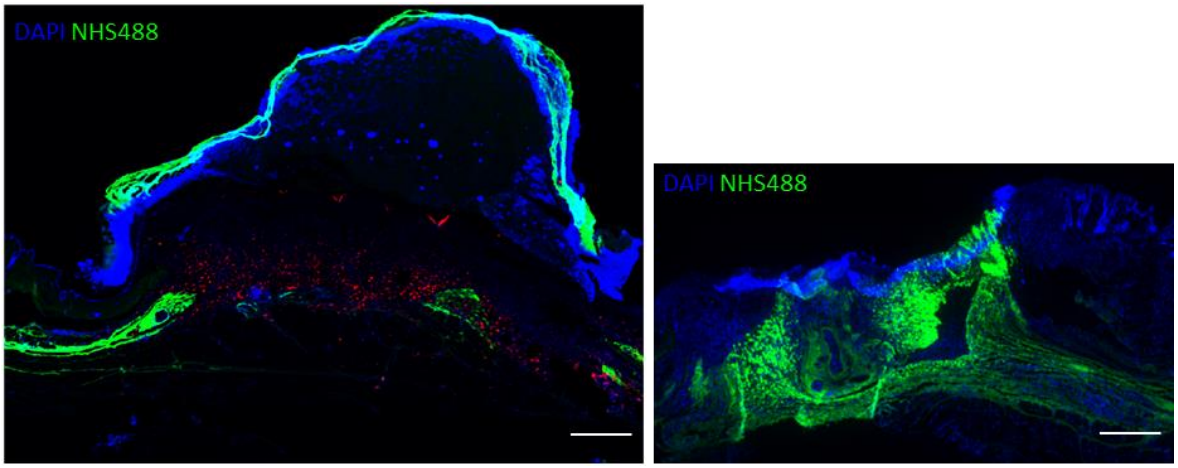
DAPI NHS488
DAPI NHS488

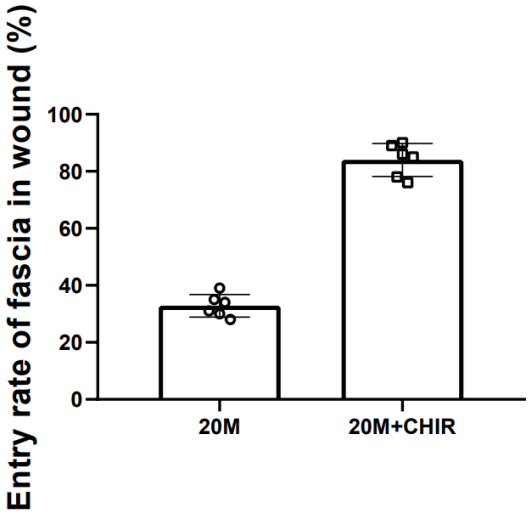
Entry rate of fascia in wound (%)
100
80
60
40
20
0
20M
20M+CHIR

F

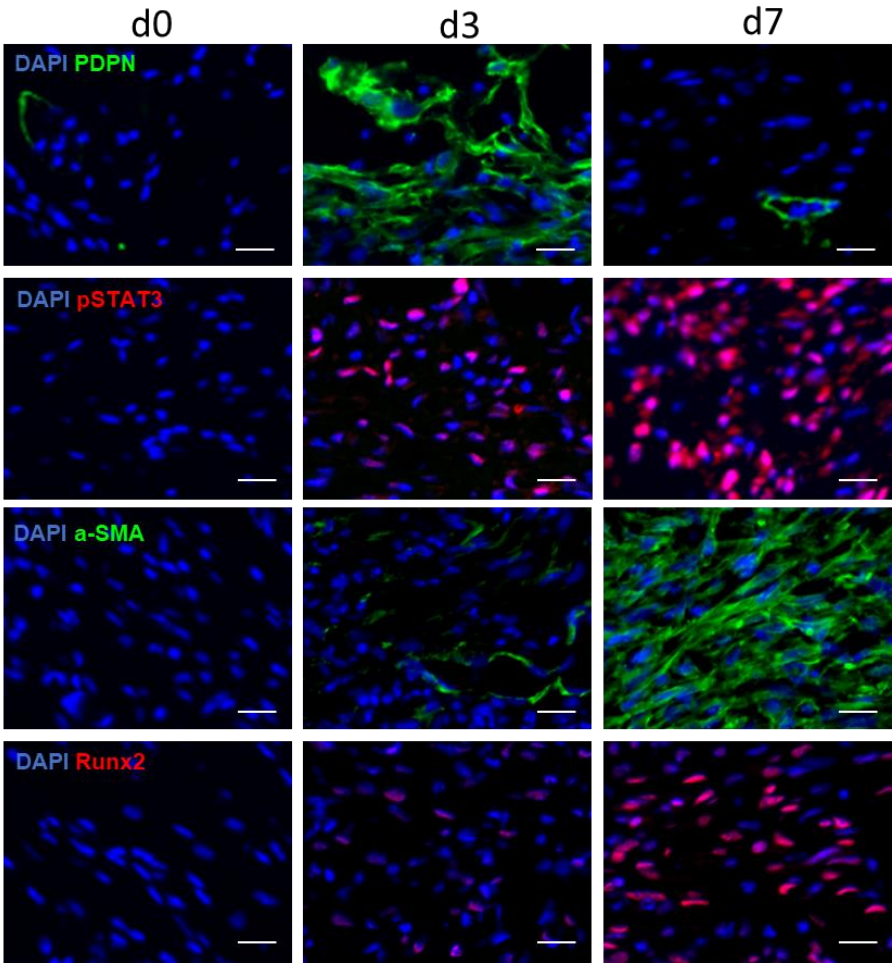
d0
d3
d7
DAPI PDPN
DAPI pSTAT3
DAPI a-SMA
DAPI Runx2

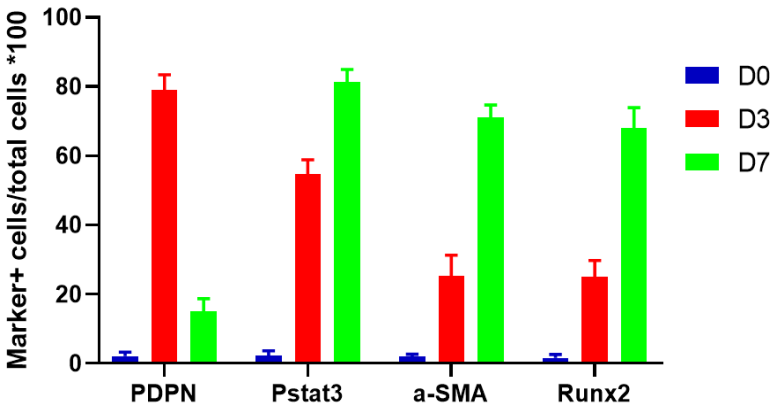
Marker+ cells/total cells *100
100
80
60
40
20
0
PDPN
Pstat3
a-SMA
Runx2
D0
D3
D7

G

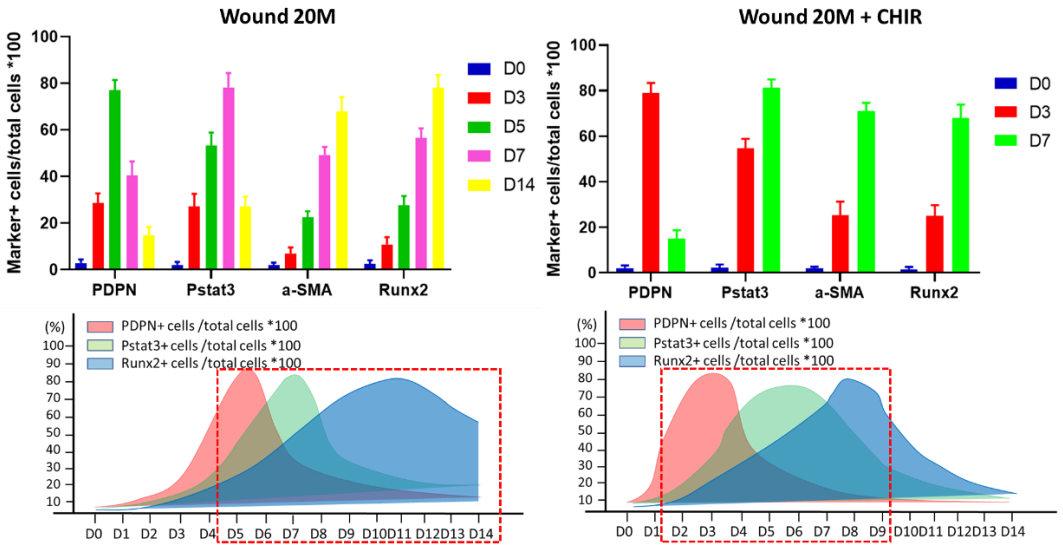

Fig.14 CHIR enhances the differentiation of aging fibroblasts and accelerates wound healing

(**A**) Suspension cultures of aging fascia and aging fascia with CHIR and quantitative analysis of their contractility index (**B**) Immunofluorescence staining of cultured aging fascia with CHIR, there are four groups of D0, D3, D6 and D10, each group was stained with PDPN, pSTAT3, a-SMA and Runx2 respectively. Then, a quantitative analysis of the expression of different genes in the four groups of fascia tissue was carried out. (**C**) During fascia suspension culture, PDPN, pSTAT3, a-SMA and Runx2 in expression differences in aging fascia and aging fascia with CHIR. (**D**) Healing differences and quantitative analysis of excisional wounds in aging mouse and aging mouse with CHIR (**E**)The labeling experiment of fascia. The left side of the figure is the situation of the labeled fascia entering the wound on the seventh day of aging, and the right side of the figure is the situation of the labeled fascia entering the wound on the seventh day of aging with CHIR, and the bottom of the figure is the corr esponding Quantitative analysis. (**F**) Immunofluorescence staining of the aging wound with CHIR, there are three groups of D0, D3 and D7, each group was stained with PDPN, pSTAT3, a-SMA and Runx2 respectively. Then, a quantitative analysis of the expression of different genes in the three groups of the aging wound with CHIR was carried out. (**G**) The differential expressions of PDPN, pSTAT3, a-SMA and Runx2 in aging mice and aging mice with CHIR during healing. All p-values (p) indicated were obtained from two-tailed T-tests. Scale bars (B, F) = 20 μm, Scale bars(E) = 500 μm.

4. Discussion

4.1 Fibroblast-mediated contraction of fascia leads to wound closure

This study is based on previous findings by our group, linking fascia transport toscar formation and wound healing (Correa-Gallegos et al., 2019)(Wan et al., 2021). Here, we expand on these early studies and analyze the cellular and molecular processes in the fascia that occur during wound healing and ageing. We designed fascia ECM labelling experiments, as shown in Fig. 1, to pre-label the fascia, then generate wounds on the fourth day after labelling, and then collect samples at different time points for analysis. When the skin is not injured, the labelled fascia ECM remains immobile beneath the PC muscle layer, and when the skin is injured, the labelled fascia transports toward the wound bed to quickly fill the wound with provisional scar tissue, corroborating our previous findings (Correa-Gallegos et al., 2019; Jiang et al., 2020; Jiang and Rinkevich, 2021b; Wan et al., 2021). When we used scissors to remove the fascia around the wound, the closure of the wound slowed, due to lack of fascia transport, and the resulting scar was significantly diminished. This suggests that the fascia is the key factor leading to wound healing, that the transport of the fascia into wounds is the basis for scar formation, and skin contraction. When fascia is removed or blocked, wound closure is significantly delayed, resulting in delayed wound healing.

Traditionally, skin contraction and wound closure is thought to occur by the panniculus carnosus muscle followed by epidermal proliferation to breach open wounds (Zomer and Trentin, 2018b). However, our experiments presented here indicate that the contraction of the full-thickness skin depends on fascia tissue alone, whereas panniculus carnosus muscle does not shrink or contract. Moreover, that this contractility of the fascia is dependent on its fibroblasts. Genetically depleting fascia fibroblasts blocks contraction. Furthermore, reinstating fibroblast into the fascia could recreate the contracture phenotypes, whereas neutrophils and macrophages could not cause fascia contraction. Indeed, lymph node contraction is also mediated by its resident reticular fibroblasts, (Acton et al., 2014; Astarita et al., 2015; Kopanska et al., 2015; Horsnell et

al., 2022), implying for common mechanisms of tissue contraction amongst different tissues/organs of the body.

4.2 Fascia fibroblasts undergo differentiation to contract skin

Most mammalian and human organs have the ability to respond to tissue damage by forming scar tissue (Plikus et al., 2021; Soliman et al., 2021; Tomasek et al., 2002; “Wound repair and regeneration | Nature,” n.d.). Our single-cell sequencing results, shows that fibroblasts in wounds undergo different stages of differentiation, from stable Procr+ fibroblasts to PDPN+ proinflammatory fibroblasts, and then to Pstat3+ proto-myofibroblasts, Finally, fibroblasts differentiate into myofibroblast that express RUNX2+. Our findings reveal the stepwise differentiation that occurs during wound repair to elicit myofibroblast differentiation, tissue contraction and wound healing. Furthermore, we corroborate the universality of our findings, by showing that human fascia, we found undergoes the same differentiation trajectory as in mouse fascia.

4.3 Inhibiting fascia fibroblast differentiation delays wound healing

HIF1a is a basic helix-loop-helix PAS domain-containing protein that is considered a master transcriptional regulator of cellular and developmental responses to hypoxia(Iyer et al., 1998). HIF1-a has a regulatory role in skin healing (Hong et al., 2014). Researchers at Stanford University School of Medicine demonstrated that HIF1A activation can prevent and treat chronic wounds in diabetic and aged mice (University et al., 2015), and can accelerate wound healing. In addition, HIF-1A modulation has been described to have pro-regenerative effects on aged skin (Bonham et al., 2018; Duscher et al., 2015) (Bonham et al., 2018).

When we used HIF1-α inhibitors and Pstat3 antagonists to culture the fascia in vitro, the fascia no longer contracted, indicating that inhibiting fibroblast differentiation processes directly blocks skin contraction, further linking fascia fibroblasts to wound

contraction. In vivo experiments, wound closure was greatly slowed down after the use of HIF-α inhibitors, and the expressions of PDPN, Pstat3, and RUNX2 were sharply reduced, indicating that HIF-α inhibitors inhibited the conversion of Procr+ fibroblasts to PDPN+ proinflammatory fibroblasts. The cellular transformation, reduction of PDPN+ proinflammatory fibroblasts also indirectly led to the reduction of Pstat3+ and RUNX2+ fibroblasts. Pstat3 antagonists then inhibited the differentiation of PDPN+ proinflammatory fibroblasts to Pstat3+ proto-myofibroblasts, as did the fascia no longer shrink. Therefore, the contraction of the fascia is mainly caused by the transformation of the proto-myofibroblast of Pstat3+ to the myofibroblast of RUNX2+. If any step of this transformation process is inhibited, the contraction of the fascia will be inhibited. Then in our conditional knockout experiment, after PDPN conditional knockout, the contractility of the cultured fascia in vitro was greatly weakened, and the wound closure speed in the in vivo experiment was greatly slowed down. This further suggests a role for the differentiation of wound fibroblasts in wound healing. The traditional theory of wound healing is that fibroblast progenitor cells proliferate and differentiate into myofibroblasts, and then myofibroblasts express a-SMA to cause wound contraction. From our experimental results, the fascia tissue in vitro expresses a-SMA on the sixth day, and in vivo also expresses a-SMA on the seventh day, but the fascia in vitro began to shrink on the second day, and the in vivo fascia began to shrink on the second day. The wound closed quickly on the second day of the experiment, so the contraction of the fascia and the rapid closure of the wound were not caused by a-SMA positive cells, but by the differentiation of Pstat3 positive fibroblasts to Runx2 positive fibroblasts.

Keloid, also known as keloid disorder and keloidal scar(Lee et al., 2004; Tan et al., 2019), is the formation of a scar that, depending on its maturity, consists primarily of type III (early) or type I (late) collagen. This is the result of overgrowth of granulation tissue (type 3 collagen) at the site of healing skin damage, which is then slowly replaced by type 1 collagen. In human skin keloid samples, the normal skin part did not undergo the process of fibroblast transformation, while the fibroblasts in the keloid part continued to express Runx2, while the normal skin part did not express Runx2. Because the skin undergoes fibroblasts after injury The transformation of cells returns to static fibroblasts at the later stage of the wound, and the fibroblasts are no longer transformed. However, in keloids, fibroblasts continue to express Runx2 and no longer continue to transform into static fibroblasts. The obstacle to this transformation may be the cause of keloid formation and may become a clinical target for keloid treatment.

4.4 Fascial fibroblasts heterogeneity leads to differences in wound healing

When the skin undergoes aging, we can find that the thickness of the dermis and the fascia layer is thinner, the adipose tissue in the aging skin layer is also greatly increased, and the density of cells in the aging fascia layer is also relatively reduced compared to the young fascia layer. Aged wound closure slowed when the skin was injured, with no significant difference in wound closure between 2- and 9-month-old mice. Histologically it can also be seen that re-epithelialization of aged wounds is also greatly slowed relative to young mice.

Then, through the fascia labeling experiment, we can also see that after the aging skin is injured, the labeled fascia hardly surges to the center of the wound, which is also a direct factor that slows down the closure of the aging wound. Then in the in vitro fascia suspension experiment, the contractility of the aged fascia was weakened compared to that of the young fascia, which can be seen more clearly in the live-image. Using the skin chimeric transplantation experiment, we can see that the young fascia surges more towards the wound and contributes more to the healing of the wound.

The migration ability of fibroblasts can be obtained from the 3D culture results, and the migration ability of fibroblasts is also weakened after fascia aging. Then, it can be clearly seen from the 3D imaging that the young fibroblasts are more stretched and slenderer, while the old fibroblasts are thicker and curled up. From the live image, the difference in fibroblast migration can be seen in real time. Finally, in the type I collagen contraction experiment, we added the same number of different cells to type I collagen. It can be seen that the contraction ability of young mouse fascial fibroblasts is stronger than that of aged fascial fibroblasts. The contractility of fibroblasts is very small, which also indicates that fascial fibroblasts are mainly responsible for wound healing, and the aging of fibroblasts leads to the weakening of the contractility of fascia, causing the discordance of aging wounds to slow down. Then human-derived fibroblasts have stronger contractility than mouse fibroblasts, which may also be the main factor responsible for the difference in wound healing between humans and mice.

4.5 CHIR can rejuvenate senescent fibroblasts and accelerate wound healing

Then in our in vitro fascia experiments, we found that the contraction of aging fascia is slower than that of young fascia, and in the type I collagen experiment, we have shown that it is because of the aging of fibroblasts. Fibroblast differentiations in aged fascia were then found to have longer periods of differentiation relative to fibroblast differentiations in young fascia from our fluorescent staining of fascial tissue in vitro. From the quantitative graph of the in vitro experiment, we found that the differentiation period of young fascia is roughly from the 2nd to the 7th day of culture, but the differentiation period of the aged fascia is delayed, which occurs from the 5th day to the 11th day of culture, so A direct factor leading to the slowing down of aging fascia contraction is due to the differentiation disorder of aging fibroblasts. Then in our in vivo experiments, the contraction of fascia is a direct factor in causing wound closure, and the turnover of fascial fibroblasts in aged wounds is also delayed relative to that in young wounds, which directly leads to decreased wound closure in aged wounds.

CHIR 99021 is a chemical that acts as an inhibitor of the GSK-3 enzyme, it has been shown to be useful in molecular biology applications involving the conversion of one cell type into another(An et al., 2010; “Chemical compound-based direct reprogramming for future clinical applications - PMC,” n.d.; Singh et al., 2015). When we used CHIR and aged fascia for co-culture, the contraction rate of the fascia was greatly accelerated, and it returned to the state of young fascia. It can be seen from the immunofluorescence results that the use of CHIR makes the differentiation period of the fascia cultured in vitro earlier, which is also the essential reason for the accelerated contraction of the fascia. In our in vivo results, the closure of aged wounds was accelerated after treatment with CHIR, followed by increased fascia entry into the wound, returning to the healing phenotype of young wounds. As shown by immunofluorescence, CHIR is an advanced fibroblast differentiation cycle in aging wounds, which leads to accelerated healing of aging wounds.

5. Summary

This thesis characterizes the differences in wound healing between young and aged skin by focusing on the fascia. The ability of aged fascia to contract is greatly diminished, resulting in slower wound closure. The reduced contractility of aged fascia is due to the reduced ability of fibroblasts in the fascia to fully complete cellular differentiate after injury. We then used a drug, CHIR, that reactivates the differentiation capacity of aged fibroblasts, thereby accelerating the contracture of aged fascia and promoting the healing of aged skin wounds. Therefore, in this study, we uncover the molecular mechanisms underlying aged wound healing, and found that CHIR can reactivate the differentiation vitality of aging fibroblasts, thereby accelerating the healing of aged wounds.

References

Acton, S.E., Farrugia, A.J., Astarita, J.L., Mourão-Sá, D., Jenkins, R.P., Nye, E., Hooper, S., van Blijswijk, J., Rogers, N.C., Snelgrove, K.J., Rosewell, I., Moita, L.F., Stamp, G., Turley, S.J., Sahai, E., Reis e Sousa, C., 2014. Dendritic cells control fibroblastic reticular network tension and lymph node expansion. Nature 514, 498–502. https://doi.org/10.1038/nature13814

Ahn, A.C., Kaptchuk, T.J., 2011. Spatial anisotropy analyses of subcutaneous tissue layer: potential insights into its biomechanical characteristics. J. Anat. 219, 515–524. https://doi.org/10.1111/j.1469-7580.2011.01407.x

Amano, K., Naito, M., Matsuo, M., 2020. Morphological study of human facial fascia and subcutaneous tissue structure by region through SEM observation. Tissue Cell 67, 101437. https://doi.org/10.1016/j.tice.2020.101437

An, W.F., Germain, A.R., Bishop, J.A., Nag, P.P., Metkar, S., Ketterman, J., Walk, M., Weiwer, M., Liu, X., Patnaik, D., Zhang, Y.-L., Gale, J., Zhao, W., Kaya, T., Barker, D., Wagner, F.F., Holson, E.B., Dandapani, S., Perez, J., Munoz, B., Palmer, M., Pan, J.Q., Haggarty, S.J., Schreiber, S.L., 2010. Discovery of Potent and Highly Selective Inhibitors of GSK3b, in: Probe Reports from the NIH Molecular Libraries Program. National Center for Biotechnology Information (US), Bethesda (MD).

Astarita, J.L., Cremasco, V., Fu, J., Darnell, M.C., Peck, J.R., Nieves-Bonilla, J.M., Song, K., Kondo, Y., Woodruff, M.C., Gogineni, A., Onder, L., Ludewig, B., Weimer, R.M., Carroll, M.C., Mooney, D.J., Xia, L., Turley, S.J., 2015. The CLEC-2-podoplanin axis controls the contractility of fibroblastic reticular cells and lymph node microarchitecture. Nat. Immunol. 16, 75–84. https://doi.org/10.1038/ni.3035

Bainbridge, P., 2013. Wound healing and the role of fibroblasts. J. Wound Care 22, 407–408, 410–412. https://doi.org/10.12968/jowc.2013.22.8.407

Baroni, A., Buommino, E., De Gregorio, V., Ruocco, E., Ruocco, V., Wolf, R., 2012. Structure and function of the epidermis related to barrier properties. Clin. Dermatol. 30, 257–262. https://doi.org/10.1016/j.clindermatol.2011.08.007

Bartos, F., 1970. [Function of local fibroblasts in the process of wound healing]. Biologia (Bratisl.) 25, 893–897.

Bonham, C.A., Rodrigues, M., Galvez, M., Trotsyuk, A., Stern-Buchbinder, Z., Inayathullah, M., Rajadas, J., Gurtner, G.C., 2018. Deferoxamine can prevent pressure ulcers and accelerate healing in aged mice. Wound Repair Regen. Off. Publ. Wound Heal. Soc. Eur. Tissue Repair Soc. 26, 300–305. https://doi.org/10.1111/wrr.12667

Cabanac, M., 1975. Temperature regulation. Annu. Rev. Physiol. 37, 415–439. https://doi.org/10.1146/annurev.ph.37.030175.002215

Campisi, J., 1998. The role of cellular senescence in skin aging. J. Investig. Dermatol. Symp. Proc. 3, 1–5.

Chemical compound-based direct reprogramming for future clinical applications - PMC [WWW Document], n.d. URL https://www.ncbi.nlm.nih.gov/pmc/articles/PMC5938430/ (accessed 8.28.22).

Choi, E.H., 2019. Aging of the skin barrier. Clin. Dermatol. 37, 336–345. https://doi.org/10.1016/j.clindermatol.2019.04.009

Correa-Gallegos, D., Jiang, D., Christ, S., Ramesh, P., Ye, H., Wannemacher, J., Kalgudde Gopal, S., Yu, Q., Aichler, M., Walch, A., Mirastschijski, U., Volz, T., Rinkevich, Y., 2019. Patch repair of deep wounds by mobilized fascia. Nature 576, 287–292. https://doi.org/10.1038/s41586-019-1794-y

Draelos, Z.D., 2018. The science behind skin care: Moisturizers. J. Cosmet. Dermatol. 17, 138–144. https://doi.org/10.1111/jocd.12490

Driskell, R.R., Lichtenberger, B.M., Hoste, E., Kretzschmar, K., Simons, B.D., Charalambous, M., Ferron, S.R., Herault, Y., Pavlovic, G., Ferguson-Smith, A.C., Watt, F.M., 2013. Distinct fibroblast lineages determine dermal architecture in skin development and repair. Nature 504, 277–281. https://doi.org/10.1038/nature12783

Duscher, D., Neofytou, E., Wong, V.W., Maan, Z.N., Rennert, R.C., Inayathullah, M., Januszyk, M., Rodrigues, M., Malkovskiy, A.V., Whitmore, A.J., Walmsley, G.G., Galvez, M.G., Whittam, A.J., Brownlee, M., Rajadas, J., Gurtner, G.C., 2015. Transdermal deferoxamine prevents pressure-induced diabetic ulcers. Proc. Natl. Acad. Sci. U. S. A. 112, 94–99. https://doi.org/10.1073/pnas.1413445112

Effective use of mesenchymal stem cells in human skin substitutes generated by tissue engineering - PubMed [WWW Document], n.d. URL https://pubmed.ncbi.nlm.nih.gov/30924522/ (accessed 8.31.22).

Elçin, Y.M., İnanç, B., Elçin, A.E., 2016. Differentiation of Human Embryonic Stem Cells on Periodontal Ligament Fibroblasts. Methods Mol. Biol. Clifton NJ 1307, 223–235. https://doi.org/10.1007/7651_2014_130

Eming, S.A., Krieg, T., Davidson, J.M., 2007. Inflammation in wound repair: molecular and cellular mechanisms. J. Invest. Dermatol. 127, 514–525. https://doi.org/10.1038/sj.jid.5700701

Fatima, Q., Choudhry, N., Choudhery, M.S., 2018. Umbilical Cord Tissue Derived Mesenchymal Stem Cells can Differentiate into Skin Cells. Open Life Sci. 13, 544–552. https://doi.org/10.1515/biol-2018-0065

Gruber, F., Kremslehner, C., Eckhart, L., Tschachler, E., 2020. Cell aging and cellular senescence in skin aging - Recent advances in fibroblast and keratinocyte biology. Exp. Gerontol. 130, 110780. https://doi.org/10.1016/j.exger.2019.110780

Han, Y., Chai, J., Sun, T., Li, D., Tao, R., 2011. Differentiation of human umbilical cord mesenchymal stem cells into dermal fibroblasts in vitro. Biochem. Biophys. Res. Commun. 413, 561–565. https://doi.org/10.1016/j.bbrc.2011.09.001

Hoffman, M., MD, n.d. The Skin (Human Anatomy): Picture, Definition, Function, and Skin Conditions [WWW Document]. WebMD. URL https://www.webmd.com/skin-problems-and-treatments/picture-of-the-skin (accessed 8.30.22).

Hong, W.X., Hu, M.S., Esquivel, M., Liang, G.Y., Rennert, R.C., McArdle, A., Paik, K.J., Duscher, D., Gurtner, G.C., Lorenz, H.P., Longaker, M.T., 2014. The Role of Hypoxia-Inducible Factor in Wound Healing. Adv. Wound Care 3, 390–399. https://doi.org/10.1089/wound.2013.0520

Horsnell, H.L., Tetley, R.J., De Belly, H., Makris, S., Millward, L.J., Benjamin, A.C., Heeringa, L.A., de Winde, C.M., Paluch, E.K., Mao, Y., Acton, S.E., 2022. Lymph node homeostasis and adaptation to immune challenge resolved by fibroblast network mechanics. Nat. Immunol. 23, 1169–1182. https://doi.org/10.1038/s41590-022-01272-5

Hu, R., Ling, W., Xu, W., Han, D., 2014. Fibroblast-like cells differentiated from adipose-derived mesenchymal stem cells for vocal fold wound healing. PloS One 9, e92676. https://doi.org/10.1371/journal.pone.0092676

Ishida, T., Takeuchi, K., Hayashi, S., Kawata, S., Hatayama, N., Qu, N., Shibata, M., Itoh, M., 2015. Anatomical structure of the subcutaneous tissue on the anterior surface of human thigh. Okajimas Folia Anat. Jpn. 92, 1–6. https://doi.org/10.2535/ofaj.92.1

Iyer, N.V., Kotch, L.E., Agani, F., Leung, S.W., Laughner, E., Wenger, R.H., Gassmann, M., Gearhart, J.D., Lawler, A.M., Yu, A.Y., Semenza, G.L., 1998. Cellular and developmental control of O2 homeostasis by hypoxia-inducible factor 1α. Genes Dev. 12, 149–162.

Jiang, D., Christ, S., Correa-Gallegos, D., Ramesh, P., Kalgudde Gopal, S., Wannemacher, J., Mayr, C.H., Lupperger, V., Yu, Q., Ye, H., Mück-Häusl, M., Rajendran, V., Wan, L., Liu, J., Mirastschijski, U., Volz, T., Marr, C., Schiller, H.B., Rinkevich, Y., 2020. Injury triggers fascia fibroblast collective cell migration to drive scar formation through N-cadherin. Nat. Commun. 11, 5653. https://doi.org/10.1038/s41467-020-19425-1

Jiang, D., Rinkevich, Y., 2021a. Distinct fibroblasts in scars and regeneration. Curr. Opin. Genet. Dev. 70, 7–14. https://doi.org/10.1016/j.gde.2021.04.005

Jiang, D., Rinkevich, Y., 2021b. Furnishing Wound Repair by the Subcutaneous Fascia. Int. J. Mol. Sci. 22, 9006. https://doi.org/10.3390/ijms22169006

Kanitakis, J., 2002. Anatomy, histology and immunohistochemistry of normal human skin. Eur. J. Dermatol. EJD 12, 390–399; quiz 400–401.

Katoh, N., Tennstedt, D., Abellan van Kan, G., Saint Aroman, M., Loir, A., Bacqueville, D., Duprat, L., Guiraud, B., Bessou-Touya, S., Duplan, H., 2018. Gerontodermatology: the fragility of the epidermis in older adults. J. Eur. Acad. Dermatol. Venereol. JEADV 32 Suppl 4, 1–20. https://doi.org/10.1111/jdv.15253

Khavkin, J., Ellis, D.A.F., 2011. Aging skin: histology, physiology, and pathology. Facial Plast. Surg. Clin. N. Am. 19, 229–234. https://doi.org/10.1016/j.fsc.2011.04.003

Kodera, S., Gomez-Tames, J., Hirata, A., 2018. Temperature elevation in the human brain and skin with thermoregulation during exposure to RF energy. Biomed. Eng. Online 17, 1. https://doi.org/10.1186/s12938-017-0432-x

Kopanska, K.S., Bussonnier, M., Geraldo, S., Simon, A., Vignjevic, D., Betz, T., 2015. Quantification of collagen contraction in three-dimensional cell culture. Methods Cell Biol. 125, 353–372. https://doi.org/10.1016/bs.mcb.2014.10.017

Krieg, T., Aumailley, M., 2011. The extracellular matrix of the dermis: flexible structures with dynamic functions. Exp. Dermatol. 20, 689–695. https://doi.org/10.1111/j.1600-0625.2011.01313.x

Krutmann, J., Schikowski, T., Morita, A., Berneburg, M., 2021. Environmentally-Induced (Extrinsic) Skin Aging: Exposomal Factors and Underlying Mechanisms. J. Invest. Dermatol. 141, 1096–1103. https://doi.org/10.1016/j.jid.2020.12.011

Lee, D.H., Oh, J.-H., Chung, J.H., 2016. Glycosaminoglycan and proteoglycan in skin aging. J. Dermatol. Sci. 83, 174–181. https://doi.org/10.1016/j.jdermsci.2016.05.016

Lee, H., Hong, Y., Kim, M., 2021. Structural and Functional Changes and Possible Molecular Mechanisms in Aged Skin. Int. J. Mol. Sci. 22, 12489. https://doi.org/10.3390/ijms222212489

Lee, J.Y.-Y., Yang, C.-C., Chao, S.-C., Wong, T.-W., 2004. Histopathological differential diagnosis of keloid and hypertrophic scar. Am. J. Dermatopathol. 26, 379–384. https://doi.org/10.1097/00000372-200410000-00006

Lefèvre-Utile, A., Braun, C., Haftek, M., Aubin, F., 2021. Five Functional Aspects of the Epidermal Barrier. Int. J. Mol. Sci. 22, 11676. https://doi.org/10.3390/ijms222111676

Li, W., Ahn, A.C., 2011. Subcutaneous fascial bands--a qualitative and morphometric analysis. PloS One 6, e23987. https://doi.org/10.1371/journal.pone.0023987

Liu, J., Zhao, B., Zhu, H., Pan, Q., Cai, M., Bai, X., Li, X., Hu, X., Zhang, M., Shi, J., Zheng, Z., Yang, A., Hu, D., 2020. Wnt4 negatively regulates the TGF-β1-induced human dermal fibroblast-to-myofibroblast transition via targeting Smad3 and ERK. Cell Tissue Res. 379, 537–548. https://doi.org/10.1007/s00441-019-03110-x

Matejuk, A., 2018. Skin Immunity. Arch. Immunol. Ther. Exp. (Warsz.) 66, 45–54. https://doi.org/10.1007/s00005-017-0477-3

McCarley, K.D., Bunge, A.L., 2001. Pharmacokinetic models of dermal absorption. J. Pharm. Sci. 90, 1699–1719. https://doi.org/10.1002/jps.1120

Mokry, J., Pisal, R., 2020. Development and Maintenance of Epidermal Stem Cells in Skin Adnexa. Int. J. Mol. Sci. 21, E9736. https://doi.org/10.3390/ijms21249736

Monika, P., Waiker, P.V., Chandraprabha, M.N., Rangarajan, A., Murthy, K.N.C., 2021. Myofibroblast progeny in wound biology and wound healing studies. Wound Repair Regen. Off. Publ. Wound Heal. Soc. Eur. Tissue Repair Soc. 29, 531–547. https://doi.org/10.1111/wrr.12937

Moreci, R.S., Lechler, T., 2020. Epidermal structure and differentiation. Curr. Biol. CB 30, R144–R149. https://doi.org/10.1016/j.cub.2020.01.004

Nguyen, A.V., Soulika, A.M., 2019. The Dynamics of the Skin's Immune System. Int. J. Mol. Sci. 20, E1811. https://doi.org/10.3390/ijms20081811

Otaka, H., Shimakura, H., Motoyoshi, I., 2019. Perception of human skin conditions and image statistics. J. Opt. Soc. Am. A Opt. Image Sci. Vis. 36, 1609–1616. https://doi.org/10.1364/JOSAA.36.001609

Plikus, M.V., Wang, X., Sinha, S., Forte, E., Thompson, S.M., Herzog, E.L., Driskell, R.R., Rosenthal, N., Biernaskie, J., Horsley, V., 2021. Fibroblasts: Origins, definitions, and functions in health and disease. Cell 184, 3852–3872. https://doi.org/10.1016/j.cell.2021.06.024

Pondeljak, N., Lugović-Mihić, L., 2020. Stress-induced Interaction of Skin Immune Cells, Hormones, and Neurotransmitters. Clin. Ther. 42, 757–770. https://doi.org/10.1016/j.clinthera.2020.03.008

Rawlings, A.V., Harding, C.R., 2004. Moisturization and skin barrier function. Dermatol. Ther. 17 Suppl 1, 43–48. https://doi.org/10.1111/j.1396-0296.2004.04s1005.x

Rippa, A.L., Kalabusheva, E.P., Vorotelyak, E.A., 2019. Regeneration of Dermis: Scarring and Cells Involved. Cells 8, E607. https://doi.org/10.3390/cells8060607

Rodero, M.P., Khosrotehrani, K., 2010. Skin wound healing modulation by macrophages. Int. J. Clin. Exp. Pathol. 3, 643–653.

Sato, T., Liu, X., Basma, H., Togo, S., Sugiura, H., Nelson, A., Nakanishi, M., Kanaji, N., Wang, X., Kim, M., Li, Y., Michalski, J., Farid, M., Sharp, J.G., Rennard, S.I., 2011. IL-4 induces differentiation of human embryonic stem cells into fibrogenic fibroblast-like cells. J. Allergy Clin. Immunol. 127, 1595-1603.e9. https://doi.org/10.1016/j.jaci.2011.01.049

Shin, J.-W., Kwon, S.-H., Choi, J.-Y., Na, J.-I., Huh, C.-H., Choi, H.-R., Park, K.-C., 2019. Molecular Mechanisms of Dermal Aging and Antiaging Approaches. Int. J. Mol. Sci. 20, E2126. https://doi.org/10.3390/ijms20092126

Singh, V.K., Kumar, N., Kalsan, M., Saini, A., Chandra, R., 2015. Mechanism of Induction: Induced Pluripotent Stem Cells (iPSCs). J. Stem Cells 10, 43–62.

Skin Acute Wound Healing: A Comprehensive Review - PubMed [WWW Document], n.d. URL https://pubmed.ncbi.nlm.nih.gov/31275545/ (accessed 8.25.22).

Soliman, H., Theret, M., Scott, W., Hill, L., Underhill, T.M., Hinz, B., Rossi, F.M.V., 2021. Multipotent stromal cells: One name, multiple identities. Cell Stem Cell 28, 1690–1707. https://doi.org/10.1016/j.stem.2021.09.001

Sorg, H., Tilkorn, D.J., Hager, S., Hauser, J., Mirastschijski, U., 2017. Skin Wound Healing: An Update on the Current Knowledge and Concepts. Eur. Surg. Res. Eur. Chir. Forsch. Rech. Chir. Eur. 58, 81–94. https://doi.org/10.1159/000454919

Sorrell, J.M., Caplan, A.I., 2004. Fibroblast heterogeneity: more than skin deep. J. Cell Sci. 117, 667–675. https://doi.org/10.1242/jcs.01005

Sotiropoulou, P.A., Blanpain, C., 2012. Development and homeostasis of the skin epidermis. Cold Spring Harb. Perspect. Biol. 4, a008383. https://doi.org/10.1101/cshperspect.a008383

Stecco, C., Macchi, V., Porzionato, A., Duparc, F., De Caro, R., 2011. The fascia: the forgotten structure. Ital. J. Anat. Embryol. Arch. Ital. Anat. Ed Embriologia 116, 127–138.

Strutz, F., Okada, H., Lo, C.W., Danoff, T., Carone, R.L., Tomaszewski, J.E., Neilson, E.G., 1995. Identification and characterization of a fibroblast marker: FSP1. J. Cell Biol. 130, 393–405. https://doi.org/10.1083/jcb.130.2.393

Stunova, A., Vistejnova, L., 2018. Dermal fibroblasts-A heterogeneous population with regulatory function in wound healing. Cytokine Growth Factor Rev. 39, 137–150. https://doi.org/10.1016/j.cytogfr.2018.01.003

Tan, S., Khumalo, N., Bayat, A., 2019. Understanding Keloid Pathobiology From a Quasi-Neoplastic Perspective: Less of a Scar and More of a Chronic Inflammatory Disease With Cancer-Like Tendencies. Front. Immunol. 10, 1810. https://doi.org/10.3389/fimmu.2019.01810

Taylor, S.C., 2002. Skin of color: biology, structure, function, and implications for dermatologic disease. J. Am. Acad. Dermatol. 46, S41-62. https://doi.org/10.1067/mjd.2002.120790

Thulabandu, V., Chen, D., Atit, R.P., 2018. Dermal fibroblast in cutaneous development and healing. Wiley Interdiscip. Rev. Dev. Biol. 7. https://doi.org/10.1002/wdev.307

Tigges, J., Krutmann, J., Fritsche, E., Haendeler, J., Schaal, H., Fischer, J.W., Kalfalah, F., Reinke, H., Reifenberger, G., Stühler, K., Ventura, N., Gundermann, S., Boukamp, P., Boege, F., 2014. The hallmarks of fibroblast ageing. Mech. Ageing Dev. 138, 26–44. https://doi.org/10.1016/j.mad.2014.03.004

Togo, S., Sato, T., Sugiura, H., Wang, X., Basma, H., Nelson, A., Liu, X., Bargar, T.W., Sharp, J.G., Rennard, S.I., 2011. Differentiation of embryonic stem cells into fibroblast-like cells in three-dimensional type I collagen gel cultures. In Vitro Cell. Dev. Biol. Anim. 47, 114–124. https://doi.org/10.1007/s11626-010-9367-2

Tomasek, J.J., Gabbiani, G., Hinz, B., Chaponnier, C., Brown, R.A., 2002. Myofibroblasts and mechano-regulation of connective tissue remodelling. Nat. Rev. Mol. Cell Biol. 3, 349–363. https://doi.org/10.1038/nrm809

University, © Stanford, Stanford, California 94305, 2015. Skin patch could help heal, prevent diabetic ulcers, study finds [WWW Document]. Welcome Bio-X. URL https://biox.stanford.edu/highlight/skin-patch-could-help-heal-prevent-diabetic-ulcers-study-finds (accessed 8.28.22).

Uyar, B., Palmer, D., Kowald, A., Murua Escobar, H., Barrantes, I., Möller, S., Akalin, A., Fuellen, G., 2020. Single-cell analyses of aging, inflammation and senescence. Ageing Res. Rev. 64, 101156. https://doi.org/10.1016/j.arr.2020.101156

van Smeden, J., Janssens, M., Gooris, G.S., Bouwstra, J.A., 2014. The important role of stratum corneum lipids for the cutaneous barrier function. Biochim. Biophys. Acta 1841, 295–313. https://doi.org/10.1016/j.bbalip.2013.11.006

Wan, L., Jiang, D., Correa-Gallegos, D., Ramesh, P., Zhao, J., Ye, H., Zhu, S., Wannemacher, J., Volz, T., Rinkevich, Y., 2021. Connexin43 gap junction drives fascia mobilization and repair of deep skin wounds. Matrix Biol. J. Int. Soc. Matrix Biol. 97, 58–71. https://doi.org/10.1016/j.matbio.2021.01.005

Wang, P.-H., Huang, B.-S., Horng, H.-C., Yeh, C.-C., Chen, Y.-J., 2018. Wound healing. J. Chin. Med. Assoc. JCMA 81, 94–101. https://doi.org/10.1016/j.jcma.2017.11.002

Wang, Y., Xu, R., He, W., Yao, Z., Li, H., Zhou, J., Tan, J., Yang, S., Zhan, R., Luo, G., Wu, J., 2015. Three-Dimensional Histological Structures of the Human Dermis. Tissue Eng. Part C Methods 21, 932–944. https://doi.org/10.1089/ten.TEC.2014.0578

What to know about skin [WWW Document], n.d. URL https://www.bbraun.co.uk/en/patients/wound-healing/knowledge-series.html (accessed 8.31.22).

Wilkinson, H.N., Hardman, M.J., 2020. Senescence in Wound Repair: Emerging Strategies to Target Chronic Healing Wounds. Front. Cell Dev. Biol. 8, 773. https://doi.org/10.3389/fcell.2020.00773

Williams, I.R., Kupper, T.S., 1996. Immunity at the surface: homeostatic mechanisms of the skin immune system. Life Sci. 58, 1485–1507. https://doi.org/10.1016/0024-3205(96)00042-2

Wlaschek, M., Maity, P., Makrantonaki, E., Scharffetter-Kochanek, K., 2021. Connective Tissue and Fibroblast Senescence in Skin Aging. J. Invest. Dermatol. 141, 985–992. https://doi.org/10.1016/j.jid.2020.11.010

Wong, R., Geyer, S., Weninger, W., Guimberteau, J.-C., Wong, J.K., 2016. The dynamic anatomy and patterning of skin. Exp. Dermatol. 25, 92–98. https://doi.org/10.1111/exd.12832

Woodley, D.T., 2017. Distinct Fibroblasts in the Papillary and Reticular Dermis: Implications for Wound Healing. Dermatol. Clin. 35, 95–100. https://doi.org/10.1016/j.det.2016.07.004

Wound repair and regeneration | Nature [WWW Document], n.d. URL https://www.nature.com/articles/nature07039 (accessed 8.26.22).

Yamaguchi, K., Kanno, E., Tanno, H., Sasaki, A., Kitai, Y., Miura, T., Takagi, N., Shoji, M., Kasamatsu, J., Sato, K., Sato, Y., Niiyama, M., Goto, Y., Ishii, K., Imai, Y., Saijo, S., Iwakura, Y., Tachi, M., Kawakami, K., 2021. Distinct Roles for Dectin-1 and Dectin-2 in Skin Wound Healing and Neutrophilic Inflammatory Responses. J. Invest. Dermatol. 141, 164-176.e8. https://doi.org/10.1016/j.jid.2020.04.030

Yao, L., Rathnakar, B.H., Kwon, H.R., Sakashita, H., Kim, J.H., Rackley, A., Tomasek, J.J., Berry, W.L., Olson, L.E., 2022. Temporal control of PDGFRα regulates the fibroblast-to-myofibroblast transition in wound healing. Cell Rep. 40, 111192. https://doi.org/10.1016/j.celrep.2022.111192

Yousefzadeh, M.J., Zhu, Y., McGowan, S.J., Angelini, L., Fuhrmann-Stroissnigg, H., Xu, M., Ling, Y.Y., Melos, K.I., Pirtskhalava, T., Inman, C.L., McGuckian, C., Wade, E.A., Kato, J.I., Grassi, D., Wentworth, M., Burd, C.E., Arriaga, E.A., Ladiges, W.L., Tchkonia, T., Kirkland, J.L., Robbins, P.D., Niedernhofer, L.J., 2018. Fisetin is a senotherapeutic that extends health and lifespan. EBioMedicine 36, 18–28. https://doi.org/10.1016/j.ebiom.2018.09.015

Zhao, B., Guan, H., Liu, J.-Q., Zheng, Z., Zhou, Q., Zhang, J., Su, L.-L., Hu, D.-H., 2017. Hypoxia drives the transition of human dermal fibroblasts to a myofibroblast-like phenotype via the TGF-β1/Smad3 pathway. Int. J. Mol. Med. 39, 153–159. https://doi.org/10.3892/ijmm.2016.2816

Zomer, H.D., Trentin, A.G., 2018a. Skin wound healing in humans and mice: Challenges in translational research. J. Dermatol. Sci. 90, 3–12. https://doi.org/10.1016/j.jdermsci.2017.12.009

Zomer, H.D., Trentin, A.G., 2018b. Skin wound healing in humans and mice: Challenges in translational research. J. Dermatol. Sci. 90, 3–12. https://doi.org/10.1016/j.jdermsci.2017.12.009

Zorina, A., Zorin, V., Kudlay, D., Kopnin, P., 2022. Age-Related Changes in the Fibroblastic Differon of the Dermis: Role in Skin Aging. Int. J. Mol. Sci. 23, 6135. https://doi.org/10.3390/ijms23116135

Acknowledgements

Along the way, I have walked many roads and suffered many hardships. The heart firmly believes that to keep a positive initial heart, naturally there is a day to keep the clouds open to see the moon.

I was born in a remote mountainous village in Jiangxi, and I was the first university student, the first master and the first doctor in the village. In the rural areas, educational resources and its lack, I remember reading the first and second grade, our entire grade only one teacher, he is responsible for all the curriculum. Then in the third grade I started to go to school, leaving at six in the morning and returning home at six in the evening. In fourth and fifth grade, I started to live in school and went home once a week. Elementary school was a very difficult and poor life, but I felt very happy because we did not have any pressure to go on to higher education, there was simply happiness every day. During my three years of junior high school, I also lived in a residential school, and my grades were always among the best, and there was no great pressure to go on to higher education. Because in rural areas, parents feel that reading depends on themselves, can read to continue to read, cannot go to school early out of work is also very good. I still remember that there were more than 80 people in our class in the first year of junior high school, and only half of them were left to take the exam in the third year. At the end of junior high school, I got into a key high school class with the third highest score in the junior high school. After entering high school, I began to find it uncomfortable to get used to the freedom of learning. High school learning belongs to the kind of filler education, every day from six in the morning to twelve at night, are sitting in the classroom, all the time is learning, but I did not find myself at that time is not suitable for this high-pressure learning state, just know a head buried inefficient learning. The first college entrance examination, unexpectedly I did not get into the second school, and then back to high school to repeat a year, still high intensity and low efficiency of learning, the second year of college entrance examination, I exceeded a line 5 points, lucky pressure into the Nanchang University School of Public Health Medical Laboratory study. My college life was very full, in addition to learning professional knowledge, actively participate in a variety of activities, perfect through the college time. When I was about to graduate from my undergraduate degree, I was still a bit confused, not knowing whether to work directly or continue to graduate school, so I was all prepared at that time. But when looking for a job but was slapped

hard by reality, in the hospital without contacts, the hospital finally chose a specialist. Then I went on to prepare for the graduate school, due to inadequate preparation time, and eventually did not get into the school of my choice, and finally transferred to the basic medicine program at Nanchang University. I was very fortunate to meet a very good supervisor for my master's degree, who had a great influence on me, especially in how to behave. The supervisor also gave me enough support in research. After graduating from my master's degree, it was very difficult to find a job in basic medicine, and I chose to continue my doctoral studies because I still had a love for research.

I have gained a lot from my four years of study in Germany. First of all, I would like to thank Yuval for giving me the opportunity to pursue my PhD here. I am grateful to Yuval for giving me the opportunity to study for my PhD. He has given me a lot of guidance and a lot of foreword ideas during my time in the lab, and he has also supported me with equipment and experimental materials. At the end of my CSC scholarship, I would like to thank Yuval for giving me a year of funding.

Many thanks to my PhD supervisor team, Prof. Dr. med. Jürgen Behr, Prof. Dr. Silke Meiners and Dr. Yuval Rinkevich, who gave me invaluable advice on the subject. Thanks to CPC research school for the doctoral program and every member (PD Dr. Claudia Staab-Weijnitz, Karin Agnes Herbert, Dr. Doreen Franke, Dr. Melanie Penning) for their dedication.

Thanks to Dongsheng, who helped me a lot during my PhD. From the interview at the beginning, to the initial arrival in the lab, Dongsheng taught me some experimental operations and many experimental ideas. In the subsequent research life, I would discuss with Dongsheng every time I had questions, and Dongsheng would answer them for me in detail. Dongsheng also gave me great support on some problems in the animal room. I am grateful to Donovan for his great help in my experiments. He gave me a lot of good suggestions in animal experiments, immunofluorescence staining and other experiments, especially in single-cell data analysis, and gave me full support. She also gave me a lot of valuable advice on my project.

Thanks to Aydan, she is the best foreign friend I have ever had here. From the beginning of the PhD program, to the help in animal experiments, to the help in life, Aydan has always helped me wholeheartedly. I would like to thank Binbin for his constant care and encouragement, as my close friend who has always given me the motivation to move forward in my research and life. Thank you to Ruoxuan Dai, Yiqun Su and Yue Lin for their help in experiments and care in life, and for often having dinner parties together to add color to the boring lab life. Thanks to Xiangyu Zhang, Ruiji Gui, Wei

Han, Shaoping Hu, Jin Xu, Jiazheng La, Jiakuan Zhao, Li Wan and Qing Yu for their help in my experiments and care in my daily life. Thanks to Junfu Luo, Ruolan Gong, Hengyi Fan, Shiqi Cheng and Fangteng Liu, with whom I enjoyed a good time of study tour. Thanks to Bikram Dasgupta, Sandra Schiener, Natalja Ring for their help in my contract and visa. Thanks to Andy Quarri, Pushkar Ramesh, Martin Mueck-Hauesl, Adrian Fischer, Tankut Gokhan Guney, Ryo Ichijo, Safouane Kadri, Ravinder Kandi, Christoph Deisenhofer, George Vogelaar, Stella Sem-melrath, Vijayanand Rajendran for their help in general. Everyone in the lab has made their own contribution to the development of the lab. Thanks to Juliane Wannemacher, Sibylle Sabrautzki and all colleagues in Unit 34 / Core Facility Laboratory Animal Services (CF-LAS) for taking care of my aging mice and for some advice.

Thank you to all my relatives, teachers, close friends and classmates. Your encouragement gives me the motivation to keep going. Thanks to the China Scholarship Council, which gave me the CSC study abroad scholarship to support my study overseas, I will also continue to work hard and return to China as soon as possible to contribute to the socialist construction.

Finally, I would like to thank my parents, my brother and my girlfriend Jiequ Ji, who I met by chance in a sea of people and fell in love at first sight and attracted each other. Thanks to her constant support and understanding, I am full of hope for our future. For the rest of my life, I will have you all the way, and I will hold my son's hand and grow old with him. Thank you to my parents and my brother, who have always been supportive of me, both in biochemical and academic aspects are giving me slow positive energy and selfless dedication. It is not easy to raise a PhD from a poor mountainous area, and they usually go through a lot of hardships for me and bear a lot of public pressure for me.

I will continue to work hard and will not let them down. I have a long road ahead of me, but I will not forget my original intention and continue to move forward.

----------Ye.haifeng

Affidavit

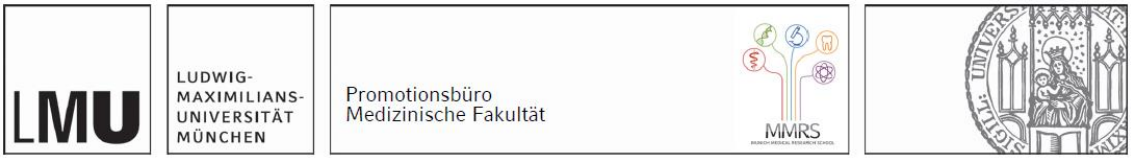

Affidavit

Ye, Haifeng

Surname, first name

Street

Zip code, town, country

I hereby declare, that the submitted thesis entitled:

Cellular and molecular mechanisms of tissue repair by fascia

is my own work. I have only used the sources indicated and have not made unauthorised use of services of a third party. Where the work of others has been quoted or reproduced, the source is always given.

I further declare that the dissertation presented here has not been submitted in the same or similar form to any other institution for the purpose of obtaining an academic degree.

Planegg, 19.04.2023

place, date

Haifeng Ye

Signature doctoral candidate

Confirmation of congruency

LMU LUDWIG-MAXIMILIANS-UNIVERSITÄT MÜNCHEN | Promotionsbüro Medizinische Fakultät | MMRS

Confirmation of congruency between printed and electronic version of the doctoral thesis

Ye, Haifeng

Surname, first name

Street

Zip code, town, country

I hereby declare, that the submitted thesis entitled:

Cellular and molecular mechanisms of tissue repair by fascia

is congruent with the printed version both in content and format.

Planegg, 19.04.2023

place, date

Haifeng Ye

Signature doctoral candidate